SKB

TECHNICAL REPORT 85-17

Sealing of rock fractures
A survey of potentially useful methods and substances

Roland Pusch*, Mikael Erlström, Lennart Börgesson

Swedish Geological Co, Lund
* also Lund University of Technology and Natural Sciences, Lund
October 1985

SVENSK KÄRNBRÄNSLEHANTERING AB
SWEDISH NUCLEAR FUEL AND WASTE MANAGEMENT CO

BOX 5864 S-102 48 STOCKHOLM
TEL 08-665 28 00 TELEX 13108-SKB

SEALING OF ROCK FRACTURES
A Survey of Potentially useful Methods and Substances

Roland Pusch*, Mikael Erlström, Lennart Börgesson

Swedish Geological Co, Lund

* also Lund University of Technology and Natural Sciences, Lund

December 1985

SWEDISH GEOLOGICAL CO
Div of Engineering Geology
Roland Pusch/JS

Date: 1985-12-31
ID-no: IRAP 86500

SEALING OF ROCK FRACTURES

A SURVEY OF POTENTIALLY USEFUL METHODS AND SUBSTANCES

Roland Pusch*
Mikael Erlström
Lennart Börgesson

Swedish Geological Co, Lund
December 1985

* also Lund University of Technology and Natural Sciences, Lund

Key words: Rock sealing, fractures, grouting, cement, clay

CONTENTS

SUMMARY

The major water-bearing fractures in granite usually form fairly regular sets but the extension and degree of connectivity is varying. This means that only a few fractures that are interconnected with the deposition holes and larger water-bearing structures in a HLW repository are expected and if they can be identified and cut off through sealing it would be possible to improve the isolation of waste packages very effectively.

Nature's own fracture sealing mechanisms may be simulated and a survey of the involved processes actually suggests a number of possible filling methods and substances. Most of them require high temperature and pressure and correspondingly sophisticated techniques, but some are of potential interest for immediate application with rather moderate effort. Such a technique is to fill the fractures with clayey substances which stay flexible and low-permeable provided that they remain physically and chemically intact. Clay grouting has been tried for many years with very moderate success by applying a constant, static pressure. It is demonstrated in the report that effective grouting requires a very low viscosity and shear strength of the substance and this can be achieved by mechanical agitation as demonstrated in this report. Thus, by superimposing static pressure and shear waves induced by percussion hammering at a suitable frequency, clays and fine-grained silts as well as cement can be driven into fractures with an average aperture as small as 0.1 mm. A suitable consistency of the grouts is that corresponding to their Atterberg liquid limit.

Experiments were made in the laboratory using concrete and steel plates, and a field pilot test was also conducted under realistic conditions on site in Stripa. They all demonstrated the practicality of the "dynamic injection technique" and that the fluid condition of the grouts yielded complete filling of the injected space to a considerable distance from the injection point. The field test indicated a good sealing ability as well as a surprisingly high resistance to erosion and piping. Long term tests are required, however, to demon-

strate the durability of such sealings and it is also required to show that the fillings are chemically stable in repository environment.

1 SCOPE OF STUDY

HLW storage concepts that are based on the use of clay-enveloped canisters located in drilled holes in crystalline rock, can be very much improved if it is also implied that water-bearing fractures in the surrounding rock are effectively sealed. Thus, if fractures which intersect the holes can be sealed so that the groundwater flow becomes virtually none within a distance of 1-2 meters from the periphery of the 1.5 m diameter KBS 3 holes, the chemical stability of smectite canister overpacks may be preserved over millions of years. Furthermore, the resistance to diffusional migration of dissolved agents that affect the integrity of the metal canisters or the transfer of radioactive substances to shallow groundwater after canister corrosion is increased by at least two orders of magnitude.

There are three major difficulties in long term sealing of water-bearing fractures: firstly to determine the hydraulic character, the orientation and the extension of individual fractures or fracture sets, secondly to select a suitable sealing substance, i.e. a material with required longevity and physical properties, and thirdly to apply a technique that is sufficiently effective to bring in the substance deep enough into the fracture. The matter is currently dealt with in the SKB research, the present report being a first survey.

2 THE ORIGIN OF FRACTURES IN CRYSTALLINE ROCK

2.1 Introduction

Crystalline rock as we see outcrops of it today, originally had the form of a molten mass of semi-solid magma in which the stress conditions were largely isotropic. This cannot have changed considerably in the course of crystallization of large masses with a homogeneous chemical composition. After solidification, however, the stress conditions were determined by numerous processes that produced the presently observed discontinuities. A number of these were formed by overstressing which yielded more or less systematic sets of fractures. A basic understanding of fracture-forming mechanisms as well as of stress-related changes in aperture and extension of such discontinuities is of great importance for successful sealing and the matter is therefore touched upon in this introductory chapter.

2.2 Earth crust stresses

Recent studies including stress measurements, analysis of earthquake data, and observations of rock strata buckling ("pop-ups") indicate that high horizontal stresses are common in the earth crust (1). There also seems to be a tendency at depth for one of the horizontal stress components to be greater than the other, although this difference is less obvious in Paleozoic rock of sedimentary origin than in underlying Precambrian rock, probably because of stress relaxation through creep in the more ductile rock. In the Canadian shield the major stress component has a direction trending approximately north-northeast, while in Scandinavia the major principal stress, which is usually almost horizontal, is generally directed west-northwest. It is also understood from such studies that the principal horizontal stress increases with depth (Fig 1).

Crustal stresses are caused by subsidence, erosion and uplift, hot spot migration, continental glaciation, large plutonic injections, metasomatic expansion, thermally induced volume changes, and plate tectonics due to magma convection.

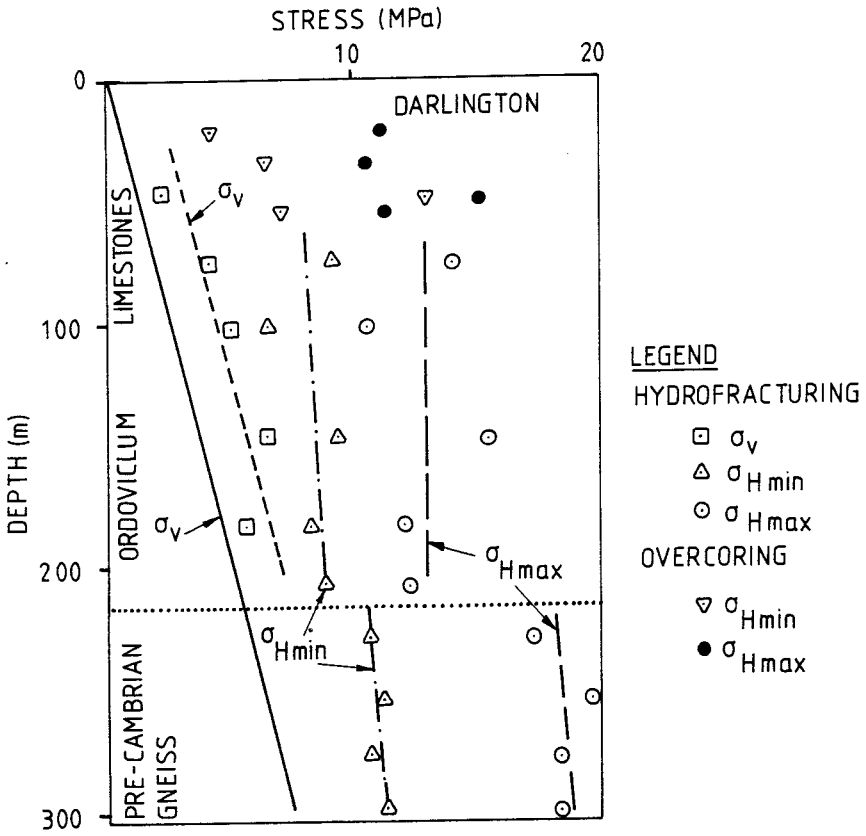

Fig 1. Typical distribution of principal stresses in the Canadian shield (2)

2.3 Stress-induced natural fractures

2.3.1 Large-scale faults

As long as the deviatoric stresses were lower than the shear strength of the lithosphere, stable conditions prevailed in the earth crust. The build-up of high, anisotropic, tectonically induced regional stresses induced creep in weak zones, which may ultimately have reached a failure condition with concomitant development of large-scale slip. This resulted in fault zone patterns like the one in Fig 2, which relates Canadian fracture rejuvenation to salt dissolution. The stress conditions leading to macroscopic failure through creep is demonstrated by Fig 3 in which a) represents stable conditions with shear stresses below the maximum stress level, while failure is developed in b) and c) because of a drop in shear strength resulting from the accumulation of strain-induced structural defects under constant deviatoric stress conditions. Like in laboratory-tested

samples of soil and rock materials that exhibit fully developed shear failure under triaxial stress conditions, macrostructurally intact, i.e. relatively fracture-free elements are confined by the oblique shear zones (Fig 4). Still, they contain flaws which are assumed to originate from initial structural heterogeneities like pores and incomplete grain contacts and which constitute the larger part of the water-bearing discontinuities that we are concerned with.

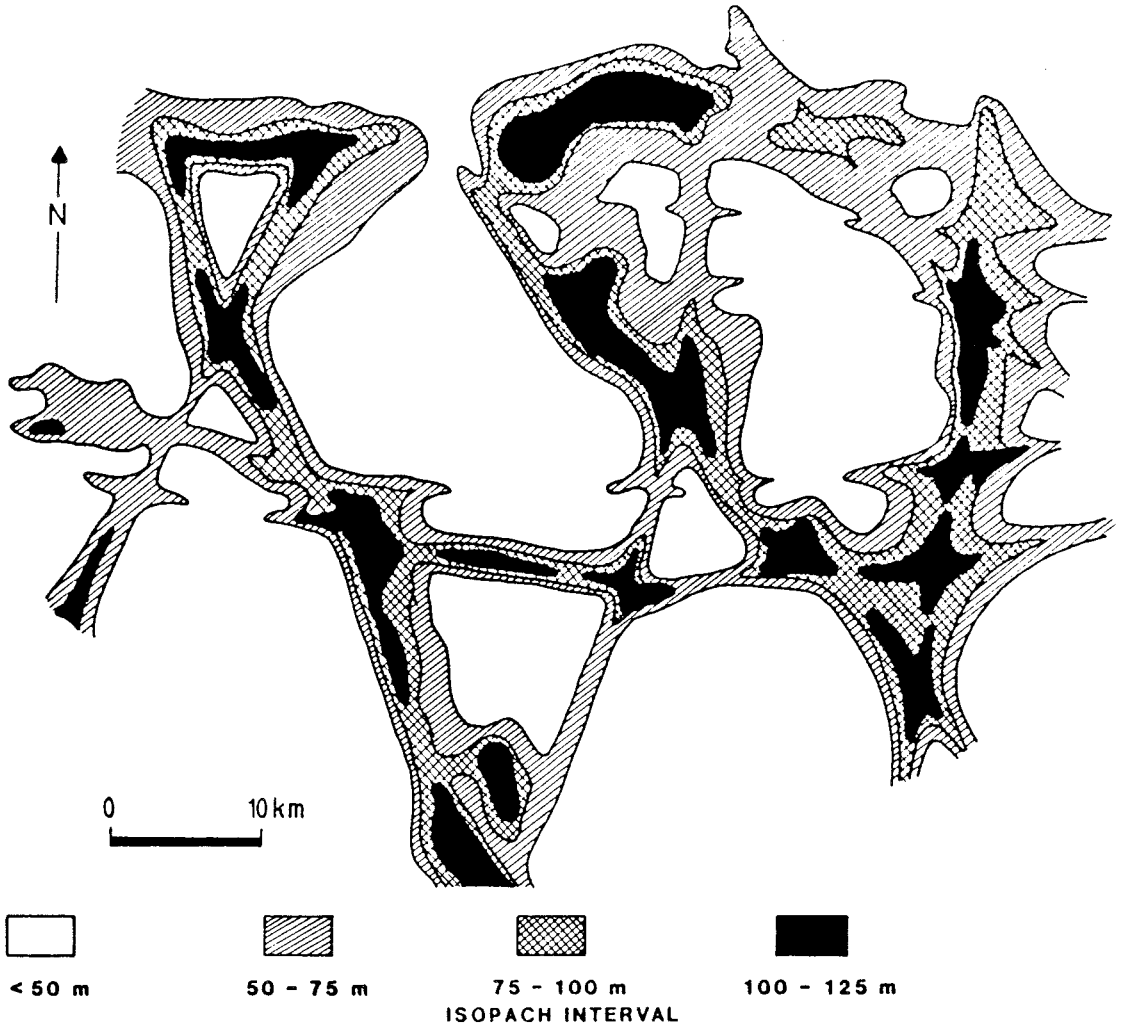

Fig 2. Anomalous thickness of upper Silurian carbonate deposits in salt dissolution cavities, the depth of which indicates the location of major fracture zones (3)

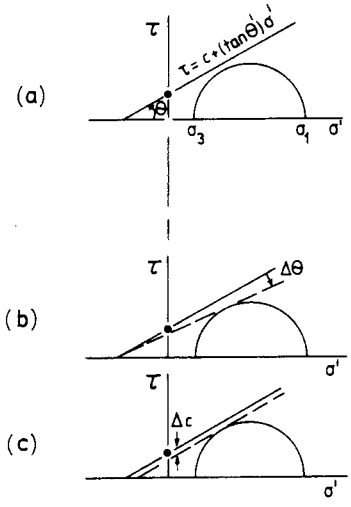

Fig 3. Mohr-Coulomb stress circle with failure envelope. a) Stable conditions, b) Failure due to a strain-induced drop in internal friction, c) Failure due to a strain-induced drop in cohesion

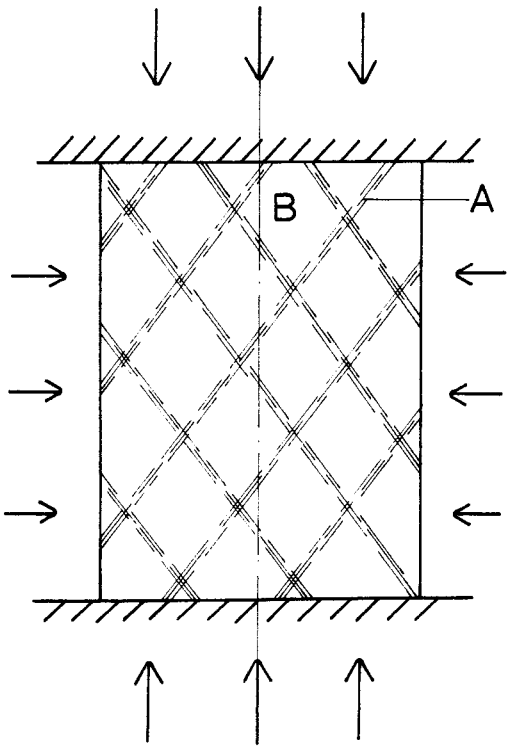

Fig 4. Large strain, developed in slip zones (A) with macro-structurally apparently intact material retained between them (B)

2.3.2 Generation of small-scale macroscopic fractures

Various investigators, such as Gramberg (4) and Paul & Gangal (5), who based their reasonings on Griffith's physical theory (1, 7), assumed that microstructural irregularities are very frequent in polycrystalline rock. Implying these irregularities to have the form of very oblate elliptical voids in a plane strain analysis, or ellipsoids in 3D analyses, it can be shown by using ordinary continuum mechanics that the tangential stress is tensile over a certain portion of their boundaries also when the entire element is in a triaxial compressive state. This generates tension fracture (Fig 5), the tendency being that such fractures propagate in the direction of the major principle stress. According to Paul & Gangal, a necessary condition for the development of a single fracture of this sort is that Griffith's failure envelope is reached (point C in Fig 6). For complete macroscopic failure the major principal stress has to be further increased, and this also initiates fractures at the tips of previously stable, differently oriented voids.

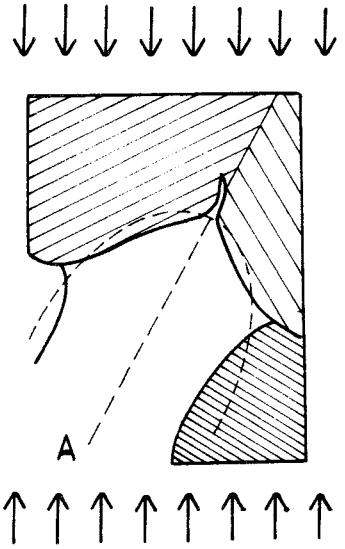

Fig 5. Generation of tensile fracture at crystal boundary according to Gramberg

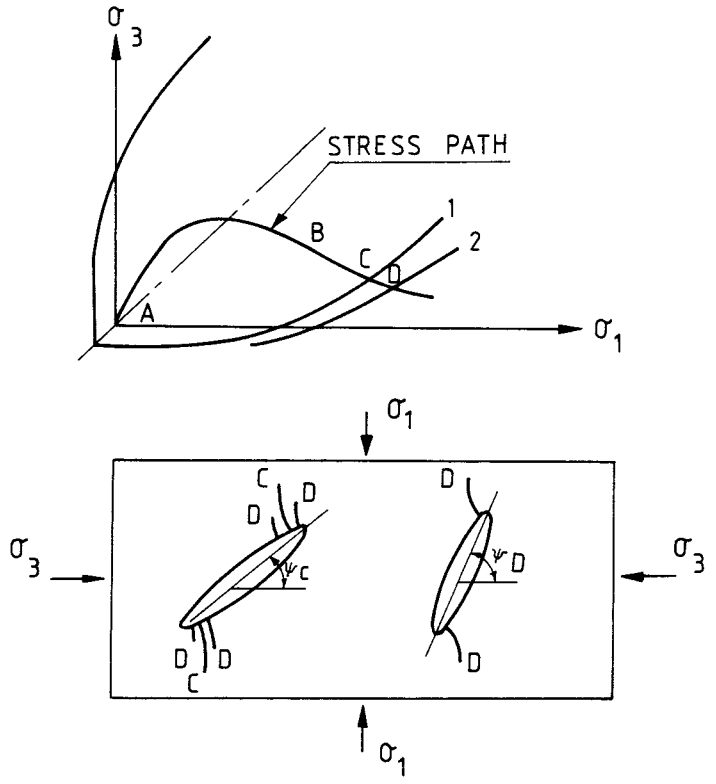

Fig 6. a) Stress diagram with primary (1) and secondary (2) Griffith failure envelopes according Paul & Gangal. b) Formation of primary tensile fractures (C) and secondary sets (D) at increased major principal stress

The resulting macroscopic failure has the form of axial cleavage (Fig 7) as demonstrated by comprehensive laboratory test series on various rock materials (4) in which the cleavage invariably developed parallel to the plane containing the major and intermediate principal stresses. This has been taken as an explanation of the formation also of large-scale, planar fractures in nature. Thus, the rather common subhorizontal joints which have a trace length of several hundred meters in Swedish crystalline bedrock and are presently filled with glacial soil or pre-Quaternary limestone (cf. p. 48) may be of this origin (8). Also many of the steeply oriented open fractures of large extension later filled by intrusions forming diabase and pegmatite dikes may be of similar origin. Both types may have resulted from high horizontal rock stresses, the flat fractures possibly in connection with the intrusion of hydrothermal solutions at high pressure.

The rock confined by features of this sort must have been exposed to the same regional stress field, i.e. one characterized by an almost horizontally oriented, high major principal stress and a steep or flat minor principal stress, but without development of large fracture features. Embryotic defects representing early stages of axial cleavage would be expected however, and this suggests ubiquitous occurrence of major sets of almost horizontal and steeply oriented sets of fractures, both of varying extension. This is also what we see in igneous rock where there are usually two nearly orthogonal sets of discontinuities, the integrated fracture pattern being more or less like that in Fig 8. Practical examples are shown in Fig 9. Identification of such regularities is of great importance for the planning of successful sealing operations.

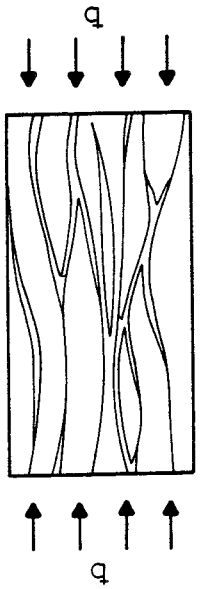

Fig 7. Schematic picture of fractures developed through axial cleavage in a uniaxially compressed rock sample with friction-free ends

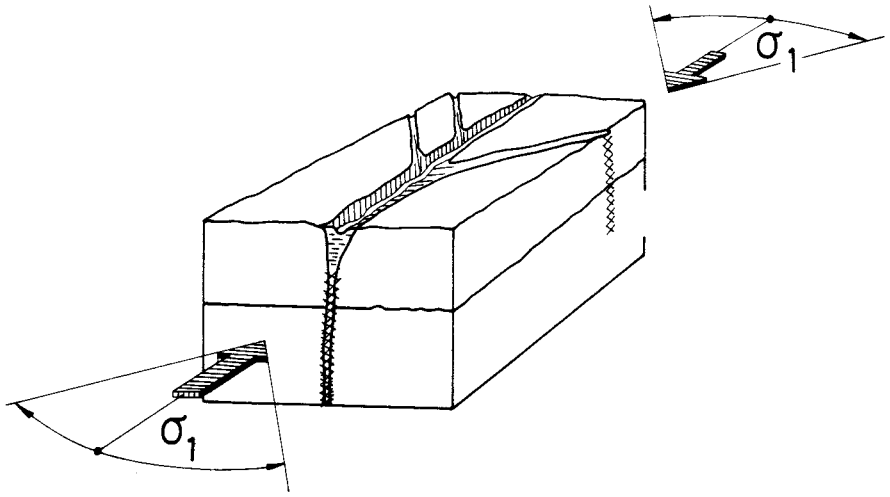

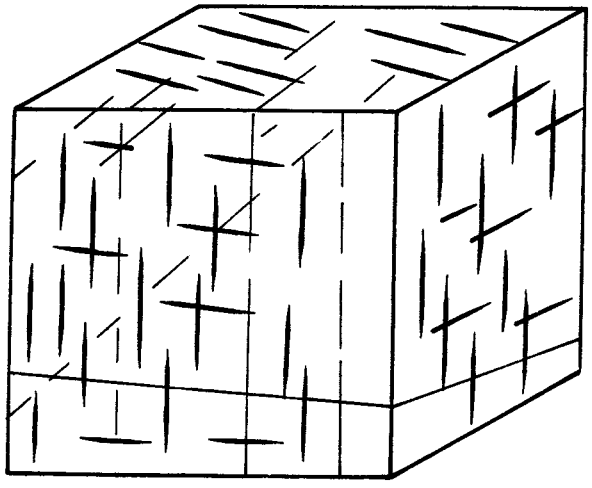

Fig 8. Large- and small-scale fracture patterns in bedrock with a high horizontal stress component

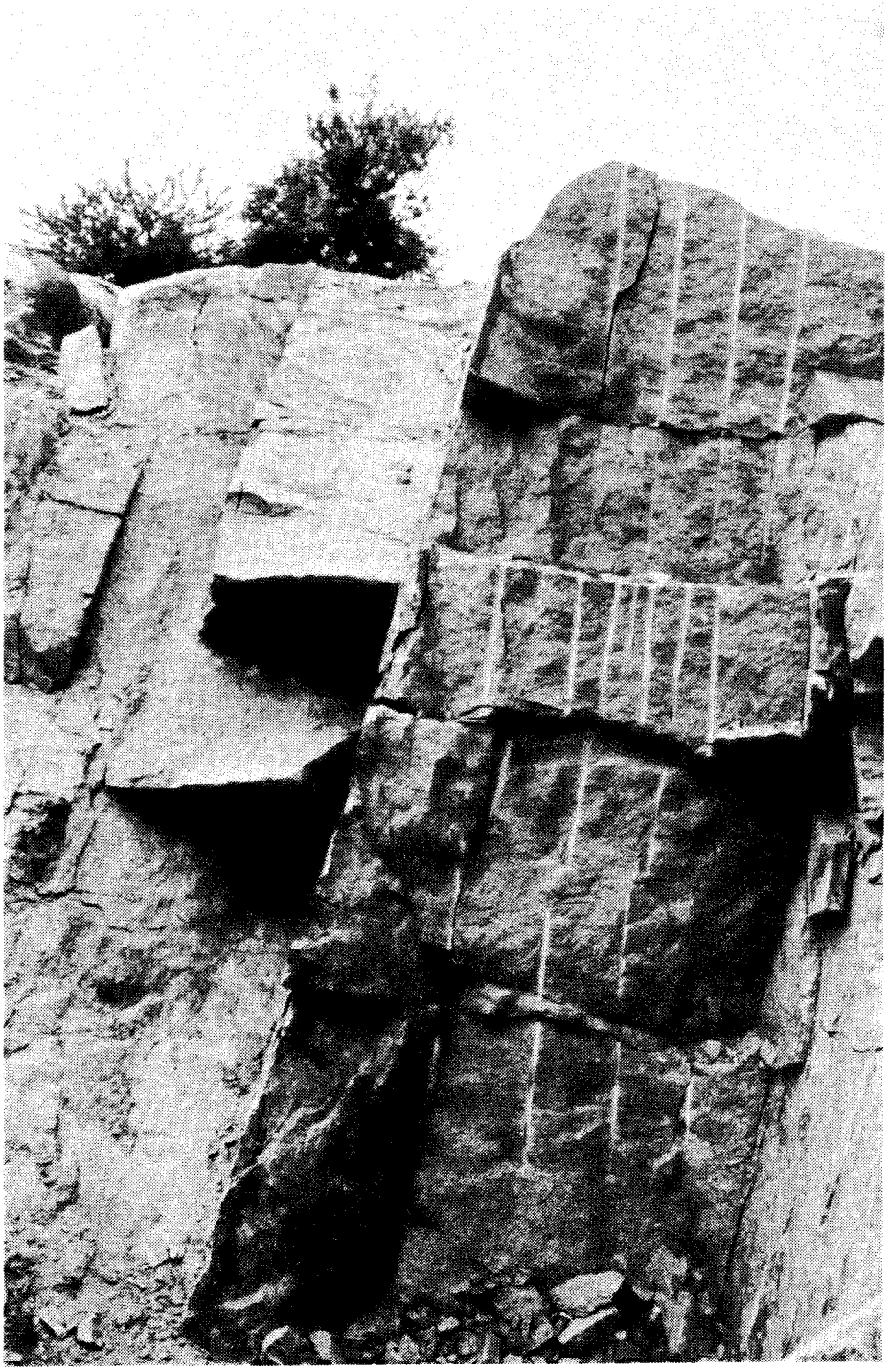

Fig 9. Typical fracture sets in granite (Bornholm)

2.4 Natural fractures

2.4.1 General

Local variations in mineral composition and structure produce inhomogeneities in any stress field and this explains why fracture patterns always deviate from regular theoretically deduced patterns like the one shown in Fig 8. Thus, depending on the rate and magnitude of the deformation at the fracture formation as well as on the deviator stress and brittleness of the rock, which are in turn functions of its mineral composition and temperature, the spacing, extension and surface characteristics of the fractures became rather irregular. This is particularly obvious for rock that has been exposed to heating and cooling cycles such as those resulting from glaciation.

2.4.2 Geometry

Major fracturing probably took place in connection with larger tectonic processes like the post-Cambrian uplifts of the Caledonian ridge. As most physical processes in nature, stochastic variations in stress/strain properties and composition, also of apparently isotropic matter, yielded a spectrum of geometries as manifested by the appearance of the open fractures we see today.

The Gramberg/Paul/Gangal fracture theory implies that fractures formed under three-dimensional compressive stress conditions propagate a certain distance and then become stable, provided that the stress field remains constant. In fact, the ultimate fracture geometry is reached after delayed failure resulting from creep caused by various mechanisms such as corrosion (9) and strain-induced stress redistribution (10). Since the regional as well as local stress conditions have not been constant since the generation of the initial fractures, whenever they were formed, some of them subsequently propagated and became widened while some were closed instead. Many of the fractures which remained open, were later partly or completely sealed by precipitated matter originating from hydrothermal processes, or derived by pressure solution in the rock matrix (11). This kind of reactions resulted in a wide range of mineral species, commonly quartz, calcite, feldspar, biotite and chlorite, and was probably the dominating

filling process in fractures interconnected so that hydrothermal solutions could percolate.

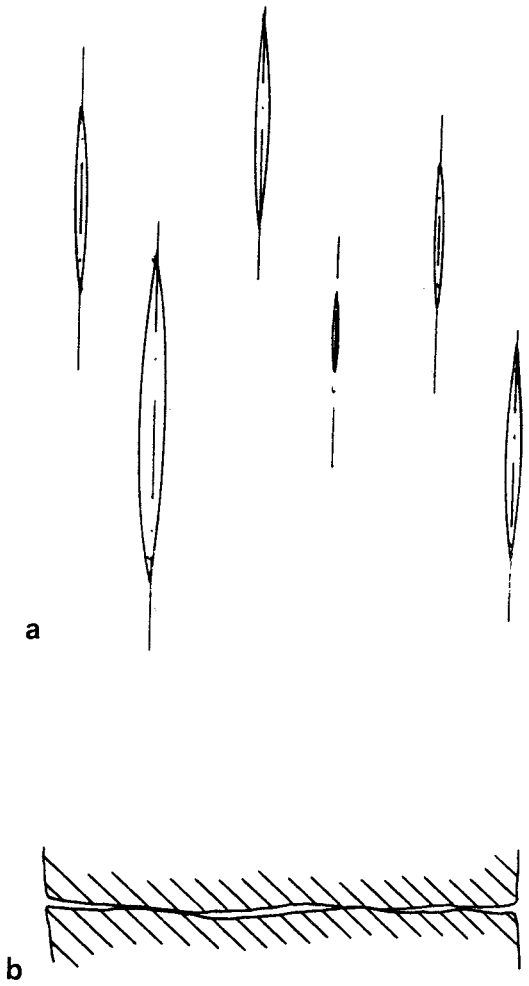

Fig 10. a) Uniaxial set of hypothetical ellipsoidal fractures.
b) Actual shape of fractures. The apertures are largely exaggarated

Fractures produced by axial cleavage are usually slightly irregular and rough, forming very thin, oblate slots with very sharply rounded edges. The general shape can approximately be taken as ellipsoidal, meaning that freshly formed fractures constitute sets of macroscopic Griffith cracks. One such set may appear as in Fig 10a in which the ratio of aperture/length is strongly exaggerated. In practice, partial filling through precipitation, or creep-induced closure leading to the formation of local contacts ("asperities") usually produced considerable deviations from the hypothetic ellipsoidal shape, the real geometry being more like that in Fig 10b. While the ellipsoidal approach cannot be directly applied for true hydromechanical modelling of the rock it may be useful for semi-quantitative evaluation of stress-related compression and changes in the interconnectivity of hydraulically active fractures, and thereby of the groutability of the rock.

2.4.3 Spacing

The number of discontinuities that are of importance with respect to hydrology and rock sealing is usually very low in crystalline rock as illustrated by the empirical rock classification scheme given in Table 1. This clearly shows that only very few water passages need to be sealed in order to make relatively large rock volumes virtually impermeable. Large zones of sheared and crushed rock are usually very fracture-rich and represent hydraulically active zones of the first order. They are not considered specifically in this report because canister deposition holes will not be located in such structures.

Table 1. Fracture classification based on Bergman's division (12)

Type	Average fracture distance, m	Occurrence
Large rock elements	>1.5	Common structure in massive igneous rock
Intermediate rock element size	0.5-1.5	Common structure in metamorphic rock except shales
Finely fractured	<0.5	Crushed zones, shear zones, also common in sedimentary and metamorphic rock

A well documented example of the frequency of open joints and fractures is offered by the Stripa granite, which is an intrusive in leptite and which has an apparent homogeneity and relative lack of foliation. A comprehensive study by the Lawrence Berkeley Laboratory (LBL) showed that this granite is characterized by four main fracture sets with the spacing of individual fractures shown in Table 2 (cf also Fig 11). As a rough rule, the average spacing of joints and fractures which are determinants of the mechanical and hydraulic properties of the rock mass, is 0.5-1.0 m. This is illustrated by the mapping of discontinuities in the six large heater holes in the Stripa Buffer Mass Test (Figs 12 and 13).

Table 2. Fracture spacing parameters of Stripa granite (13)

Set no	Mean vertical spacing, m	Mean dip angle, (°)	Normal spacing, m
1	0.73	41	0.55
2	0.50	59	0.25
3	0.32	39	0.25
4	0.42	0	0.42

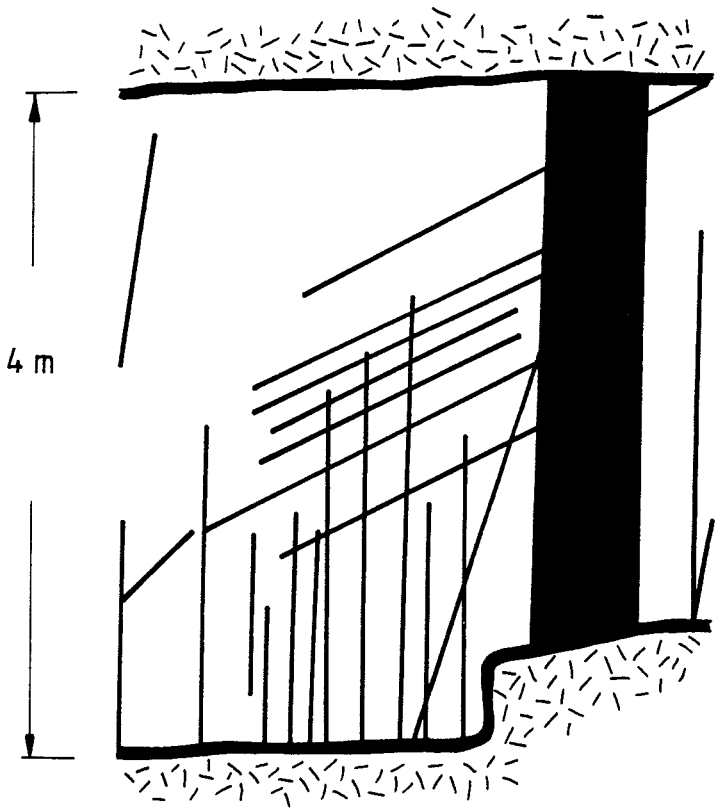

Fig 11. Regular fracture sets in granite associated with a large diabase intrusion. Inner end of the Tunnel Plug test site at Stripa. Not all the fractures give off measuable quantities of water

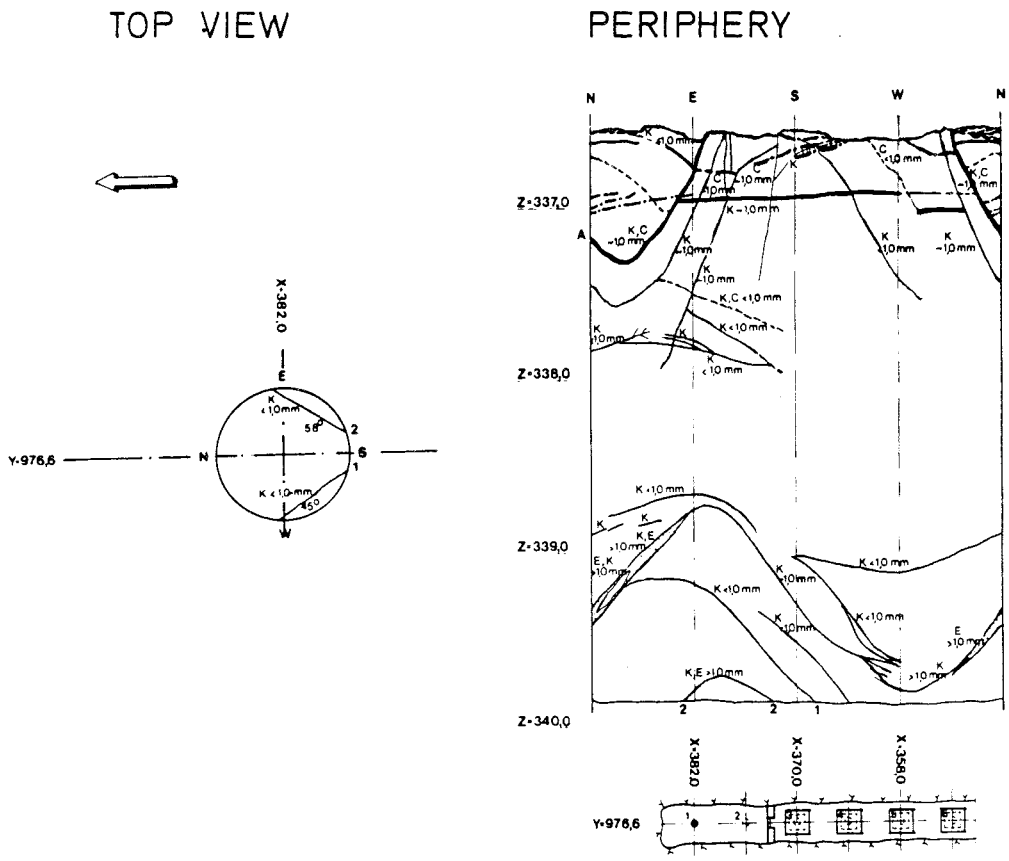

Fig 12. Major fractures exposed in the "wet" BMT hole no 1. Clearly waterbearing fractures are marked by heavy lines (14). Z-values give level in meters

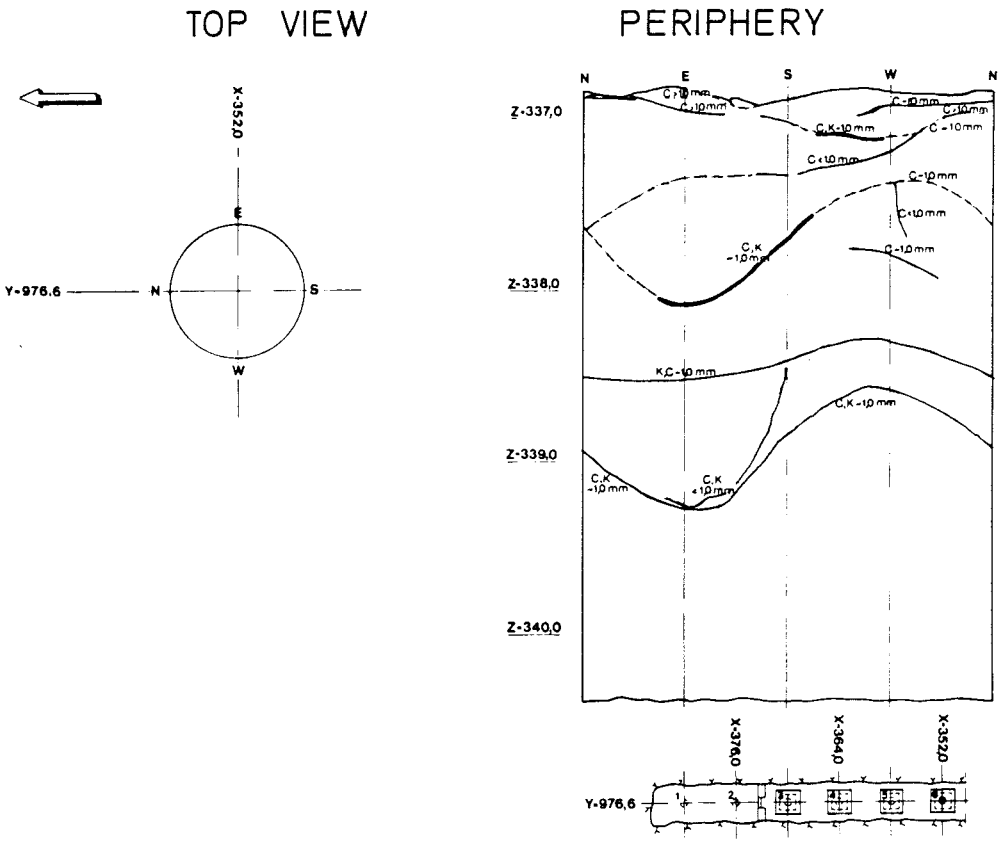

Fig 13. Major fractures exposed in the "dry" BMT hole no 6. Clearly water-bearing fractures are marked by heavy lines (14)

2.4.4 Persistence

The persistence, or trace length, is known to be rather small in general. Thus, it is concluded from various investigations, i.a. the LBL study, which demonstrated that only 15 % of the total number of clearly identified fractures in the Stripa granite persist more than 4 meters. Only about 2 % have a trace length of 7 m. The distribution of the persistence, which is usually log-normal (15), is of profound importance since it determines the degree of cross-linking and thereby governs the gross hydraulic conductivity. From the point of rock sealing it means that only a few, easily identified fractures are responsible for the major part of the gross hydraulic conductivity of rock hosting deposition holes.

2.4.5 Aperture

Direct measurement of joint apertures as they appear in boreholes or on exposed blasted rock surfaces is difficult to perform and hardly accurate, since the aperture varies considerably over the fracture plane. Rock stresses due to gravitation and tectonics have to be transferred across individual discontinuities to adjacent block units, which requires local contact regions in the form of asperities also in joints which appear to be open at ocular inspection. The spacing of such contacts is determined by the bulk strength and creep properties of the rock; it can hardly be more than a few meters in open, slot-shaped joints which have persisted for a long time at large depths since creep and creep fracturing would lead to local closure unless the rock stress state is extreme. Larger, more or less spherical voids, caves etc may of course be stable for a very long time due to arching.

The usual practical way of estimating the aperture is by steady-state injection testing. It yields equivalent "hydraulic" apertures assuming ideally smooth, parallel plate flow. This way of evaluating the aperture of joints and fractures is too inexact to form a basis of a rock model that integrates typical hydrological and stress/strain behavior, and it is not relevant with respect to the modelling of migration of injected grouts. An alternative approach would be to apply stochastic principles and pay attention to the actual variation

in persistence and cross-linking, the matter being discussed later in this report.

2.5 Influence of excavation on rock fractures

2.5.1 General

We will confine ourselves here to consider, qualitatively, the effect of stress changes on the fracture geometry and the associated alteration of the hydraulic properties and groutability of rock hosting drilled deposition holes and tunnels as well as of blasted shafts and tunnels. In principle, the removal of rock to produce such excavations induces changes in normal stress as well as shear stress and contraction of certain fractures will take place while others will expand. Propagation of some fractures also occurs at highly stressed sites. To that comes the dynamic influence by blasting which generates new fractures, widens older ones, and alters the stress situation by which delayed fracture propagation may be initiated.

2.5.2 Influence of altered stress state

2.5.2.1 General

A large number of small-scale investigations dealing with stress-induced changes in fracture aperture have been reported in literature (16). They tend to show that the compression of fractures is roughly proportional to log stress, except at very low and very high stresses (17). Similarly, the fractures expand when the normal stress is diminished. In the case of a perfectly isotropic primary stress state practically all fractures, except those which are perpendicular to the axis of a circular tunnel or shaft, become widened by stress release in the vicinity of such excavations. This yields an increased hydraulic conductivity in the axial direction of the immediate surroundings of the excavations, a phenomenon that has been frequently predicted on a theoretical basis (17, 18) and practically demonstrated by the Stripa Buffer Mass Test. In the usual case of anisotropic primary stresses, the response of the fractures to excavation is more complex as indicated by the following example, which refers to a rather common stress situation (Fig 14).

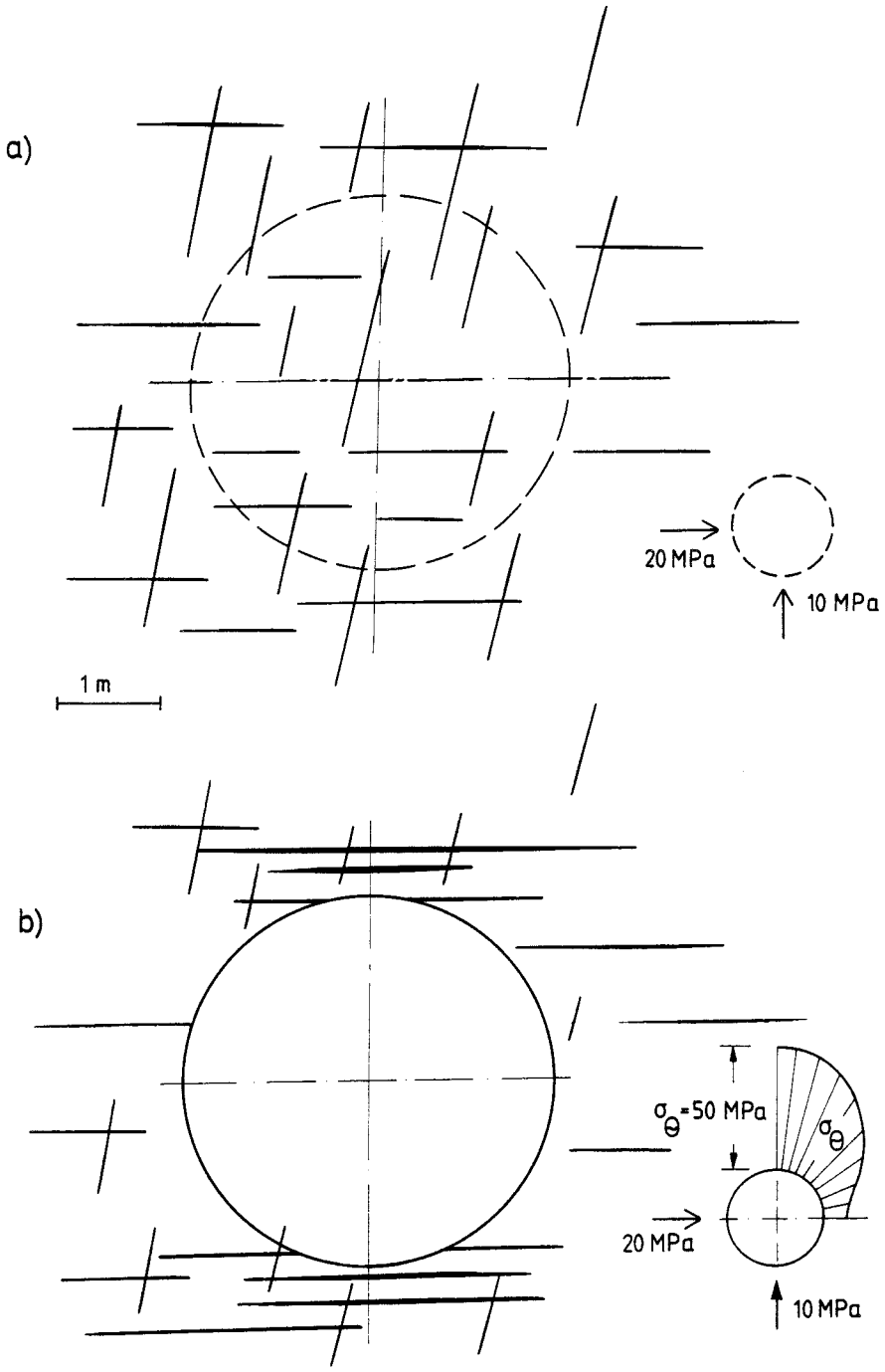

Fig 14. Hypothetic stress-induced alteration of fracture geometry. a) Initial pattern. b) Altered geometry. Notice expansion and generation of subhorizontal fractures at crown and base

The primary rock stresses in the horizontal plane are assumed to be 20 and 10 MPa, respectively, while the vertical stress is taken as 10 MPa. The excavation required to form a circular cross section of a tunnel results in a tangential stress of about 10 MPa at mid-height of the section, which would tend to leave most fractures unchanged here. At the tunnel crown and base, on the other hand, the high tangential stresses and the possibility of inward displacement of rock slabs favors propagation and expansion of existing subhorizontal fractures, as well as formation of new sets of discontinuities oriented in this same fashion. In very brittle rock, tangential stresses of this order of magnitude may produce spalling. It is concluded from this that injection of sealing substances at the crown and base of many tunnels need to be made by applying very moderate pressures in order to avoid disintegration of shallow rock.

2.5.2.2 Simplified model

A simple rock model (19) serves to illustrate the general influence of stress changes on the fracture pattern. Its main features are:

a) Three mutually perpendicular sets of fractures

b) The fractures are ellipsoids with a varying distance between their centers

c) The fracture ellipsoids have a constant a/b/c ratio, where a is the largest and c is the smallest diameter, while b is the intermediate diameter

d) The maximum aperture of the fractures (i.e. the c diameter) is a function of the normal stress. Thus, if the stress is increased in the direction that is parallel to the c-axis of each fracture set, the aperture is reduced and with it also the dimensions a and b. If the stress is instead reduced in the same direction, c increases and a and b are expanded. These changes affect the effective hydraulic section and the interconnection between the individual fractures and thereby also the hydraulic conductivity and the groutability

e) The porosity of the rock is of the common order of magnitude, i.e. 0.5-1 %, half of which is assumed to be due to hydraulically active features.

A physical, simplified version of the fracture model with a constant distance between the center of gravity of all the ellipsoidal fractures is shown in Fig 15. In practice, the distributions of size, shape and spacing may be of the types shown in Fig 16. We see that this anisotropic model resembles natural rock in the sense that the crystal matrix with no visible fissures or fractures forms a coherent mass, which contains partly intersecting, narrow oblate voids of limited extension.

At no stresses acting on the outer boundaries, the fractures have a certain "zero stress" geometry, while an increased uniaxial stress tends to compress those fractures which have their small diameters oriented in the direction of compression. Ascribing actual figures to the model for the present purpose of illustrating the influence of stress changes, the ellipsoids are assumed to have a long diameter that is twice the intermediate diameter and 20.000 times the smallest diameter (maximum aperture). Assuming then the side length of a considered cubical rock body to be 3 m in order to set the scale and applying the distributions in Fig 16, we find that the 27 m^3 rock volume holds 21 fractures with the generalized data specified in Table 3. They are taken to be characteristic for an isotropic stress condition with the effective pressure 10 MPa.

Table 3. Main fracture data of the 27 m^3 cubical rock

Number	Long diameter, m	Intermediate diameter, m	Small diameter, m
7	3	1.5	1.5×10^{-4}
7	2	1.0	10^{-4}
7	1	0.5	5×10^{-5}

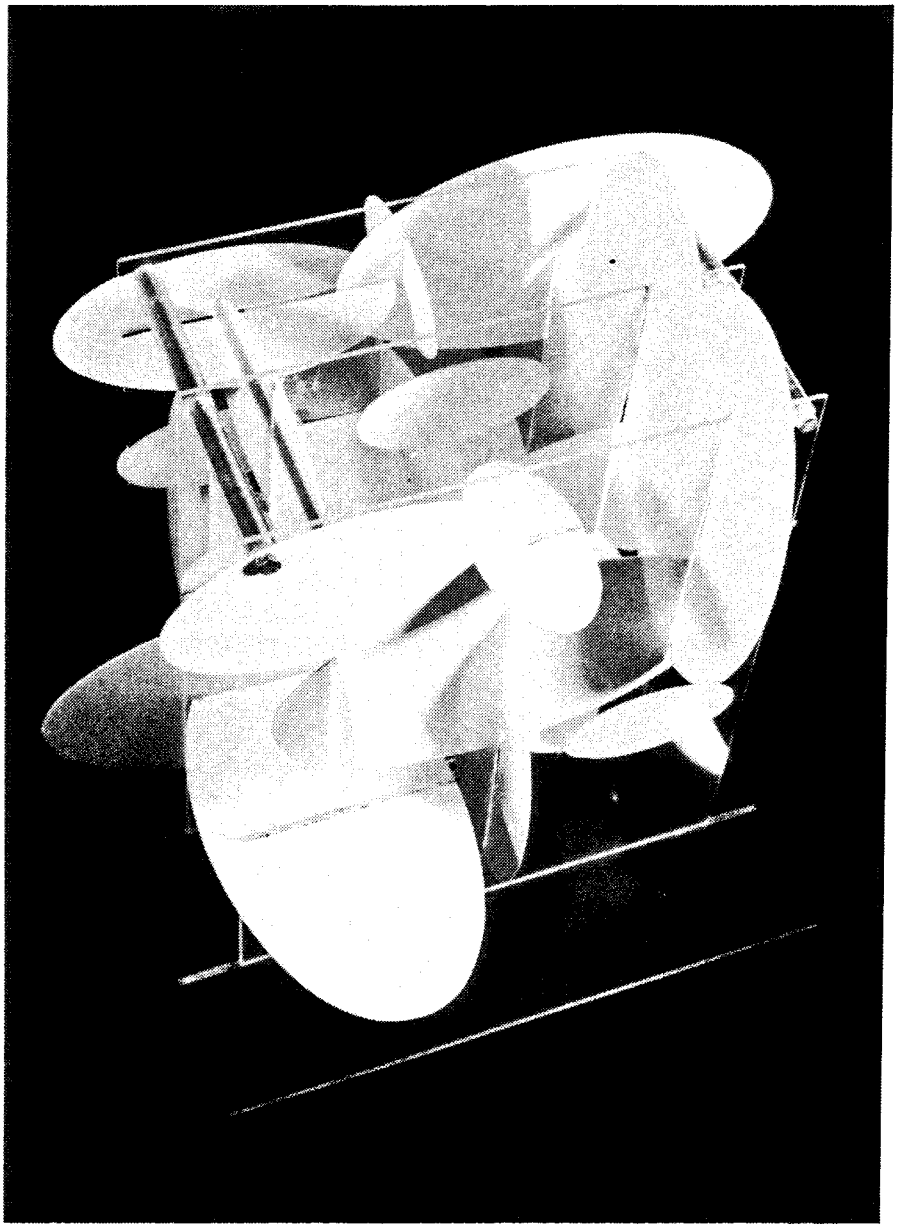

Fig 15. Physical fracture model. The ellipsoidal fractures appear as white discs

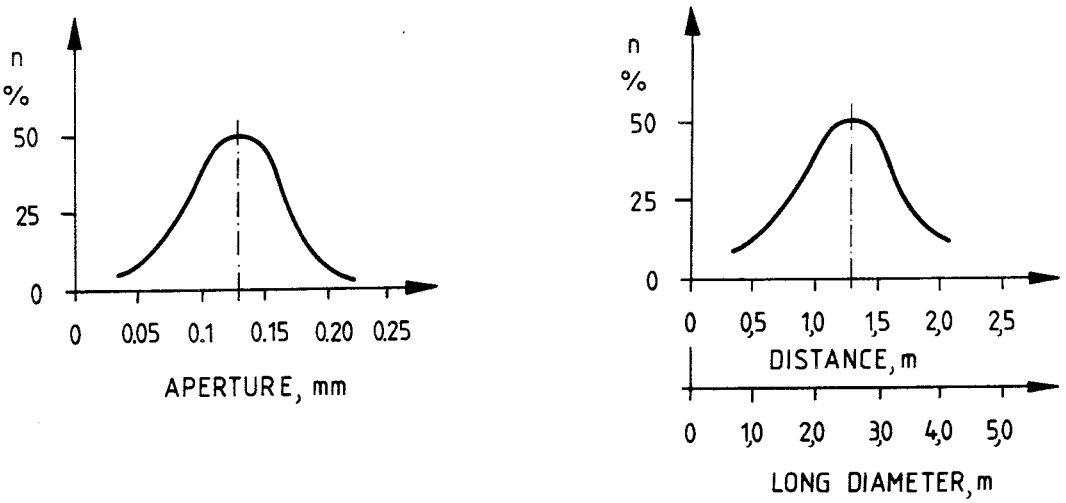

Fig 16. Example of distribution of aperture, maximum diameter and fracture spacing

These fracture sets yield a rock porosity of common magnitude, i.e. about 0.4 % and a continuous fracture network, which in turn results in flow paths across the rock body in all three dimensions. The maximum compression of the 27 m^3 block model leading to closure of all fractures would correspond roughly to 0.6 mm, which represents a uniaxial strain of about 2×10^{-4}. With the rather common bulk E-modulus 10^5 MPa, such closure would require a uniaxial stress of about 20 MPa assuming that Poisson's ratio is very low. A 3 m long borehole with a diameter of 0.76 m traversing the block would yield coherent cores with a length varying from a few decimeters to about 2 m, which was also the actual size interval for the Buffer Mass Test heater holes which had exactly this size.

It is noticed that the open fractures form a large part of certain critical sections. Thus, the model correctly suggests that there is no single unique relationship between rock shear strength and element size and that the strength is a function not only of the stress situation but also of the orientation and location of potential shear planes.

As to the hydraulic properties and groutability of the fractures, the flow rate naturally depends on the number of clear paths offered by interconnecting passages. Although the dimensions and positions of their intersections are determinants of the flow and need to be defined when applying the model, its overall behavior can be illustrated by estimating the uniaxial flow across an arbitrary section of the 27 m^3 rock volume. On an average, it would represent flow through 4 to 7 fractures, the effective flow section roughly corresponding to that of the a/c plane of the intermediate ellipsoid of Table 3, where a denotes the maximum diameter and c the minimum. Applying Poiseuille's law we find the flow at the hydraulic gradient i to be 10^{-5}x(i) to 10^{-7}x(i) m^3/s, which corresponds to an average flow rate of about 10^{-6}x(i) to 10^{-8}x(i) m/s over the 9 m^2 cross section. Expressed in terms of average hydraulic conductivity of the rock this would correspond to 10^{-6} m/s to 10^{-8} m/s. The actual tor-tuosity of the flow paths brings down the conductivity by one or two orders of magnitude, which yields values that are in reasonable agreement with actually recorded flows through rock with a few major flaws. Altering the boundary stresses in one of the directions perpendicular to the flow from 10 to 30 MPa yields a theoretical reduction in flow by about 20 %, while a drop from 10 to 1 MPa results in an increase by about 100 % assuming a reasonable lin strain/log stress relationship between aperture change and normal stress (17). Although this example only approximates the stress-induced alteration of the interconnectivity of fractures that the model actually allows for, and which dominates the effect of stress changes, we see that the mechanical response is in general agreement with the behavior of rock that was outlined in the preceding chapter.

2.5.3 Influence of blasting

Charge detonation yields a very high gas overpressure of short duration which breaks up rock by brittle fracture. Cracks are formed that extend radially from charged boreholes and prismatic blocks are loosened due to the tensile stresses that are set up by the reflection of the shock wave in the presence of a free surface like in bench blasting.

The extension of radial fractures generated by detonation can be roughly estimated by assuming that the crack volume is equal to the reduction in rock volume due to its compression in the crack generation phase (20). Such calculations lead to theoretical penetration depths in homogeneous rock of only a few decimeters if the amount of explosives is kept at minimum in careful blasting of tunnels. This appears to be in agreement with the experience from a number of practical tunnel blasting operations, according to which fractures are formed or widened to within a distance in meters that is equal to the charge in kilograms per meter borehole length (21). Smooth blasting technique is accordingly said to limitate the radial extension of the disturbed zone to about 0.5 m (Fig 17).

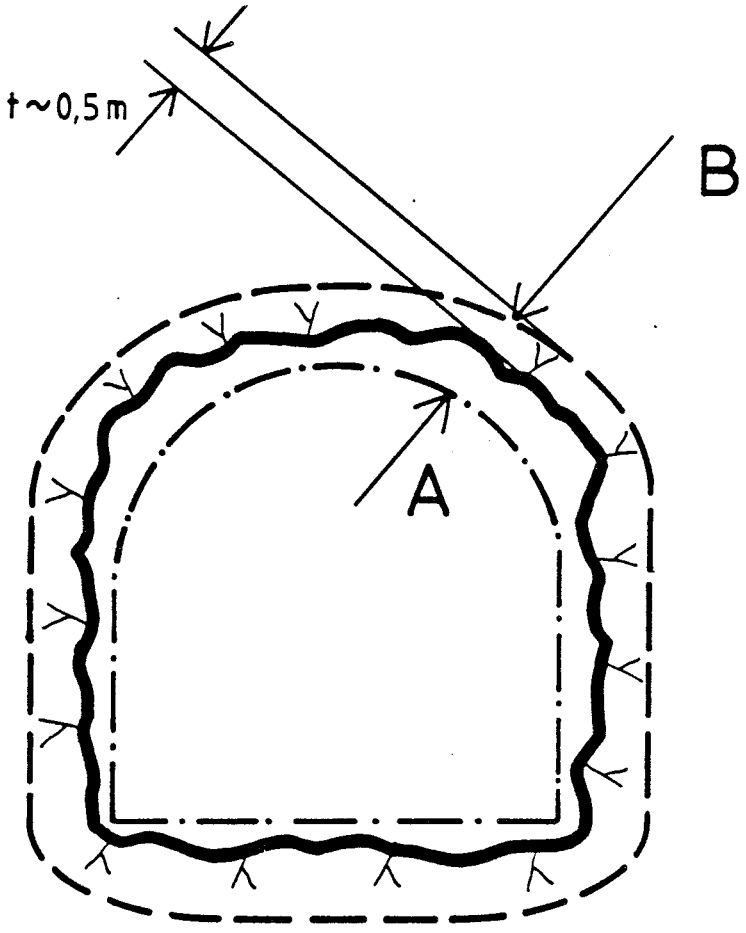

Fig 17. Generalized picture of the disturbed zone (B) by blasting. The A contour represents the theoretical propile

In principle, blasting can produce fractures in three ways (cf Fig 18):

1 Expansion and propagation of existing, natural fractures that are intersected by or located close to the charged hole

2 Creation of one or a few planar, radially oriented fractures

3 Creation of a large number of fractures, "crushed zone"

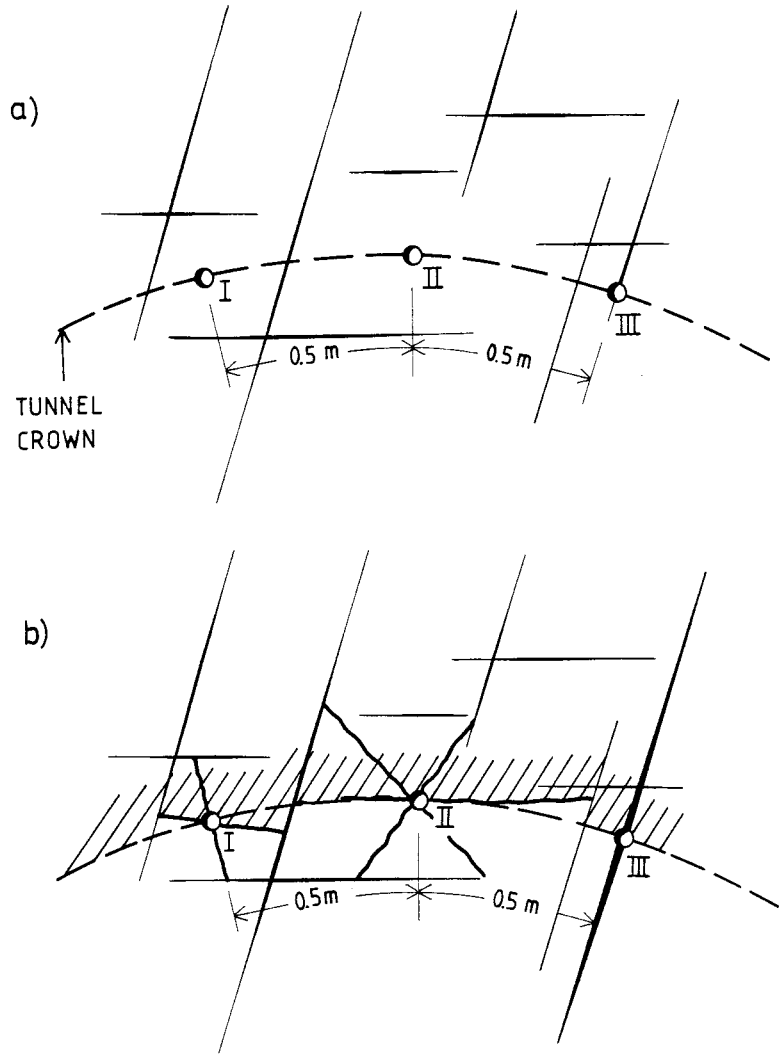

Fig 18. Hypothetic fracture pattern and influence of blasting. Thick lines represent generated fractures. a) Natural condition, b) After detonation

Assuming an instant gas pressure at detonation of 100 MPa and a compression modulus of the rock of K=E/3 (1-2 ν), which yields K $\sim 5 \times 10^4$ MPa for reasonable values of the E-modulus and Poisson's ratio, it is clear that the first case, represented by the fracture traversed by hole no III in Fig 18, will be instantly widened by at least 1 mm, part of the expansion being permanent. The most important effect would be that the fracture will propagate in the axial direction of the tunnel thereby creating an improved connectivity of hydraulically active fractures in this direction.

If radial fractures are generated as assumed in the case of holes I and II they would obtain an aperture in the range of a few tens to a few hundred microns, keeping in mind though, that the rock pressure conditions will usually cause partial closure and contacts through asperities. Despite this, there will be a largely increased connectivity of the fractured peripheral rock zone, which therefore logically will have a relatively high hydraulic conductivity in radial as well as in the axial direction of the tunnel.

The elastic rebound towards the center of the tunnel that follows after the detonation phase is associated with a mass movement in the same direction, which yields a reduced continuity of the rock matrix in the peripheral rock zone around the tunnel. Although the block elements still transfer significant stresses at points of contact, which also helps to keep the blocks in position through arching effects, there must be a substantial drop in tangential stress close to the tunnel periphery. This effect should be particularly obvious in the walls of tunnels located in rock with high horizontal primary stresses.

2.6 Conclusions and comments

The main pattern of water-bearing passages in many types of rock is that of regular sets of fractures with rather small, stochastically distributed trace lengths and apertures. Their sensitivity to stress changes would imply expansion of critically oriented fractures in anisotropic stress fields, such as that illustrated in Fig 17. This is expected to produce an increased connectivity of hydraulically active fractures in the axial direction of most tunnels, shafts, and

drilled canister deposition holes, and therefore by an increased hydraulic conductivity in the same direction. This shows that sealing is required in order to restore the original hydraulic conductivity of the near-field of canister holes. The fractures which are prone to stress-induced widening and therefore most suitable for sealing, are easily identified by optical inspection and simple inflow tests. Rock stress measurements should be very helpful.

Fracture generation and propagation, particularly in combination with blasting, is likely to produce large changes in stress transfer between adjacent rock elements. This effect is expected to yield a poorly defined stress condition at the periphery of tunnels and shafts due to the mass movement towards the opening. Thus, the slight angular displacement of a block assembly that is associated with such movements in anisotropic stress fields will produce very high stresses in local contacts and complete relaxation close to these spots (Fig 19). This induces creep with successive redistribution of stresses tending to yield an overall increase in hydraulic conductivity and a drop in average "tangential stress" in the peripheral, shallow rock zone around blasted tunnels and shafts.

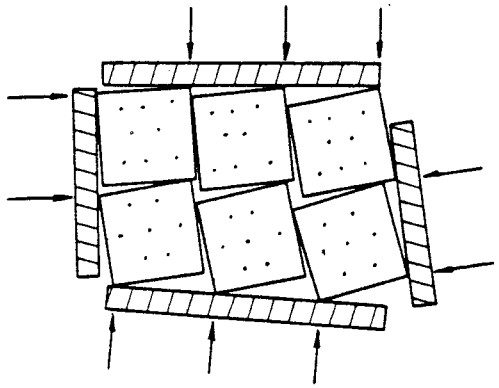

Fig 19. Schematic picture of shear displacement in dilating block assembly

3 NATURAL FRACTURE FILLING SUBSTANCES IN CRYSTALLINE ROCK

3.1 Introduction

The search for suitable techniques to seal fractures logically starts with a survey of the modes of formation of the most common natural fracture-filling minerals with particular respect to the possibility of reproducing nature's own genetic mechanisms. The aim is to find out whether it is feasible at all to seal fractures at reasonable cost by simulating processes through which dissolution/precipitation, or even injection of fine-grained sealing substances can take place. The matter is difficult and complex since many minerals are final products of coupled processes which are governed by thermodynamics and several of them cannot be produced artificially. Keeping in mind the rather small rock volumes that need to be treated by chemical sealing or grouting it would still be possible to manipulate fractured rock so that suitable crystalline, glassy or colloidal substances can be formed under controlled conditions in hydraulically active joints or fractures. It should be added here that the entire problem of mineral formation is actually also that of mineral stability, which is a research field of profound interest to waste repository technology but which is beyond the scope of this report.

The present report summarizes a number of general aspects of mineral formation as well as some ideas of possible practical means of rock sealing by filling fractures with suitable minerals. Particular emphasis is put to the properties of clayey fracture fillings.

3.2 Mineral genesis in general

3.2.1 Classification

Several systems for classification of mineral formation have been suggested in the literature and various versions have been used for different purposes. A relatively recent scheme that has turned out to be very useful in genetic modelling was introduced by Lindgren (22) in 1933 and has since been applied world-wide with only minor changes. Its major features are the following:

Main mode of formation		Temperature:
1	Minerals formed by mechanical processes	Independent
2	Minerals formed by chemical processes	
2.1	In surface waters	
2.1.1	By reaction	0-70°C
2.1.2	Evaporation	0-70°C
2.2	In bodies of rock	
2.2.1	Concentrations of substances contained within rocks	
	a) By weathering	0-100°C
	b) By groundwater	0-100°C
	c) By metamorphism	0-400°C
2.2.2	By introduced substances	
2.2.2.1	Without igneous activity	0-100°C
2.2.2.2	Related to igneous activity	
	a) By ascending solutions (hydrothermal)	
	By epithermal solutions	50-200°C
	By mesothermal solutions	200-300°C
	By hypothermal solutions	300-500°C
	b) By direct igneous emanations	
	By pyrometasomatic deposits	500-800°C
	By sublimates	100-600°C
3	Minerals formed by differentiation of magmas	
3.1	Magmatic primary deposits	700-1500°C
3.2	Pegmatites	575°C

The following chapters summarize major literature-derived information of important groups of endogenic mineral deposits. High temperature and pressure products are treated first.

3.2.2 Igneous, magmatic or primary processes

Minerals formed by magma solidification can be accumulated in several ways through magmatic differentiation and recrystallization.

Pegmatites, ore deposits, vapor, gases and mineralizing solutions are some of the magmatic products that were created by differentiation. They usually crystallized near the location where the magma stagnated but they also appeared at larger distances, as in the case of hydrothermal solutions percolating through solid primary rock. The solutions were oversatured or reacted with minerals exposed in flow passages, thereby forming precipitates such as fracture fillings and dikes.

All magmas have undergone some kind of differentiation before they crystallized. On cooling, this process usually first yielded crystallization of the least soluble minerals such as magnetite and other low-silica minerals. The remaining liquid solution became depleted of these constituents and with decreasing temperature silica-containing minerals like feldspars were then successively formed. At the end of the crystallization phase the solution became rich in silica by which the generated rocks became typically granitic.

The resulting sequence of mineral formation is usually expressed in terms of Bowens' reaction series for crystallization of silicate-rich melts (Fig 20). The latest phase of precipitation yielded minerals like micas and quartz with simultaneous differentiation of hot water and volatiles, the ultimate product being pegmatite, which is commonly found in most igneous rocks. After crystallization of the pegmatites hot water and vapor were the only remaining constituents of the original magma.

A more detailed picture of the temperature-related processes, which also gives a rough indication of the character of the precipitated matter and of the possibility of producing it artificially, is given in the subsequent text.

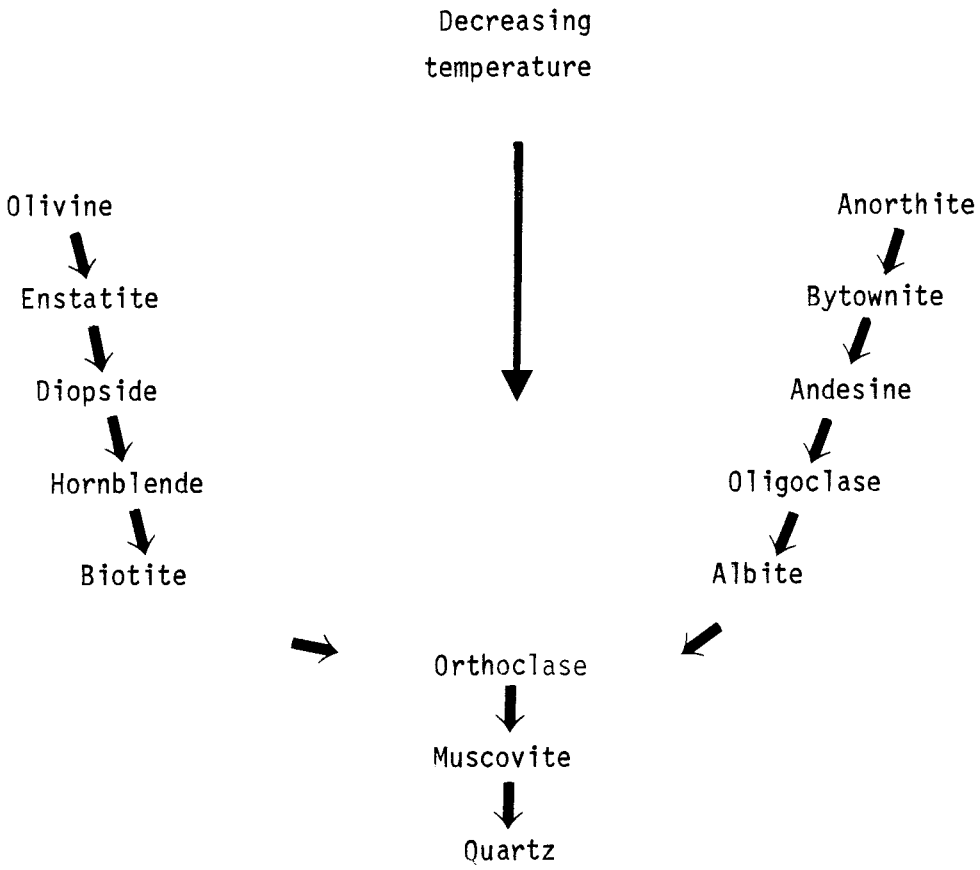

Fig 20. Bowens' reaction series for crystallization of silicate-rich melts

3.2.3 Orthomagmatic processes

Precipitates from orthomagmatic processes represent the major constituents of most igneous rocks, such as granite, gabbro and dolorite, which all crystallized from magma at temperatures between approximately 500 and 1500^{o}C.

The first phase of the orthomagmatic crystallization produced anhydrous silicious minerals followed by hydroxyl-bearing silicates. The exact temperature at which these processes took place depended on the volatiles present.

In the initial stages of magma cooling the first-formed crystals floated freely in the solution. As the crystals multiplied, they took up more space in the solution and the new crystals formed were interstitial among the earlier formed euhedral crystals. For purely geo-

metrical reasons the crystal growth left small pores in the crystal matrix and in these minute openings a relatively electrolyte-rich solution remained. Its concentration was not sufficient to yield precipitation even at low temperatures but it probably contributed to the interstitial "salt water" that is now commonly found at large depths in crystalline bedrock.

When pyroxene-producing components were sufficiently abundant to constitute more than 42 % of the melt, this mineral formed first. With increasing concentration of the required components the crystallization started at higher temperature (cf. Fig 21).

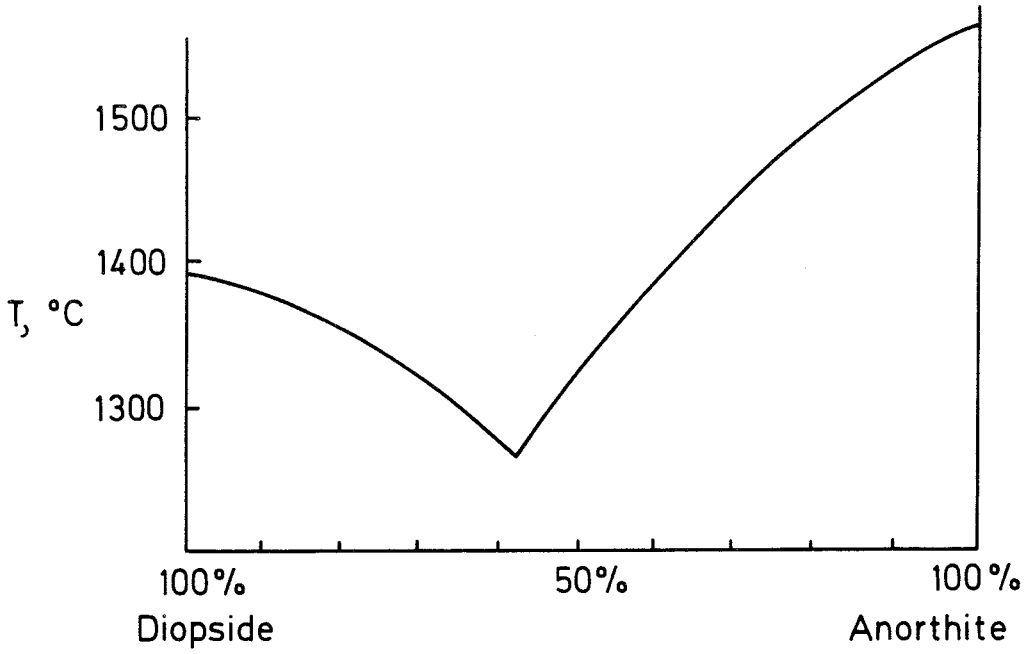

Fig 21. Binary crystallization diagram: Diopside-anorthite

When plagioclase-producing components were present in amounts that would form more than 58 % of the melt, this mineral appeared prior to pyroxene. Those minerals which were present in excess were gradually abstracted by crystallization and the residual melt therefore became progressively richer in the other components. Since the number of possible precipitation species was usually very large, it is clear that local variations in melt composition and slight temperature differences produced substantial variations in the rock mineral composition. This is amply demonstrated by ocular inspection of any exposed outcrop of crystalline rock.

An important structure-forming process was the contraction of the first-formed minerals caused by the successive drop in temperature. This yielded incomplete grain boundaries and elongated pores of various size especially where different mineral species met. It is reasonable to believe that locally available residual solutions were sucked into such discontinuities.

3.2.4 Pegmatitic - pneumatolytic processes

In the course of the crystallization of magma components, the volatiles became concentrated in the residual solution. If the first-formed solid rock contained large fractures and openings, the viscous solution was squeezed into these discontinuities and solidified as pegmatite veins. The composition of pegmatite depends largely on the nature of the parent magma and the differentiation processes. Three major types can be identified in this respect:

a) Veins without sulphides
b) Silicate-sulphide veins
c) Carbonate veins

The first type includes quartzofeldspathic veins and the more uncommon quartz and epidote veins. The first-mentioned type is representative of moderately high pressure and temperature environment and shows the largest variation in mineralogy, the main minerals being quartz, plagioclase and potassium feldspar. This type also contains substantial amounts of mica and compounds like epidote, spodumene, tourmaline and beryll.

Silicate-sulphide veins characteristically contain many important ore-minerals and it seems as if sulphides of magmatic origin have been effective agents in interacting with parent rock to form metals like iron, copper, lead, zink and silver. They appear to have been formed in connection with the common vein-filling minerals quartz, feldspars and different types of silicates.

Carbonate veins are often of low-temperature origin and they are usually found in connection with large scale structures such as dolerite intrusion into carbonate-rich rocks where calcite precipitation occurred in the metasomatic region of the intrusion.

The gas components of the magmatic residuals consisting of water/vapor with elements like F, B and S, were not chemically active but combined to form pneumatolytic mineral deposits. The most common representatives of the pneumatolytic volatiles are fluorine, hydrofluoric acid and boron fluorides. Pneumatolytic processes are often considered as separate stages.

1 **Tourmalinization**: Formation of tourmaline when boron-rich volatiles react with pre-existing minerals

2 **Greisening**: Results in mica-rich deposits formed by influence of fluorine-rich vapors on granites

3 **Ore mineralization**: Fluorides transported pneumatolytically and reacting with water yield oxides

Many of these mineral formations cannot be unanimously interpreted as resulting from pneumatolytic processes. In some cases at least they may actually result from hydrothermal activities, usually by percolation of super-heated vapor containing boron or fluorine through fractures. The temperature was at least $550^{o}C$.

Another pneumatolytic process that may also be of potential practical use in the present context is that which results from volatiles reacting with granitic rocks yielding kaolinite ($Al_4Si_4O_{10}(OH)_8$). One such reaction is that of water with CO_2 converting feldspar as shown by Eq. (1).

$$4KAlSi_3O_8 + 2CO_2 + 4H_2O \rightarrow 2K_2CO_3 + Al_4Si_4O_{10}(OH)_8 + 8SiO_2 \quad (1)$$

This process, which is known to take place in the course of weathering of granite and gneiss under humid and warm conditions (laterite formation), is an example of a possible means of producing artificial fracture fillings. As will be shown later, however, the physical properties of this clay product are not altogether attractive.

3.2.5 Pyrometasomatic processes

Metasomatism refers to alterations caused by hot (500-800^{o}) gaseous solutions that remained in the magma after the primary solidification. Contact metamorphism is closely related to metasomatism but does not include the deposition of minerals of magmatic origin. Possible confusion between the two concepts can be avoided by applying Lindgren's scheme according to which the name pyrometasomatic deposition is given to metasomatic changes occurring under conditions of high temperature and pressure at or near contacts with very hot igneous intrusions.

Pyrometasomatic processes are usually manifested by isomorphous replacement of minerals or groups of minerals. Typical deposits of this kind are those formed at the contact of granitic intrusives and limestone. They include many important ore-minerals like magnetite (Fe_3O_4), hematite (Fe_2O_3), pyrite (FeS_2), wolfram (Fe, Mn)WO_4), galena (PbS) etc. Common gangue minerals include iron-rich silicates such as epidote, diopside, plagioclase, fluorspar and micas. The deposits are often irregularly spaced and shaped, displaying the complex paths along which the components moved in the primary rock.

3.2.6 Metamorphic processes

Metamorphic changes are always associated with the restoration of chemical equilibrium in rocks subjected to altered conditions. The physical factors controlling the environment of metamorphism are the temperature, the water pressure and the effective stress conditions (cf. Fig 22). Temperature is perhaps the most important factor and rock mineral alteration depending solely on heat changes is known as thermal metamorphism. It is often found that mineral assemblages show

a zonal arrangement which indicates that a thermal gradient existed at the time when metamorphism occurred (progressive metamorphism). The corresponding process taking place at a successively reduced temperature is known as retrogressive metamorphism.

High pressure changes the physical properties of most rocks. Pressure does also favor the development of minerals with a high density.

High anisotropic stress associated with folding, faulting and similar structural events results in mechanical degradation of the rock. At higher temperatures or in the case of high pressure of active pore fluids, high anisotropic stresses may speed up crystal growth by providing new reactive surfaces.

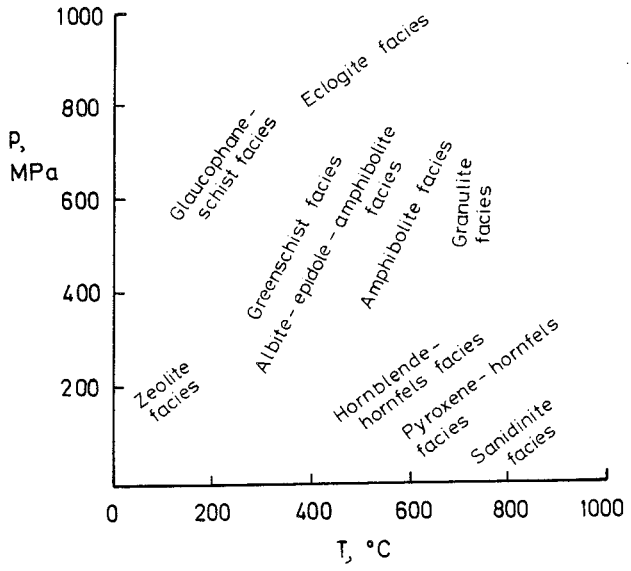

Fig 22. Pressure-temperature diagram showing possible relationships of the metamorphic facies (23)

Four types of geological metamorphism can be distinguished:

1 **Contact - metamorphism:** Caused by the heat of magmatic intrusions

2 **Autometamorphism:** Changes occuring within an igneous body during cooling

3 **Dislocation - metamorphism:** Changes caused mainly by high stresses and moderate temperature

4 **Regional metamorphism:** Alteration of large rock masses by the influence of heat and pressure (e.g. orogenic belts)

3.2.7 Hydrothermal processes

The ultimate magmatic differentiation results in residual, "hydrothermal" solutions which are the source of most endogenic minerals.

The composition of a hydrothermally formed mineral assembly depends on the temperature at the time of formation and on the distance from the original magma.

Three different groups of hydrothermal products can be specified with respect to temperature, pressure and geological conditions.

These are:

1 Hypothermal (500-300°)
2 Mesothermal (300-200°)
3 Epithermal (50-200°)

Hydrothermal solutions may turn into low-concentration water flow through precipitation in cavities and open fractures in the course of their percolation through the primary rock. They may also experience large changes in composition if replacement reactions with the primary rock takes place. The first-mentioned process is likely at low temperature and low pressures (epithermal), while the second is most typical for hydrothermal reactions.

Formation of hydrothermal products requires:

a) mineralizing solution capable of transporting the mineral components
b) openings available in the primary rock through which the solution percolates
c) sites available for mineral deposition
d) chemical reactions initiating and controlling deposition
e) sufficient concentration of mineralizing components

The mineralizing power of percolating solutions is determined by the temperature, since there is a limited interval in which the various minerals become precipitated. Certain species or rock matrix features are taken as indication of the temperature conditions that prevailed at their formation, their function being that of geothermometers. One group of geothermometers are liquid inclusions trapped in cavities of crystals. Assuming that the liquid at the crystallization event completely filled the respective cavity, the temperature at which the liquid can be brought to fill the cavity again on heating is indicative of the conditions under which this particular crystal was formed.

Other geothermometers are melting points, inversion points (temperatures at which minerals change symmetry), exsolution, recrystallization and the temperature at which there is a change in physical properties.

List of some geologic thermometers:

1391°C	Diopside	Melting point
1120°C	Galena	Melting point
995 - 1140°C	Orthorhombic pyroxene to monoclinic pyroxene	Inversion point
800°C	Magnetite-spinel	Exsolution
675°C	Mematite-ilmenite	Exsolution
573°C	Low quartz to high quartz	Inversion point
530°C	Brucite	Stable up to
450°C	Marcasite to pyrite	Inversion point
300°C	Smoky quartz	Color disappears

175°C	Fluorite	Color disappears
100°C	Zeolites	Max limit of formation

The formation of hydrothermal mineral products is governed not only by the chemical composition of the solution and by pressure and temperature, but it is also determined by the constitution of the rock that is exposed in the flow paths of the solution. Strongly reactive rock, such as limestone that is not in equilibrium with the solution, produces a rapid chemical change at the contact by which precipitation is initiated. Cooling is usually caused when the hot solution enters the primary rock which also contributes to the precipitation. Naturally, this factor becomes increasingly important at larger distances from the point of magma outflow.

The character of the passages through which the solutions flew determined the flow rate, wide fractures with smooth surfaces naturally offering the least resistance to flow. Also, pressure changes influenced the formation of hydrothermal minerals. Thus, a decrease in pressure, promoting precipitation, was usually associated with upward transport of hydrothermal solutions.

The three subdivisions of hydrothermal precipitation (hypothermal, mesothermal and epithermal) are mainly distinguished by their formation temperature (50-500°C).

Hypothermal or high temperature deposits are generally fillings of cavities and fractures by calcite, baryte, fluorspar, pyrite, blende or manganese carbonates. They often show a zonal succession because of their different solubilities. Hypothermal products may also consist of minerals formed by replacement. Quartz, pyroxene, magnetite, galena and garnet are common minerals formed by such processes.

Epithermal deposits result from precipitation of easily soluble minerals, such as feldspars, zeolites and calcite.

Before considering in detail the possibility of repeating nature's own fracture sealing mechanisms, we will examine what minerals that actually occur as filling substances, bearing in mind that those

which were formed at low temperature are also the ones which should be most easily created artificially.

3.3 Common fissure-filling minerals

Experience shows that crystalline rock usually has a high frequency of fractures which contain precipitated matter originating from the various processes that have been summarized in the preceding text. Very often the filling is not complete and also apparently healed fractures still serve as slightly pervious passages. This is demonstrated at TV-inspection of boreholes which have not been affected by blasting, the observed inflow of water from such fractures being due to incomplete precipitation of mineral matter or to reopening of the fractures due to altered stress conditions. This observation has two important implications, firstly that it is hardly possible to fill fractures completely by chemical precipitation, at least not when the filling substance undergoes cooling in the solidification process, and secondly that fillings consisting of rigid and brittle substances yield less effective sealing than a substance which is flexible and expandable. This points to the use of clays, which deserve to be examined not only as possible reaction products of chemical treatment but also as injection substances. This matter will be treated in considerable detail in a later chapter.

3.3.1 Fracture fillings formed by chemical precipitation

3.3.1.1 **Calcite** ($CaCO_3$)

There are three polymorphs of calcium carbonate, namely calcite, vaterite and aragonite (cf. Fig 23).

Calcite has been formed in various environments. When this carbonate species has a magmatic origin its was mainly precipitated as fracture or vein fillings or as carbonatites from carbonate-rich extrusive magmas. Calcite has been found to be the most common filling material of crystalline rock in many areas, such as Gideå, Finnsjön and Studsvik (24). Usually it was formed from epithermal solutions at a very moderate temperature.

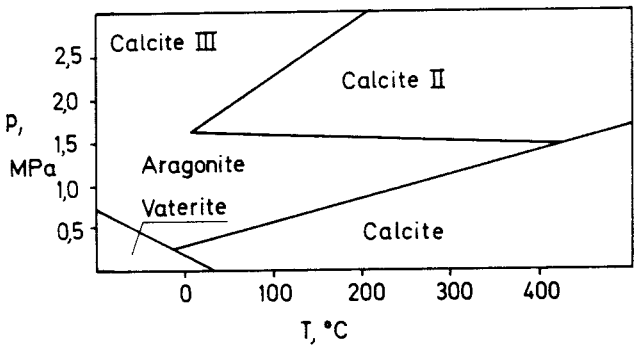

Fig 23. Stability of calcium carbonate

3.3.1.2 **Fluorite** (CaF_2)

Fluorite has also been formed in different environments and is frequently occurring in veins and ores as gangue mineral, often associated with quartz (SiO_2), calcite ($CaCO_3$), celestine ($SrSO_4$), dolomite $CaMg(CO_3)_2$, galena (Pbs), cassiterite (SnO_2), siderite ($FeCO_3$) and chalcopyrite ($CuFeS_2$). Examples of precipitations from hydrothermal solutions (25) show that fluorite usually has been formed in the epithermal region (200-300°C) in the cooling stage of such solutions. It should be mentioned that fluorite can be formed also from solutions that are not saturated with fluorine (cf. Fig 24) but pH needs to be low.

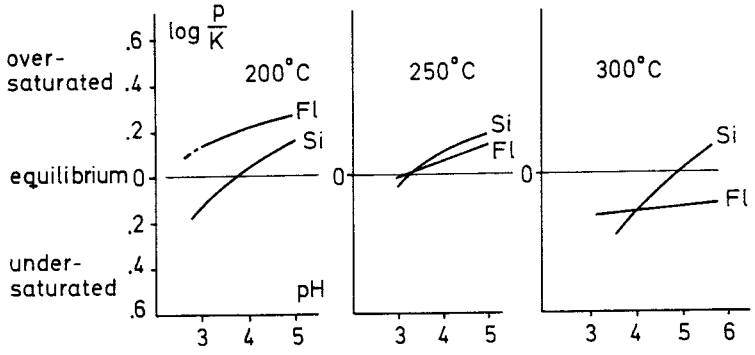

Fig 24. Saturation evolution of minerals at different temperatures (after Deloule, 1982)

3.3.1.3 Zeolites

All members of the zeolite family conform to the composition of hydrated aluminosilicates consisting of a tetrahedral framework of oxygen atoms surrounding either a Si or Al atom in their three-dimensional framework structure. The composition of the zeolites is analogous to that of feldspars, CaAl being replaceable by NaSi. An additional feature of the zeolite group is the presence of water molecules loosely bound within the framework. This yields an idealized formula for the zeolite group: $(Na_2, K_2, Ca, Ba, Sr, Mg)\ (Al, Si)O_{2n} \cdot XH_2O$. In general they are formed from hydration of feldspars and similar minerals at elevated temperature and they occur as fillings in steamholes, cavities and fractures in the rock. Usually they are associated with epithermal solutions and secondary mineralization in sedimentary rocks (26). Common zeolites in Swedish bedrock are the following:

a) **Analcime** ($NaAlSi_2O_6 \cdot H_2O$), typically occurs in cavities in basic rocks

b) **Chabazite** ($/Ca,Na_2/Al_2Si_4O_{12} \cdot 6H_2O$), common mineral filling in cavities in basic rocks

c) **Laumontite** ($CaAl_2Si_4O_{12} \cdot 4H_2O$), results from low-grade metamorphism of sedimentary rocks

3.3.1.4 Feldspars

There are three main representatives of the feldspar family: (orthoclase ($KAlSi_3O_8$), albite ($NaAlSi_3O_8$) and anorthite ($CaAl_2Si_2O_8$).

Between albite and anorthite there exists a series of solid solution mixtures produced by the substitution of NaSi by CaAl. The span between orthoclase and albite gives the intermediate species soda-orthoclase ($K,Na\ AlSi_3O_8$) and anorthoclase ($Na,K\ AlSi_3O_8$). Several different forms of feldspars appear, their constitution mainly being related to the temperature at formation. Feldspars are main rockforming minerals but do also dominate in many pegmatites and low-temperature hydrothermal deposits.

3.3.1.5 **Quartz** (SiO_2)

In addition to quartz two other versions with the composition SiO_2 occur, namely tridymite and cristobalite. They are chemically stable in different temperature ranges: quartz below 870°C, tridymite in the interval 870-1470°C, and cristobalite in the high-temperature region 1470-1713° C. This last temperature is the melting point of silica. Pure quartz can exist in two modifications; high-temperature or ß-quartz forms between 570-870°C, while at lower temperature it converts to low-temperature or L-quartz. The quartz mineral occurs in several different environments. It is a main constituent of acid rocks such as gneiss and granite but also a very common vein-filling mineral precipitated from hydrothermal solutions.

3.3.1.6 Micas

a) Muscovite ($KAl_2(AlSi_3O_{10})_2$) is a common constituent of acid plutonic rocks and pegmatites. Micas also occur as secondary minerals formed from feldspar, and are then called sericite. Muscovite, which is stable to at least 500°C like the rest of the micas, is generally considered to originate from magmatic solutions also when it is a constituent of pegmatite.

b) Biotite ($K(Mg,Fe)_3AlSi_3O_{10}(OH,F)_2$)
Biotite occurs in almost all types of igneous and metamorphic rock but is most commonly found in acid igneous rocks, schists and gneisses.

c) Phlogopite ($K\,Mg_3AlSi_3O_{10}(OH,F)_2$)
Phlogopite occurs mainly in connection with metamorphic limestone or in Mg-rich igneous rocks and pegmatites.

3.3.1.7 **Prehnite** ($Ca_2Al_2(Si_3O_{10})(OH)_2$)

Prehnite is precipitated from hypothermal solutions, usually together with calcite and zeolites. It is a common fracture filling in the Finnsjön and Studsvik areas (27, 28).

3.3.1.8 **Gypsum** ($CaSO_4H_2O$)

Gypsum usually occurs in evaporites, where it is associated with halite (NaCl), calcite ($CaCO_3$), aragonite ($CaSO_4$), dolomite ($CaMg(CO_3)_2$) sulphur (S) and quartz (SiO_2). It is also a frequent fissure-, fracture- and joint-filling mineral in Swedish crystalline rock and sediments and it is actually the most common fracture filling mineral at larger depths (29) in certain crystalline rock masses as observed in boreholes in the Karlshamn area (27). Here, it is probable that acid solutions dissolved calcite in shallow regions and produced formation of gypsum at greater depths (30). Weathering of sulphides, such as pyrite (FeS_2), gives rise to sulphuric-acid rich solutions which are capable of extracting Ca from carbonate-rich rocks and from gypsum. Many of the fractures in Scanian alun shale have been filled with gypsum formed through this process.

3.3.1.9 **Brucite** ($Mg(OH)_2$)

Brucite is most commonly found in contact-metamorphosed dolomitic limestones and in serpentinites. The latter is formed as an alteration product of olivines and pyroxenes by the process of serpentinisation (Eq. 2).

$$4\ \underset{\text{Olivine}}{Mg_2SiO_4} + 4\ H_2O + 2CO_2 \longrightarrow \underset{\text{Serpentine}}{Mg_6Si_4O_{10}(OH)_8} + 2\ \underset{\text{Magnesite}}{MgCO_3} \qquad (2)$$

Brucite, which is stable at temperatures below 500-700°C, is also common in retrograded dolomitic limestones where it is formed together with calcite, periclase (MgO) and carbon dioxide.

3.3.2 Fracture fillings formed by mechanical processes

3.3.2.1 **Fissures filled with material derived from overlying sediments**

Mineral substances originating from overlying clastic sediments or sedimentary rock are not uncommonly found in fractures, veins and fissures of granitic rocks. These fillings were predominantly formed in steeply oriented openings in which liquefied soil material from

near-sited sediments or sedimentary/rocks was accumulated. Such fillings are known from Åland, southern Finland (33, 34, 35) and possibly also in the Forsmark area. Very often such fillings are associated with mineralization of galena, pyrite or calcite, originating from subsequent metamorphic processes.

3.3.2.2 Mylonites

Intense stress and large strain of a rock mass disrupts the entire fabric and produces micro-brecciation or mylonite composed of microscopic, angular grains linked together by colloidal particles. The finely ground material of a mylonite is quite mobile and appears to have been injected into fractures by which veins were formed. Recrystallization is usually not abundant but granules of quartz and calcite may be precipitated from the pore fluid together with chlorite and sericite.

3.3.3 Secondary minerals

Clay minerals are common secondary products, usually not very well crystallized, which were formed from rock silicate minerals, mainly feldspar, micas, amphibole and pyroxene, through attack by hydrothermal solutions flowing through fracture-rich zones. They are discussed in detail later in the text.

3.4 Synthetic production of fracture fillings

3.4.1 General

In nature, the formation and deposition of minerals in open fractures, results from a series of processes. Generally, it has the form of precipitation from chemically active solutions originating from deeper magmatic regions, usually in the postorogenic phases when intrusions and volcanism took place. Fractures were initiated and percolated by solutions and vapors, which resulted from the differentiation processes that were associated with the crystallization of magma. As shown in the preceding text, the precipitation followed a certain pattern depending on the temperature and pressure, and on the distance from where the solutions began to migrate.

It was also demonstrated that the major part of the fracture filling minerals were formed in the high-temperature range from slightly acid solutions, and it is immediately realized that even if such conditions could be obtained in a fracture-sealing operation, an induced high temperature would probably create many new fractures and much damage to the rock. Artificial crystallization of low temperature minerals, which represent the final stages of hydrothermal recipitation, is much more promising since they have actually been synthesized in laboratories. Such candidate minerals are calcite, fluorite and zeolites, which are also common fracture filling minerals in Swedish crystalline rock (31).

3.4.2 Artificially produced chemical precipitates

Calcite fillings can be created in two different ways, firstly through introducing calcite melts in fractures and secondly to inject supersaturated calcium carbonate solution in pre-cooled rock. The first-mentioned technique is not realistic because of the very high required temperature (1340°C) and pressure (100 MPa), while the second may be feasible. As to the feasibility of sealing rock by use of carbonates it must be remembered that they are soluble in acid solutions and therefore not stable in a long time perspective if pH drops below 7.

Fluorite can be precipitated from fluorite melt, which unfortunately requires unrealistic temperature and pressure. Instead, a quite different approach may be applicable and that is to introduce hydrofluoric acid, which is expected to react with silica minerals exposed in the fractures, by which not only fluorite but also various F-bearing crystalline and amorphous silica compounds are produced.

Zeolites can be formed through the so-called hydrogel method. This involves percolation of aqueous phases of sodium hydroxide and silicates which form a gel from which zeolites precipitate at temperatures around 200°C. The involved chemistry is as follows:

$$\mathrm{Na(OH)(aq)+NaAl(OH)_4(aq)+Na_2SiO_3(aq)} \xrightarrow{t_1} \mathrm{(Na_a(AlO_2)_6(SiO_2)_2 \cdot NaOH \cdot H_2O)\ (GEL)} \xrightarrow{t_2} \mathrm{Na_x(AlO_2)_x(SiO_2)_4 \cdot 4H_2O} + \text{solution} \qquad (3)$$

Several of the zeolites have been successfully synthetized at temperatures between 80°C and 150°C.

Among the large group of minerals which do not result from hydrothermal solutions and which may be of potential interest, gypsum, iron oxides and hydroxides and magnesium hydroxide are the most promising candidates. Gypsum can possibly be precipitated by evaporation of saturated, injected brines, while iron oxides and hydroxides may form from iron-rich, fracture-injected saturated solutions provided that the redox and pH conditions can be properly controlled.

Magnesium hydroxide, finally, may be an excellent sealing medium formed directly from powdered magnesium oxide which hydrates in contact with water. The same goes for magnesium silicate hydrates (serpentinite) formed from finely ground, preheated serpentine rock (32). Both substances may have a potential to seal crushed zones penetrated by boreholes and possibly for sealing individual fractures with an aperture of at least 0.5 mm.

3.4.3 Clay fillings

3.4.3.1 General properties of clays

Experience shows that natural clay seams, formed by weathering of the parent rock or injected into fractures at high pressures, have remained physically and chemically intact for very long periods of time. They represent very effective barriers through their low hydraulic conductivity and through their ability to absorb certain dissolved ions and molecules. Clay fillings would serve as very effective fracture sealings if they can be formed in or brought into the rock. However, they need to be so composed or protected that mechanical degradation by erosion is prevented. The physical properties strongly depend on the granulometry and bulk density as well as on the microstructural homogeneity, particularly with respect to the distribution of the finest particles. Of even greater importance is the type of dominant clay mineral since it determines the microstructural features, specific surface area, hydration, and ion exchange properties as well as the rheological behavior. Naturally, mineral alteration and microstructural rearrangement induced by changes in

porewater chemistry can affect the barrier functions very substantially as discussed in this report.

An indication of the rather dramatic sealing efficiency of certain clay gels is the fact that illitic and smectitic gels with water contents corresponding to their liquid limits, i.e. 50-500 %, have a hydraulic conductivity of 10^{-5} to 10^{-10} m/s. Since the gross permeability of normally fractured rock is almost entirely dependent on the flow capacity of interconnected, open fractures, it is concluded that the permeability of rock in bulk is reduced by several orders of magnitude if such clay gels can be formed in or brought into the fractures. A deeper understanding of the function of such gels requires a more detailed description of the crystal constitution of the clay minerals and their arrangement, the matter being dealt with in this chapter.

3.4.3.2 Clay minerals

Clay mineral particles are phyllosilicates consisting of crystals smaller than about 2-5 microns, with a crystal structure based on composite layers of tetrahedrally and octahedrally coordinated atoms. We will distinguish here between three main groups:

* Kandites (main minerals: kaolinite and halloysite)
* Illites (main minerals: illite/hydrous mica and glauconite)
* Smectites (main minerals: montmorillonite, beidellite, nontronite)

Kandites

The crystal lattice sheets of the clay minerals belonging to this group are non-symmetric from a structural point of view (Fig 25), and adhere strongly to each other so that a kaolinite particle, for instance, usually consists of hundreds of sheets forming silt-sized

stacks. This yields a low specific surface area and a small amount of adsorbed water, which in turn results in a low plasticity and a low liquid limit, i.e. of the order of 20-40 %. If water is added to a water saturated sample in excess of the liquid limit, the clay turns semi-liquid like a silt consisting of quartz and feldspar grains. It does not show any swelling properties.

The cation exchange capacity is insignificant, while anion exchange is effective, but since the specific surface area is low the net exchange capacity is still not very important.

The small amount of strongly adsorbed water of kandites - with the exception of the rare mineral halloysite - and their microstructural arrangement with large continuous passages for water, are manifested by a much higher hydraulic conductivity than of clays dominated by the other clay minerals at one and the same bulk density.

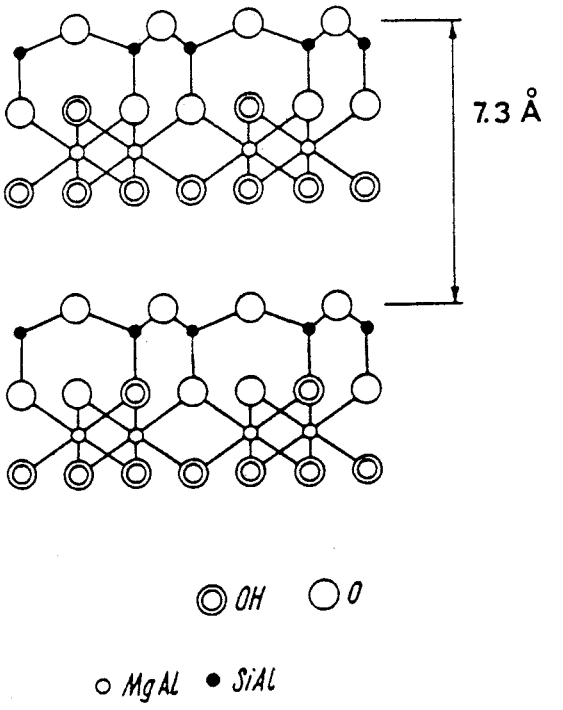

Fig 25. The crystal structure of kaolinite

Illites

Basically, illites are closely related to the micas and merge into that group by cation substitution. Their crystal structure can be regarded as a condensed version of smectite through the establishment of a firm sheet-to-sheet coupling that is caused by potassium ions in interlayer positions (Fig 26). Illites are characterized by a cation exchange capacity of about 30-40 mE/100 g dry clay. Their ability to hydrate is intermediate to that of kandites and smectites and this is manifested by a liquid limit of 70-90 % if the specimens are fine-grained and organic-free.

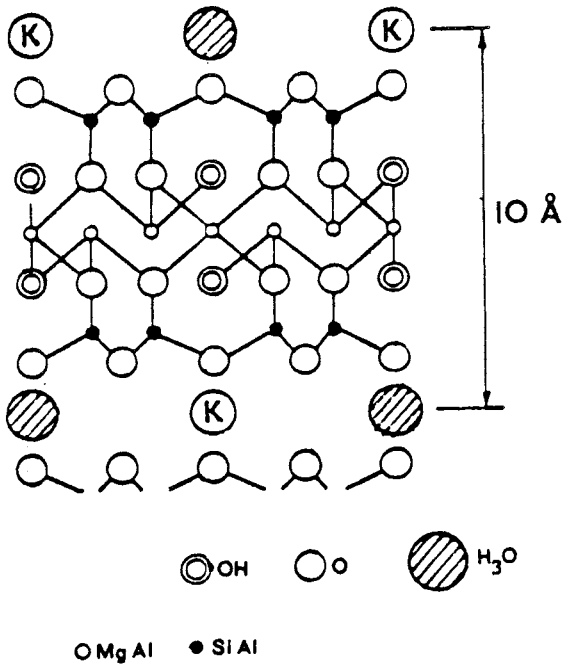

Fig 26. The crystal structure of illite

The crystal structure of illite is not very well defined; large variations in composition occur, such as interstratification of discrete lamellae of other silicates, the heterogeneity being manifested by a large variation in crystal size and shape (Fig 27). This yields a corresponding variation in mineral surface activity which, in turn, leads to a largely altered particle interaction when the porewater chemistry is changed. A well-known example of this, which is pertinent also to the present subject, is the influence of porewater chemistry on the coagulation of illitic clay gels.

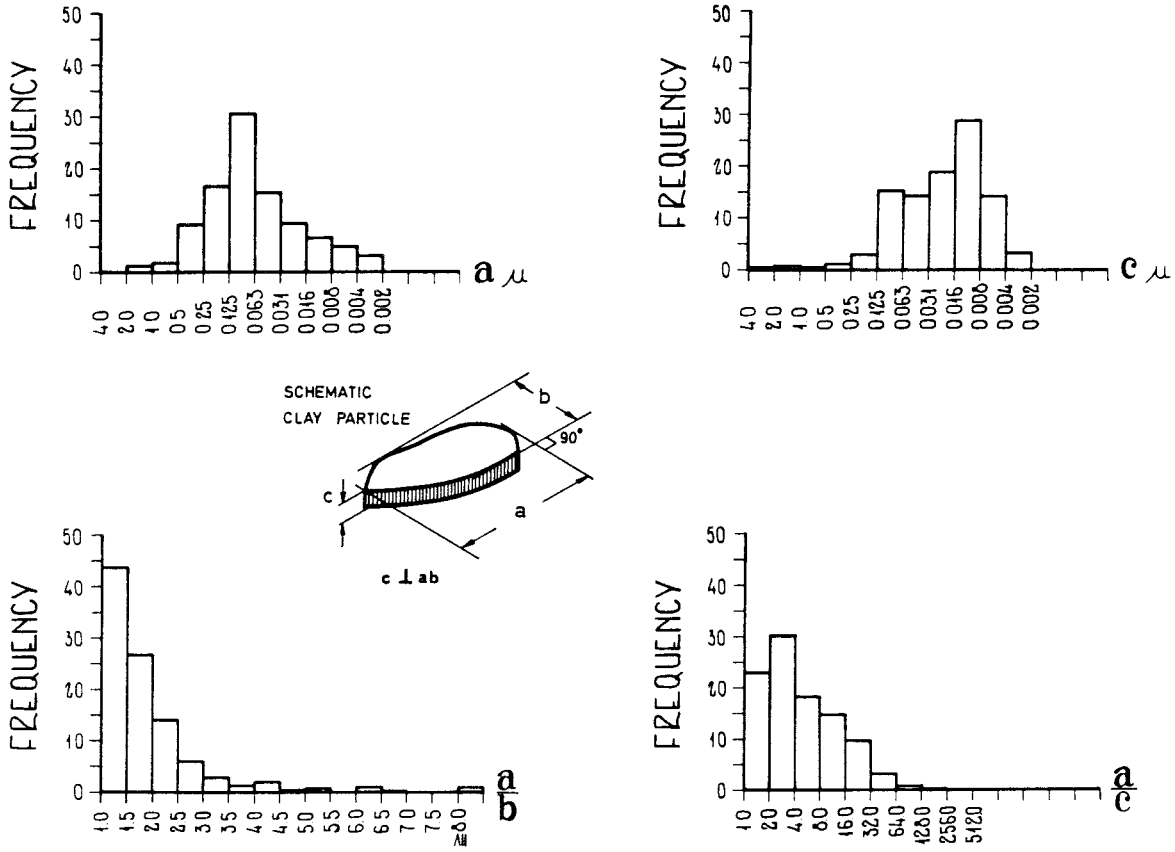

Fig 27. Clay particle size and shape in illitic clay

Smectites

Smectite crystals have an octahedral sheet coordinated with two tetrahedral layers in which oxygens are shared. Cationic substitution occurs in octahedral as well as tetrahedral sheets, which yields different properties and forms the basis of classification: montmorillonite with Si in tetrahedral positions and Al and Mg in octahedral sites, beidellite with Si and Al in tetrahedral positions and Al in octahedral sites, and nontronite with Si and Al in tetrahedral positions and Fe in octahedral sites. In practice, most smectites have a composition that deviates from the idealized versions. The most common species, montmorillonite, has a crystal structure that may have two forms depending on the ambient temperature (Fig 28). The occurrence of different smectite versions is not trivial. Thus, mineral transformation and associated large changes in physical properties may take place as a result of heating and uptake of certain cations in the course of percolation or diffusion through the clay. One such process is heat-induced conversion of montmorillonite to beidellite and subsequent transformation to illite by K-fixation. The mineral characterization is usually based on chemical analyses, the characteristic compositions* being:

Montmorillonite $(OH)_4Si_8(Al_{3.34}Mg_{0.66})O_{20}$ ($Mg_{0.66} \rightarrow Na_{0.66}$)

Beidellite $(OH)_4(Si_{6.34}Al_{1.66})Al_{4.34}O_{20}$ ($Al_{1.66} \rightarrow Na_{0.66}$)

or

Beidellite $(OH)_4(Si_6Al_2)Al_{4.44}O_{20}$ ($Al_2 \rightarrow Na_{0.66}$)

---

*After Ralph E. Grim

In the above formula, arrows are placed below the groups with charge deficiency, thus requiring the addition of cations external to the crystal lattice to balance the structure. Sodium has been taken here as balancing adsorbed cation.

Expansion or shrinkage of the smectite lattice in the range of 10-25 Å take place depending on the ionic strength, the nature of cations and anions or molecules and the available space for volume change. It is usually assumed that the amount of adsorbed water depends on the exchangeable cation species at least at low bulk densities. It is immediately seen that the expansion/contraction of smectite gels yields an excellent flexibility, which makes them fill up the fractures also in case of relatively large changes in aperture.

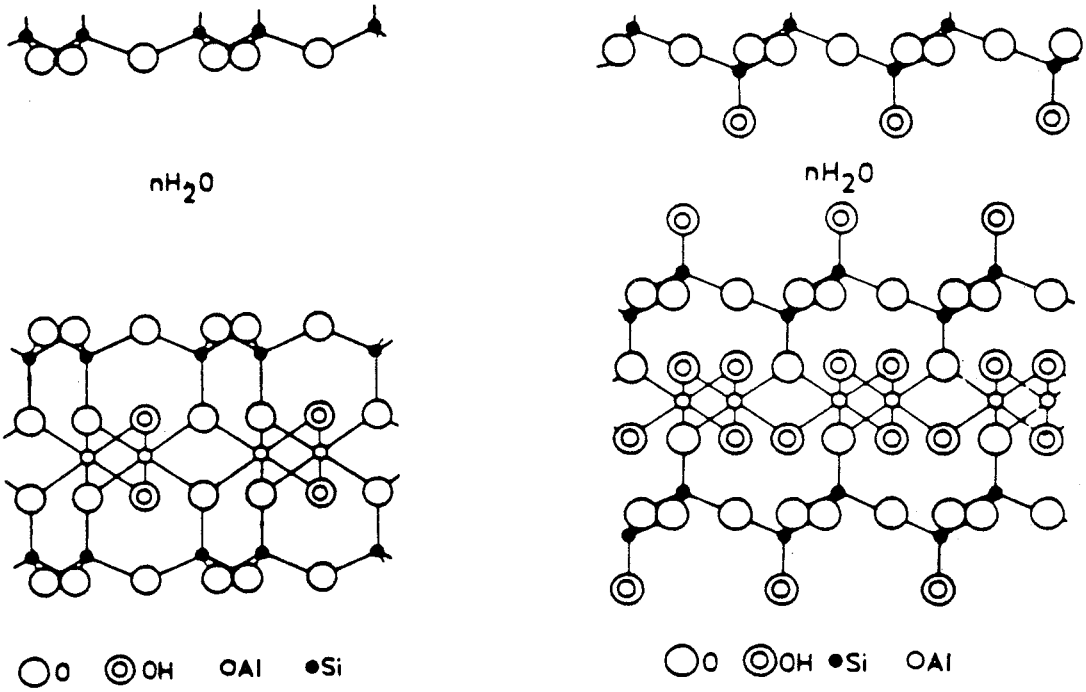

Fig 28. Possible montmorillonite structures. Left: Traditional version (Hofmann, Endell & Wilm). Right: Alternative version (Edelman & Favejee). n(H_2O) represents inter-crystalline water

3.4.3.3 Texture and microstructure

Grain size distribution

A high content of clay particles, particularly of smectite minerals, yields a high swelling potential and flexibility but it also makes the filling vulnerable to erosion. The erodibility can be very much reduced by altering the clay content, i.e. by adding silt-sized particles of rock-forming minerals like quartz. Current investigations of the importance of the clay content, i.e. the amount of clay-sized particles (minus 2 microns), and of coarser constituents demonstrate that large changes in physical properties are experienced when the clay fraction is increased from a few percent by weight to about 20 percent, and that additional, significant changes are observed when this percentage is raised to more than 50 percent. Experience shows, however, that mixing and preparation of soils for sealing purposes may not yield a very uniform spatial distribution and homogeneity of the clay component. This difficulty is particularly obvious when the relative amount of fines is small as demonstrated by a number of tests in which bentonite powder was mixed with silt/sand-type ballast material. There is actually a very obvious risk also that particles of different size become separated at the injection of diluted clay/silt/sand mixtures. Such mixtures may be of primary interest for fracture sealing since they are expected to be very resistant to erosion if their homogeneity can be preserved.

The influence of changes in porewater chemistry on the physical properties is particularly obvious at low clay contents. Fig 29 illustrates the microstructure of a clay-poor soil where the clay-sized smectite minerals form a gel that is contained in the pores of larger grains where its ability to fill up the pores is essential to achieve a low hydraulic conductivity. The gel density of clay-poor mixtures of this type commonly varies between 1.3 t/m^3 and 1.6 t/m^3. For the lower part of this range the difference in hydraulic conductivity may be significant on altering the salinity as demonstrated by Table 4, while less important influence is noticed for the higher gel density. The same tendency is actually even more obvious for the high densities intended for HLW canister overpack. The influence of porewater salinity on the hydraulic conductivity is explained by its effect on the clay particle arrangement.

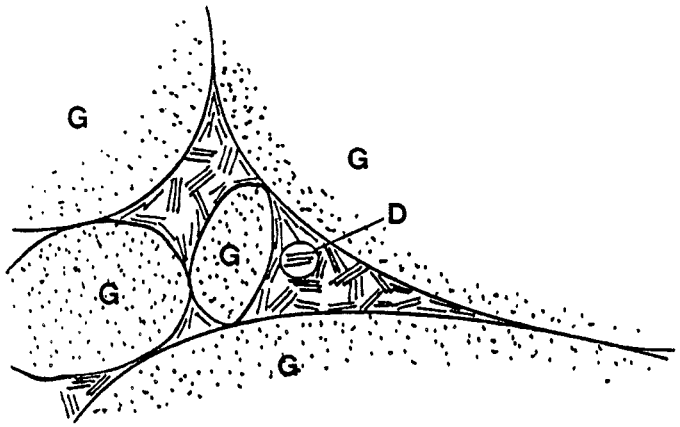

Fig 29. Schematic grain arrangement in a clay filling that is poor in fines. G are ballast grains, D is clay aggregate (domain)

Table 4. Hydraulic conductivity (k) of Na smectite at different porewater salinities (hydraulic gradient 10-100)

Bulk density t/m^3	Porewater chemistry	k m/s
1.64	Artificial sodium-rich groundwater, 300 ppm	$5x10^{-11}$
1.30	Natural sodium-rich groundwater, 9800 ppm	$6x10^{-9}$
1.60	"	$9x10^{-11}$
1.30	35000 ppm NaCl solution	$>10^{-8}$
1.60	"	$10^{-8}-10^{-9}$

Clay particle arrangement

The physical properties of clay gels are closely related to the microstructural arrangement as shown by a large number of independent investigations. The matter was brought up early in agricultural sciences, the classical question being that of the influence of porewater salinity on the hydraulic conductivity and on the erodibility. It is of equal importance in the present context where percolates are apt to affect the interparticle forces thereby influencing the microstructure, which is in turn a determinant of the physical properties in bulk.

The earliest information regarding the detailed particle arrangement in clays has been inferred indirectly from theoretical studies of interparticle forces operating between particles in colloidal suspensions. The interaction is supposed to contain a repulsive factor caused by electrical double-layers and an attractive factor due to (London-) van der Waals forces. The repulsion can be represented by an exponential function with a range approximately equal to the extension of the double-layer, whereas the attraction decreases at some inverse power of the distance. The Van der Waals forces, which create the attraction, result from the nearness of one particle to another and the concomitant overlapping of atomic forces in the crystal lattices. The range of these attractive forces is assumed to be of the order of colloidal dimensions. The influence of the concentration and kind of cations in the liquid phase on the interparticle distance is commonly explained by the theoretical properties of electrical double-layers. Thus, an increased concentration of cations reduces the zeta-potential and the range of the double-layer, thus reducing the repulsive force between the particles and favoring clay particle flocculation. In relatively dense smectite clay the disordering influence of surface-adsorbed cations on interlamellar water lattices seems to be a dominant mechanism rather than double-layer interaction (36).

From a theoretical point of view an increased cation concentration in the porewater of a clay gel should result in coagulation and formation of clusters or aggregates of particles with concomitant creation of larger pores. This is also demonstrated by microstructural inves-

tigations of natural clays which were deposited in fresh and salt water, respectively, and which had similar granulometric and mineralogic compositions (37). These studies gave microstructural data in the form of the ratio of the sectioned pore area P in percent of the total sectioned area T of ultrathin sections ("Two-dimensional porosity"). Also, the size distribution of the longest intercept a_p of individual pores was found to be a useful parameter that relates the particle arrangement to the cation concentration of the water in which the sediment was formed. A typical example of an ultrathin section for determination of the microstructural parameters is shown in Fig 30. Fig 31 shows a representative comparison of P/T-data for typical illitic fresh water clays and marine clays and this figure also illustrates the practical importance of salinity on the hydraulic conductivity (38). A similar relationship is expected also for smectitic clays.

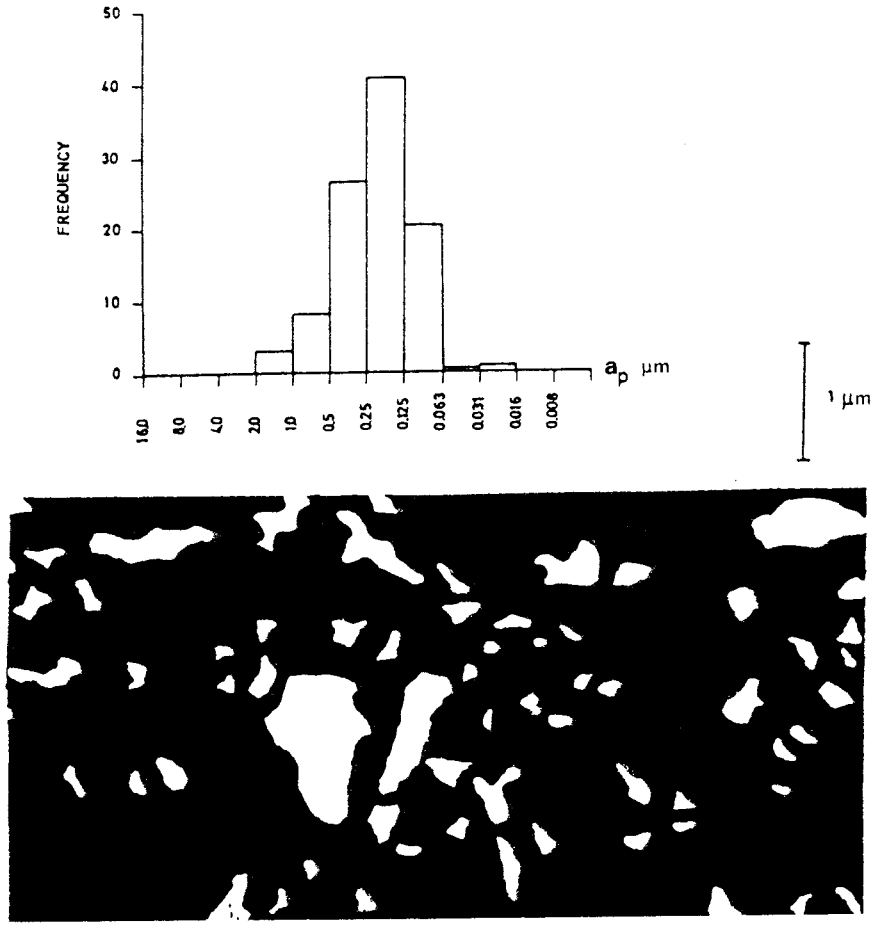

Fig 30. Example of the pore size distribution in an illitic clay deposited in fresh water

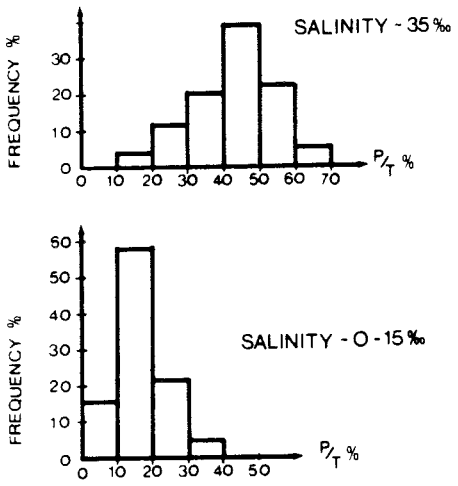

P/T versus salinity.

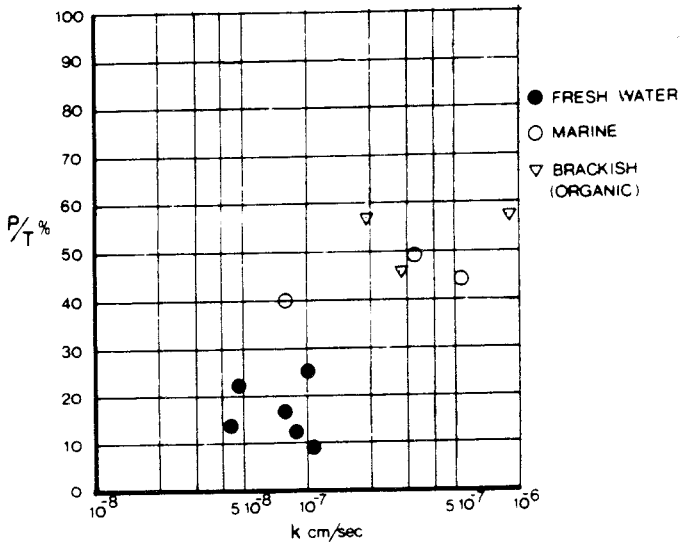

P/T versus permeability

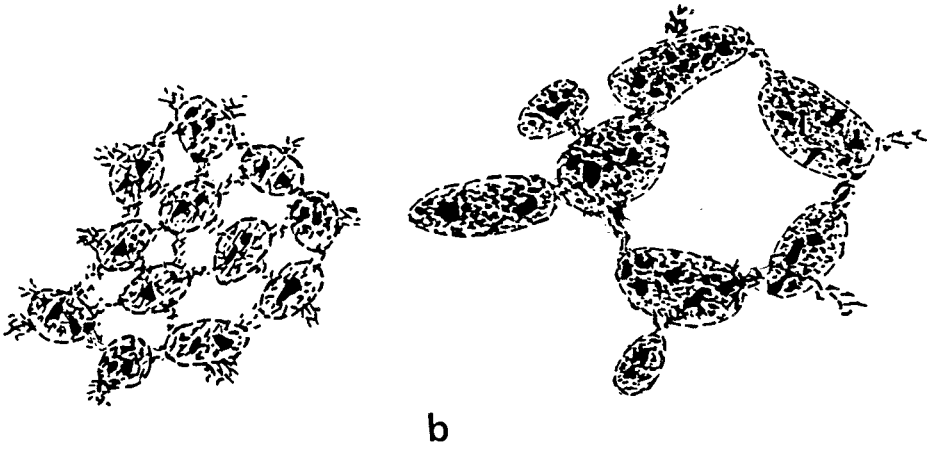

Fig 31. Typical P/T-data related to porewater salinity. Right upper picture demonstrates that high P/T:s yield high hydraulic conductivities. Lower picture shows schematic clay particle arrangement in a) Clay deposited in fresh water have relatively porous aggregates but small voids, and b) Marine clay with large, dense aggregates separated by large voids

We see that when the salinity of water with Na and Cl as major ions increases from a few hundred ppm to 35 000 ppm, the hydraulic conductivity of illitic clay with a bulk density of about 1.6 t/m^3 increases from about $5x10^{-10}$ m/s to about $5x10^{-9}$ m/s i.e. by 10 times. The effect is thus not as obvious as in the experiments with Na smectite as represented by Table 4. Keeping in mind that the erodibility is lower for illites than for smectites, the first-mentioned clay type may be a strong candidate although its sealing efficiency and swelling ability are not as good as those of smectite. If the corresponding tests are conducted with kaolinite-rich clays much higher conductivities are measured and for such clays the difference between salt and fresh water percolation rates is even smaller than for illite. All this shows that the surface activity, which is highest for smectites and lowest for kandites and which is manifested by the cation exchange capacity, determines how sensitive the clay gel microstructure and its hydraulic conductivity is to the ionic strength and composition of the percolate.

The considerably lower hydraulic conductivity of sodium smectites than of illites and kaolinites at any particular porewater salinity and density is explained by the strong hydration ability and associated swelling power of the first-mentioned clay. This yields a "dispersed", non-aggregated type of particle distribution and a small content of continuous flow paths as shown in Fig 32.

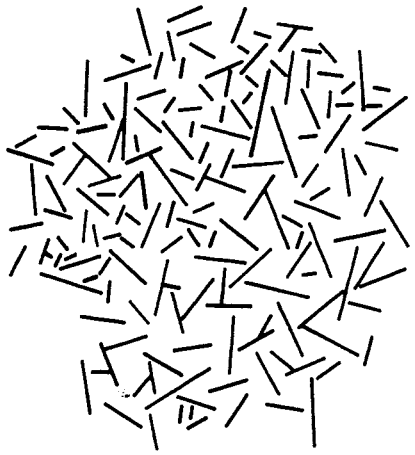

Fig 32. Schematic arrangement of montmorillonite flakes in soft or moderately dense gels

As to the influence of cations others than sodium, basic colloid chemistry is applicable in predicting their influence on the microstructure, hydraulic conductivity and diffusivity. In principle, there is a preference in cation exchange that is illustrated by the series: $Na<K<Ca<Mg<NH_4$.

Partial replacement of left end members by those to the right may take place even at low concentrations of the latter but complete exchange seems to require a strong preponderance of the replacing ion (except when this ion is Na) or possibly a very long percolation time. The important factor in this context is that the exchange from sodium to bi- and multivalent cations has approximately the same effect on the clay particle arrangement as a strongly increased concentration of the porewater salinity with Na and Cl as major ion constituents. In the case of smectite, cation exchange from sodium to calcium is known to yield dense domains of parallel flakes with simultaneous creation of larger pores between these packs (Fig 33). Percolation tests of calcium bentonite with $CaCl_2$ solutions of largely varying strength have shown that the hydraulic conductivity is 2 to 5 times that of sodium bentonite with the same bulk density (1.8-2.2 t/m^3) and total salt content. At lower bulk/densities than 1.8 t/m^3 the difference in hydraulic conductivity is expected to be even higher.

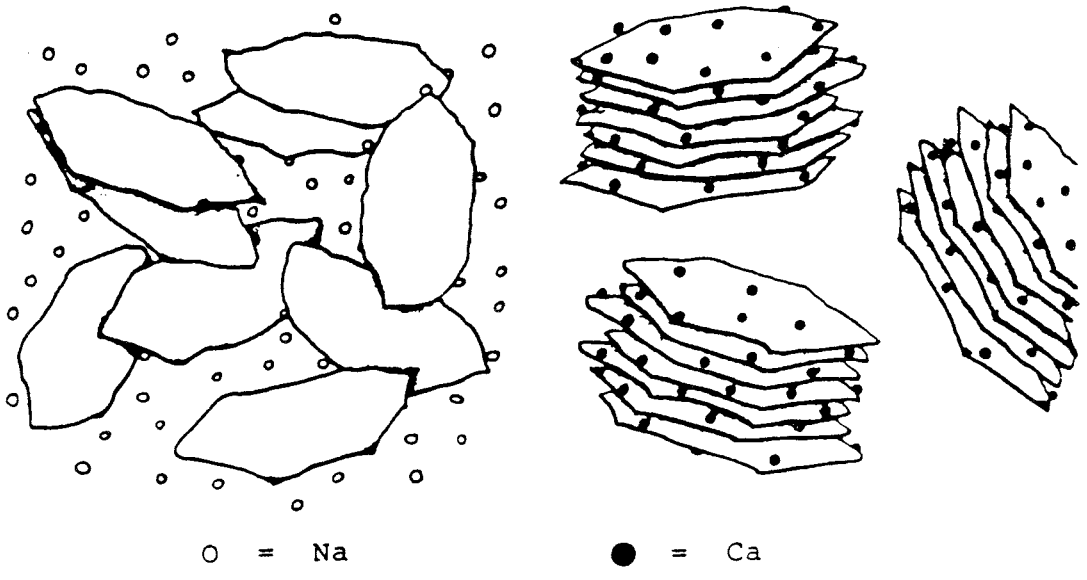

Fig 33. Schematic Na and Ca smectite microstructure

The replacement of the originally adsorbed cations by those of percolates ultimately yields saturation, which means that the barrier function of clay-based fillings to pick up and absorb cations is only temporarily effective. The amount of mineral-adsorbed substances can be calculated by using the cation exchange capacity (CEC) values since the exchange reaction is stoichiometric. CEC is approximately 5-15 mE/100 g for kaolinite and halloysite, 10-40 mE/100 g for illite and 80-150 mE/100 g for smectites.

The influence of various anions on the physical properties of percolated clays is not very significant. It is true that certain anion fixation, such as phosphate, tends to disperse clay mineral particles and transform clay gels to sols, but this is only valid for rather dilute gels which are mechanically agitated; it does hardly take place spontaneously. It is generally assumed that the geometry of the anions in relation to the clay mineral lattices is important for anion uptake and fixation. Thus, anions such as phosphate, arsenate and borate, which all have about the same size and geometry as the silica tetrahedron, are probably adsorbed at exposed edges of the tetrahedral sheets where they grow to form extensions of them. As to kaolinite, OH:s of exposed basal surfaces can take part in exchange reactions. One example of the efficiency of this exchange mechanism at neutral pH conditions is that the phosphate retained in kaolinite is almost 0.1 millimole per gram, while illite has a phosphate-retaining capacity that is only 50 % of this figure. As in the case of cations, anion screening and retainment only proceeds until saturation has been reached.

Organic molecules interact with clay minerals through functional groups like carboxyl (COOH), phenol and alcohol (OH), methoxyl (OCH_3) and carbonyl (C-O). The hydrogen of carboxyl and phenol groups can be exchanged against various bases or surface-adsorbed cations and thereby become fixed to surface-active minerals (Fig 34). This effect is naturally strongest in the case of smectite minerals and less obvious in kandites, illitic clays being intermediate in this respect.

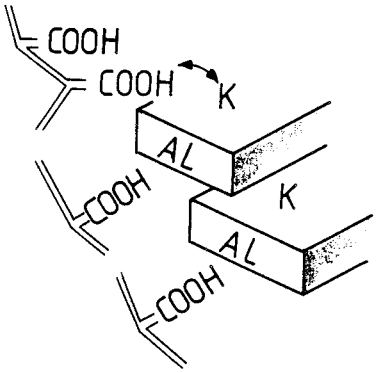

Fig 34. Example of bond mechanisms of organic molecules and clay minerals

In addition to ion adsorption mechanisms like the one in Fig 34, attraction and fixation also takes place through hydrogen bonding between carbon atoms and exposed hydroxyl groups of the crystal lattices. The OH:s of kaolinite and smectite crystallites are particularly effective in such interactions but the smaller specific surface area of kaolinite means that the net adsorption capacity is much less in this type of clay. Large molecules such as organic phosphorous compounds and proteins with or without a net charge sorb within the crystal lattice of expanding clay minerals and on kaolinite and illite through van der Waals forces. This creates expansion of dense clay particle aggregates by which the average pore size would tend to drop if the total volume is kept constant. The expected, associated physical effect would be a drop in hydraulic conductivity in the course of the percolation of many organic solutions.

3.4.4 Chemical stability of clay minerals

3.4.4.1 **Transformation of smectite to illite**

If a smectite clay filling consists of beidellite the charge deficiency of the crystal lattices favors K-uptake from percolating groundwater and fixation of these ions at the basal planes of the crystals. Thereby, the smectite flakes move together and form thick illite particle aggregates separated by large pores. At low bulk densities this process produces an almost complete loss in swelling

and self-healing ability and increases the bulk hydraulic conductivity by as much as three orders of magnitude. Montmorillonite can be converted to beidellite by heating to about 100°C, which means that clay fracture fillings applied in the form of montmorillonite can be altered to illite with concomitant reduction in swelling potential and increase in hydraulic conductivity.

3.4.4.2 Influence of pH on silicate minerals

The strong influence of pH on the solubility of silica and alumina (Fig 35) demonstrates its importance with respect to clay mineral stability.

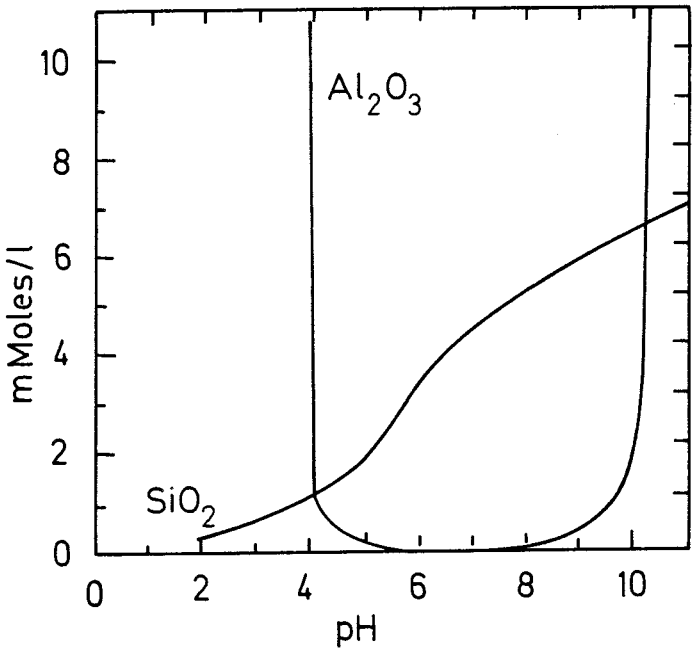

Fig 35. The solubility of silica and alumina as a function of pH (After Correns)

The diagram suggests that the octahedral sheets of clay mineral lattices break down completely at pH-values below 4 and above 10.5, which has also been verified in laboratory tests where very dilute smectite clay gels became dissolved in a few hours. In a clay filling percolated by alkaline solutions, as is expected in the vicinity of a concrete structure or cement grouts, the buffering capacity of the clay may be sufficient to maintain its overall integrity for quite a long time if the clay content is high, but the operational time is certainly restricted to a few years of injected clay fillings of low density. The products resulting from pH-induced reactions may not alter the net hydraulic conductivity substantially in the first few years but since dissolved species may be transported out from the clay fillings by flow or diffusion, the remainder becomes increasingly permeable in a longer perspective.

Considering first acid percolates, the main reaction products resulting from attack on smectite and illite are aluminum hydroxy interlayers and kaolinite, as well as free silica and alumina complexes. The optimum conditions for the formation of hydroxy interlayers is at pH 4 to 6. Such hydrolysis products are $Al(OH)_2$, $Al(OH)$ and $Al(OH)_3$. At pH values lower than 4 the $Al(H_2O)^{3+}$ ion dominates, while gibbsite /$Al(OH)_3$/ solubility is at minimum at pH=6. It is realized from the preceding chapters that alteration to kaolinite means that originally low-pervious clay fillings containing smectite or illite deteriorate strongly and offer no essential barrier effect with respect to the rate of percolation or diffusion.

In the high pH region three major reactions occur, namely formation of 1) zeolites, 2) certain alumina and magnesium compounds, and 3) amorphous alumina and silica complexes. Smectites are particularly vulnerable while kaolinite is most resistant, whereas illite is intermediate in this respect. If Ca is abundant, the zeolites chabazite ($CaAl_2Si_4O_{12} + n\cdot H_2O$), scolecite ($CaAl_2Si_3O_{10} + n\cdot H_2O$) or gismondite ($CaAl_2Si_2O_8 + n\cdot H_2O$) are formed, while in excess of Na the product will be the zeolite analcime ($NaAlSi_2O_6 + n\cdot H_2O$). The Al- and Mg- compounds may be $Al(OH)_4$, $Mg(OH)_2$, and $SiO(OH)_2$. Considering the expected moderate temperature conditions in clay fillings, amorphous gels are the most probable reaction products and their high solubility suggests that long term diffusion of their constituents through

the fillings will lead to a degradation similar to that in the low pH region. Clay/zeolite alteration yields a largely increased hydraulic conductivity but the minerals formed are very efficient cation exchangers, having cation exchange capacities even greater than those of smectites (up to 6 mol/kg). Unfortunately, this property is highly dependent on cation size and ion selectivity is therefore a typical feature. In practice, the ion retention ability is of limited value as in the case of smectites, because it does not affect the composition of the percolate after complete saturation of the ion exchanger.

It should be added here that feldspars are also likely reaction products at high pH, but at temperatures lower than 50-60° C the feldspar crystallization kinetics are so slow that this process is of no practical importance.

3.5 Options

There seems to be several options in the search for possible and suitable fracture fillings but practical problems that are associated with the use of higher temperatures than about 100°C and pressures exceeding 1 or 2 megapascals indicate that there are probably only three major possibilities:

1 Injection of vapor or solutions which react with the rock by which fracture fillings, crystalline or amorphous, are produced

2 Injection of supersaturated solutions from which precipitation and fracture filling takes place through temperature effects. It must be certified that future temperature alterations do not lead to dissolution

3 Pressure injection of suitably composed clay gels

The two first-mentioned methods are expected to yield brittle, relatively porous and incomplete fracture fillings, while the third technique may give a flexible, largely complete but porous filling.

Considering first the reaction techniques, hot CO_2-solutions are of potential interest since they may lead to very rapid "weathering" and clay formation. Also, the injection of hydrofluoric acid at normal temperature may be practical.

As to the precipitation methods it can be assumed that artificial calcite formation would be particularly feasible and that precipitation of silica-rich compounds may also be of potential interest. The importance of pH and future temperature conditions has to be considered in this context.

Smectite clays, finally, are of particular interest because of their flexibility, which makes them stick to the rock and fill up the fractures also if aperture changes take place. The major problem is to bring in clay particles into fractures with a small aperture to form a sufficiently dense and erosion-resistant gel; it probably requires a grain size composition with a relatively large amount of silt-sized grains. With a clay content of 10-50 % and the rest being silt-sized crystals of rock-forming minerals, the hydraulic conductivity and diffusivity are still acceptable. An alternative option may be to use natural illite-rich Quaternary clay which has a low swelling ability but is more erosion-resistant than smectite-rich clays.

4 GROUTING OF FINE FRACTURES

4.1 Introduction

Injection of cement suspensions and pastes, usually with chemical additives in order to improve the flow properties of the latter, has long been used for the sealing of fractured, pervious rock. Strong leakage is thereby usually reduced very much since wide fractures can be effectively blocked. However, experience shows that cement grouts cannot penetrate and fill fractures with an aperture smaller than 0.2-0.5 mm unless the injection pressure is raised to several megapascals, which has the unfortunate effect of breaking up the rock. Since such relatively narrow fractures are responsible for fast water percolation of rock in the common gross hydraulic conductivity range of 10^{-6} to 10^{-8} m/s, other substances, usually clay materials and organic chemical compounds, have therefore been tried for grouting purposes. Tests have demonstrated that smectite-rich (bentonite) suspensions can penetrate fractures with apertures down to about 0.1 mm, while "chemical grouts" like "sodium silicate" manufactured by heating of quartz sand and sodium carbonate with carboxylate hardeners, or epoxy and polyester compounds are able to enter even finer fractures. The difference in groutability is due to the low viscosity of the fluid organic solutions. However, although their solid reaction products do not seem to be very short-lived and have a longevity that is sufficient for most rock engineering purposes, long-term chemical stability has not been evidenced and there are reasons to believe that decomposition due to microbial activity or dissolution may well take place in a 10^{3}-10^{5} year perspective. This means that neither cement nor organic compounds can be accepted for rock sealing of HLW repositories without extensive further research, while suitably composed clay-based grouts seem to be of immediate potential use. The latter need to be relatively viscous, however, which presents the same difficulty in injecting them into fine fractures as does cement grouting.

This chapter is an attempt to summarize and coordinate the major conclusions from a number of published investigations of fracture sealing using cement substances and smectitic clays, respectively.

The purpose is to define the potential of such techniques with particular respect to the physical state of the injected fracture fillings. Cement is included since this material can be considered for temporary sealing purposes or as a component of mixed grouts.

4.2 Theory

4.2.1 Fracture geometry

In geohydrology and applied rock sealing, joints and fractures are usually regarded as plane slots with constant aperture because of the simple mathematics in flow calculations that is implied by this concept. As demonstrated in an earlier chapter, the aperture of most fractures varies to which comes that their extension is limited and that the net flow is largely determined by the connectivity of the fractures.

4.2.2 Theoretical flow models

4.2.2.1 General

The penetration of pressure-induced substances has the character of flow governed by the fracture aperture and pressure gradient, as well by the viscosity of the injected mass. For uniaxial flow through an infinitely large slot Eq. (4) gives the average rate of penetration provided that the Poiseuille law applies, i.e. that there is no flow at the slot boundaries and that the grouting behaves as a fluid.

$$v = \frac{d^2 \cdot g \cdot \rho}{12\eta} \qquad (4)$$

where v = flow rate, m/s
d = aperture, m
g = gravity, m/s^2
ρ = bulk density, kg/m^3
η = viscosity, Pas
i = pressure gradient

The fact that neither cement-based nor clayey grouts behave as perfect Newtonian fluids puts a restriction to the applicability of Eq.

(4). They usually exhibit a Bingham threshold shear stress, which means that the shear resistance becomes so large at a certain penetration depth that the flow stops. Theoretical considerations as well as experiments have shown that this critical depth ("Endreichwerte") can be calculated by the simple expression in Eq. (5) for cement suspensions and pastes (39).

$$r_e = \frac{d}{2\tau_o}(p_1 - p_2) \qquad (5)$$

where r_e = maximum penetration depth
d = slot aperture
τ_o = Bingham yield stress ("Fliessgrenze")
p_1 = injection pressure at point of injection
p_2 = water pressure (counterpressure) at the front of the penetrating mass (Fig 36)

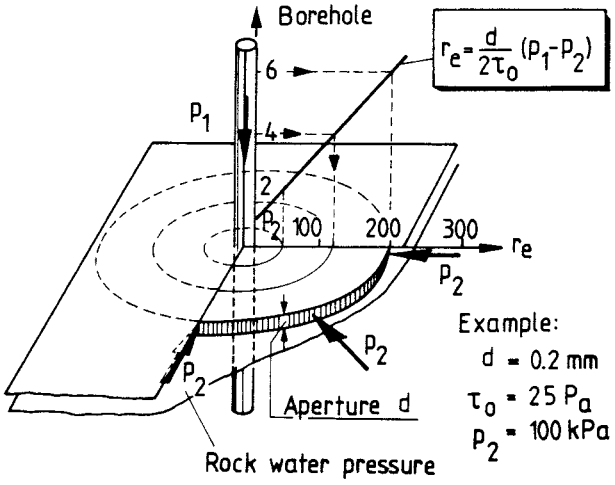

Fig 36. Theoretical maximum penetration depth at the effective injection pressure $p_i = p_1 - p_2$. After Wittke et al

A typical diagram of the flow behavior of cement pastes with a viscosity of about 0.4 Pas, and a yield stress of around 30 Pa, is shown in Fig 37. D, expressed in 1/s is the rate of shear at viscometer testing.

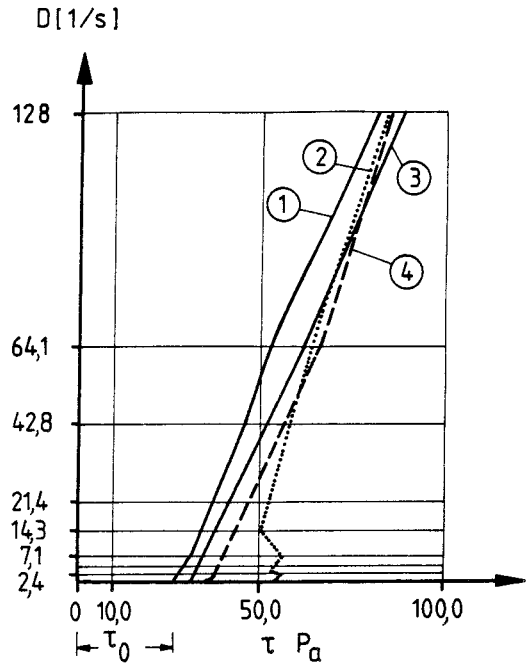

Fig 37. Flow behavior of cement paste (39)

4.2.3 Validity

Good agreement between calculated and measured penetration rates and maximum depths has been reported for cement suspensions and pastes in systematic laboratory tests in which smooth glass plates were used (39). Keeping in mind the rather rough surfaces and the non-uniform aperture of real rock fractures the effectivity of sealing is overestimated by simple models like the one in Fig 36. Actually, experience shows that injection from packer-sealed boreholes yields irregular distribution of the grout because water pressure gradients are set up which tend to drive water backward towards the free surface through interconnected fractures. This may create only partial sealing of the fractures and implies that the regular flow shown in the schematic picture in Fig 36 is not realistic at all. To that comes that sets of interconnected fractures often have the character of channels with largely varying width and abruptly changing directions.

4.3 Practical experience, preliminary literature survey

4.3.1 General

There is a large amount of reports on recorded changes in hydraulic conductivity resulting from more or less successful, large scale rock sealing operations made by contractors, and they were expected to serve as a rich source for evaluating the efficiency of grouting in the present survey. Unfortunately, the documentation usually cannot be interpreted in terms of penetration depth of the grouts into well defined fractures. Despite their limited practical applicability the authors have therefore confined the literature scanning to systematic experiments with relatively well defined fracture geometries and flow data of the grouts (cf. 40).

4.3.2 The Bergman Report R 45:1970 (41)

4.3.2.1 Experimental set-up

In 1970 the results of a series of laboratory tests were reported in which cement and bentonite had been tried as fracture grouts*. The major purpose was to find out whether finely fractured rock could be sealed effectively with these substances. The experiments were made by use of parallel 15 mm thick polished glass plates which had a size of 0.5x0.65 m and which were sealed at all ends except for one of the short edges which was left open for free drainage. The sealing substance was injected from the short edge on the opposite side under a constant injection pressure of 50 kPa, the distance between the plates being varied in the range of 0.1-0.4 mm. The temperature was kept constant at about 25^{o}C.

Three substances were used with the properties specified in Table 5, namely cement, cement/bentonite, and pure bentonite. It is obvious from this table that the cement had the consistency of a soft paste and that the other two substances were rather diluted.

---

* Chemical grouts were also used but these results are omitted here

The aperture of the "artificial fracture" was 0.1, 0.2, 0.3 and 0.4 mm, respectively. The report does not state the composition and physico/chemical condition of the bentonite but it can be assumed that sodium was the major adsorbed cation.

Table 5. Properties of the groutings

Grouting	Water content %	Viscosity Pas
Cement (Limhamn's quick-setting)	50 (vct=0.5)	1
Cement/bentonite mass ratio 4:1	400	0.5-0.7
Bentonite	2000	3

4.3.2.2 Results

The penetration pattern was similar for the three substances. At the application of the air-pressure which was used to drive the grout from a 1 liter tank to the test-device, the grouts rapidly entered the slot after which the penetration rate dropped significantly.

The cement grout could not be injected to more than about 0.15 m depth when the aperture was 0.3 mm or smaller than that. At 0.4 mm aperture it migrated right through the slot, the rate of penetration being almost constantly 0.05 meter per second.

The cement/bentonite grout entered the 0.2 mm slot to about 0.2 m depth and then stopped. At 0.4 mm aperture it migrated through the slot at an almost constant rate of penetration of about 0.01 meter per second.

The bentonite suspension was successfully injected in slots with apertures down to 0.1 mm. It entered the last-mentioned slot at a rate of 0.005 meter per second while the corresponding rate was 0.1-0.2 meter per second in a 0.4 mm slot, which was filled in a few seconds.

4.3.2.3 Comments

The investigator noticed that the cement slurry tended to be consolidated, i.e. to be compacted in the course of the injection. It is questionable, however, whether this process actually takes place in a water saturated rock fracture with less possibility of serving as a drainage. Also, he concluded that particle interaction, i.e. the tendency of aggregation, sometimes termed coagulation, is far more important for the penetrability than the viscometer-determined viscosity. The investigator finally noticed that the viscosity of the grout substance contained in the pressure vessel and injection pipe increased successively, which appeared to result in a loss in effective injection pressure. In view of the present understanding of the involved physis, the increase in viscosity is certainly expected when using Na smectite clays through its typical thixotropic behavior, and also in the case of cement suspensions if the residence time in the vessel is long.

4.3.3 The Wittke Report (39)

Based on earlier systematic tests, Wittke and coworkers gave general recommendations for the injection of cement suspensions and pastes and particularly emphasized the importance of defining and selecting a proper injection pressure. According to these investigators, the "active" injection pressure p_i is defined as in Eq (6). Thus, for a downward-directed packer-sealed hole the applied pressure is increased by the weight of the slurry while the flow resistance in the injection pipe (p_η) reduces the active pressure (cf Fig 38). Naturally, p_i must be positive, i.e. it has to overcome also the shear p_{τ_o} resistance at the penetration of the grouting:

$$p_i = p_o + p_\rho - p_\eta - p_{\tau_o} \qquad (6)$$

where $p_\rho = g(h_2 \cdot \rho - h_1 \cdot \rho_w)$

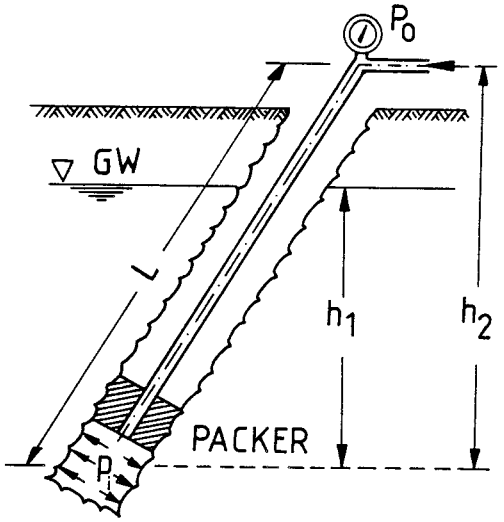

Fig 38. Evaluation of effective injection pressure (39)

In general, these investigators found that a suitable cement-based grout should have a yield stress of no more than 20-40 Pa and a viscosity lower than 0.3 Pas in order to make it effectively groutable. It was concluded from laboratory experiments as well as from injection in hydraulically well defined fractures with large extensions that it is possible to bring in a relatively soft cement paste (w=47 %)* to a depth of 0.5 to about 1.7 m in a fracture with an equivalent aperture of 0.2 mm at the rather low injection pressure 0.5 MPa (Fig 39). The subsequently recorded, insignificant reduction in gross permeability of the treated rock suggests, however, that the grout followed wider passages so that the penetration pattern was probably finger-like instead of the regular circular distribution assumed by the authors. One reason for the surprisingly large penetration depth is that 2 weight percent of flow-improving plastic monomer ("Intracrete") and 3 percent by weight of sodium bentonite had been added to the cement.

---

* In Sweden this moisture content is termed vct=0.47

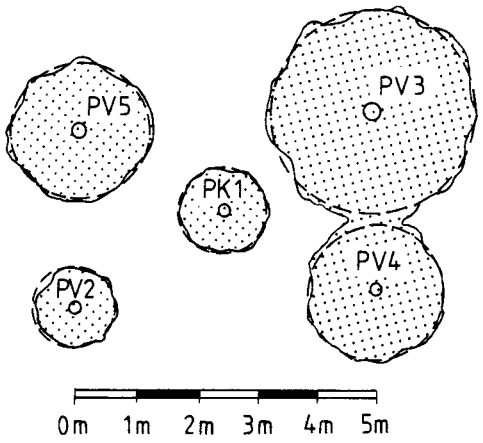

Fig 39. Assumed penetration depth in subhorizontal 0.2 mm fracture (39)

Field injection tests were also conducted with cement suspensions with water contents ranging between 60 and 90 %. These were injected in hydraulically well defined rock fractures and were concluded to have a large penetrability. However, as in the case of the cement paste the sealing was found to be incomplete and have only a small influence on the gross permeability.

The investigators pointed out that the penetration depth at prolonged treatment is very small in fractures with an average aperture of about 0.2 mm, a possible way of reaching better results being a successively increased injection pressure in the course of the treatment. The authors' recommendation that this pressure should not exceed 1.5 times the effective stress acting perpendicularly on the fracture plane, unfortunately implies that the maximum permitted injection pressure would commonly be only a few tenths of a megapascal or less than that for very shallow, subhorizontal fractures. This is in agreement with practical experience, which recommends a maximum pressure of about 1 MPa when the grouting depth is 3-10 m. All this suggests that the penetration power can not be very much improved by increasing the pressure. The risk of breaking up the rock is actually

very well illustrated by a field test, conducted by these investigators, in which the penetration was related to the propagation and expansion of the injected fracture. The experiment involved injection of a cement suspension in a packer-sealed borehole with 5 m packer distance from the rock surface, with the flow (q) plotted versus time and injection pressure in Fig 40. The very low viscosity figure indicates that the suspension behaved almost as water and that "hydraulic fracturing" took place.

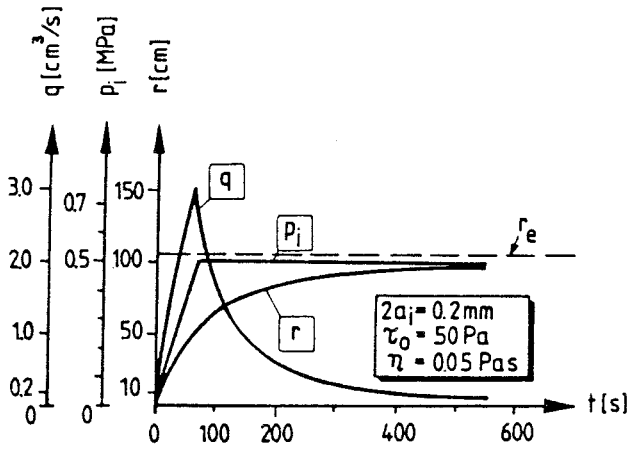

Fig 40. Example of cement injection data (39)

The diagram shows that the penetration proceeded parallel to the successively increased injection pressure and that it did not stagnate when this pressure was kept constant at 0.6 MPa after 1 minute, which points to a successive propagation of the fracture. After 8 minutes the injection pressure was reduced by which the flow almost ceased. A subsequent pressure increase to 2.5 MPa only caused insignificant, additional penetration of the grouting, which can be interpreted as resulting from consolidation of the grouting at the preceding pressure drop. This drop probably yielded partial closure of the fracture.

One of the reported cement paste injections is of particular interest since no flow-improving chemicals were added. Attempts were instead made to reduce the yield stress by adding fly-ash to the cement/ bentonite mixture. This procedure was helpful as concluded from Table 6, although the effect was moderate. All the mixtures specified in the table were reported to have filled a 0.1 mm slot in a small experimental setup to a distance of about 0.3 m at non-defined injection pressures. There is some doubt as to the aperture since the two plexiglass plates forming the slot probably deformed to give a significantly increased slot width.

Table 6. Influence of adding fly-ash to bentonite-doped cement

Water content %	Fly-ash[1] (EFA)	Na-Bentonite[1]	τ_o Pa	Pas
45	0	3	25	0.33
43	0	3	39	0.35
45	10	3	18	0.25
45	20	3	27	0.28
42	33	3	36	0.27

4.3.4 The Chan Report (42)

Canadian investigations of clay sealings have shed some light on the groutability of smectites, illitic clays and kaolinite. The tests involved injection of clay pastes and suspensions into a gap space of 0.25 mm using a pressure that was increased step-wise from 0 to 105 kPa. The relative ease of injection is illustrated in Fig 41, the respective grout being specified in Table 7.

Table 7. Properties of clay grouts used in Chan's study

Grouting	Water/solid ratio	Water content %
Black Hill, Wyoming	10:1	1000
Na bentonite	8:1	800
Avonlea, sodium-enriched	5:1	500
Ca bentonite	4:1	400
Pembina Ca bentonite	7:5	140
Sealbond, illite-bearing	1:2	50
crushed shale	5:12	42
Kaolin (kaolinite-rich	1:1	100
clay from Georgia)	4:5	80

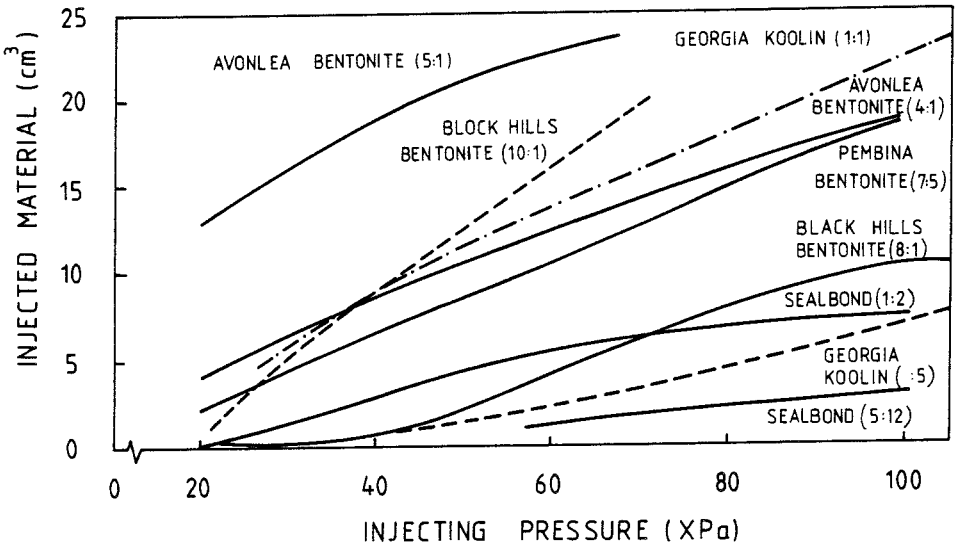

Fig 41. Quantity of injected material versus pressure in Chan's study

The results are very characteristic in the sense that effective grouting of soil-type materials, i.e. not only clays but also finely granular cement and quartz powders requires that the water content is at least of the same order of magnitude as the liquid limit. This consistency parameter is 300-500 % for sodium bentonite, 70-90 % for illitic, and 20-40 % for kaolinitic soils which explains why the wettest Georgia clay could be effectively grouted, while the test with the Sealbond clay was not very successful.

4.3.5 Application of models for predicting the penetration power of pressure-injected grouts

While Eqs (4) and (5) serve to give a rough estimate of pressure-induced penetration of pastes and suspensions for the ideal case of a plane slot, nature behaves differently. This is amply demonstrated by the fracture modes of real rock, illustrated for instance by the simple rock model in Chapter 2, i.e. the block structure with orthogonal sets of thin, ellipsoidal fractures. Assuming a constant injection pressure to be exerted on one of the faces of the block (cf Fig 42) we find that the grout will enter the widest fracture most rapidly. The penetration rate in this passage will drop successively due to the increased shear resistance and the rate of filling of finer fractures will then be the highest etc. For a finite injection time all the fractures will be filled to a certain, largely varying depth which is related to their aperture and surface characteristics, provided that thixotropic stiffening and gelation through chemical reactions do not take place rapidly. The penetration rate of grouts through fractures of the types shown in Fig 42, calculated by use of Eq (4) is illustrated in Table 8 for an injection pressure of 1.5 MPa and an assumed penetration depth of 0.5 m. It should be noticed that in practice the dimensions of the fractures are altered by the increased internal pressure caused by the injection. This is roughly incorporated in the example.

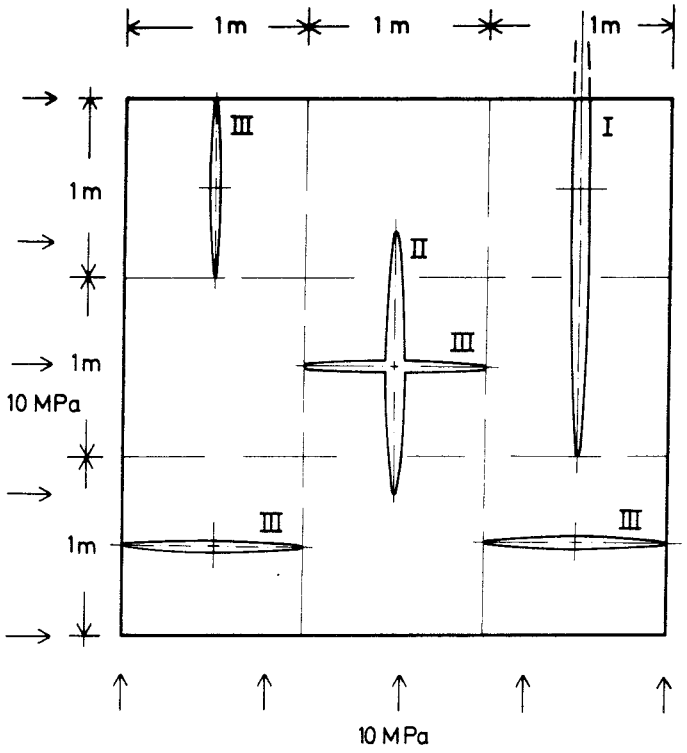

Fracture sets: I II III

Long diameter a = 3.0 m (truncated) a = 1.5 m a = 1.0 m
Short diameter c = 1.5×10^{-4} m c = 1.5×10^{-4} m c = 10^{-4} m

Fig 42. Schematic cross section through rock model with stochastically varied fracture geometry

Table 8. Approximate flow rates of grouts through the largest fractures forming the set in Fig 42

Viscosity Pas	Flow rate m/s
10^5	10^{-8}
10^4	10^{-7}
10^2	10^{-5}
10	10^{-4}
1	10^{-3}

This demonstrates that the viscosity should be well below 10 Pas in order to bring the grouting into narrow fractures, a matter that is well documented by practical experience and which will be further discussed in Chapter 5. Naturally, very low viscosities would mean high penetration rates, but unfortunately also a very low density and sealing power of the grout.

4.3.6 Miscellaneous

Electrophoretic transportation of montmorillonite particles into rock fractures appeared to be a possible alternative to pressure injection in a series of exploratory tests (43). The basic physical principle is that clay particles have a net negative electric charge in water solution and are therefore apt to migrate in a static electric field.

Plane glass plates were used to simulate rock fractures with an aperture of 0.2 mm and 0.1 mm. Each pair of plates, which were 500 mm long and 100 mm wide, were glued together at the long edges and connected to glass vessel at the short edges. One of them was filled with a bentonite slurry having a water content of 500 %, while the opposite vessel and the slot between the glass plates contained salt water. Copper electrodes were submerged in the vessels and a direct current of 240 V was applied for 3 days, the cathode being the electrode in the bentonite slurry. The average current, which tended to drop slowly, was found to be about 1.8 mA.

The clay-transporting power of the electric field was very obvious. Thus, after 2 days the 0.2 mm slot and a large part of the 0.1 mm slot were filled by a clay gel. A separate test in which the glass plates were brought into direct contact, demonstrated that smectite crystallites were transferred to the opposite end of the slot, also when the aperture was as small as about 0.01 mm. In this test, as well as in the tests with wider slots, the receiving vessel soon got its originally clear water non-transparent by transferred clay particles.

The hydraulic conductivity measured by applying a hydraulic gradient of the order of 0.2 over the slot was found to decrease to 1/1000 or less of the value before the sealing operation for the 0.1 and 0.2 mm slots. This pilot study suggested that electrophoretic treatment using bentonite slurries should be applicable for sealing narrow joints and fractures, and rock tests were therefore tried.

Theoretically, electrophoretic rock sealing requires that the fracture pattern need not be known. Clay particles are simply expected to move from the cathode to the anode along all joints extending from the hole with the cathode and the bentonite slurry, the rate of particle migration being proportional to the potential gradient according to the basic laws which govern electroosmotic as well as electrophoretic processes. These expectations were checked in a small-scale test using a 1 m^3 block of rock. The hydraulic conductivity tests showed fair to excellent sealing of hydraulically active joints and splitting of the block demonstrated that the main passages had been filled with a fairly stiff montmorillonite gel (water content ~100 %).

The promising results from the laboratory experiments suggested a larger field test which was also conducted in 1979 and 1980. The test arrangement had the form of a Ø 1 m, 3 m deep central hole and a number of circumferential holes extending downwards from the floor of a tunnel. The central hole contained the clay slurry and a negatively charged electrode while the outer holes hosted anodes. Various electrical potentials were used in a number of different setups some of which indicated a significant sealing effect. Others showed no effect at all, which gave the conclusion that the method was not

altogether a success. The reason for the negative results was most probably that the electrophoretic particle transportation was associated with an electroosmotic water transport in the opposite direction which created channels in the gel. Further development of the technique involving pump-drainage of the water at the anodes, and the application of salt-free water in the cathode hole is expected to yield significant improvement of the sealing effect.

4.4 Conclusions

A major conclusion from the cement and clay injection studies is that such substances cannot be driven far out in narrow fractures unless the yield stress and viscosity are kept lower than what has been tried so far in practice and in various experiments. It is clear, however, that the density of the groutings, which is known to be a determinant of the shear resistance, cannot be reduced too much since it is required that the fracture fillings remain physically stable in the fractures. This dilemma does not seem to be avoidable unless new grouting techniques can be developed. A necessary prerequisite for such work is to define criteria for the required properties of clay-type groutings in repository environment.

4.5 Required properties of fracture sealings

It is required from fracture sealings that they are durable and remain physically and chemically stable for very long periods of time. The stability criterion we are primarily concerned with here is that the fillings should not be easily eroded by water flow or have a structure that collapses if the rock is exposed to seismic shocks ("liquefaction") or changes in porewater chemistry.

4.5.1 Properties of injected substances at rest

4.5.1.1 Physical state

Expandable fracture sealings are very favorable, and ductile fillings with smectite as a major or important constituent are of primary interest. They are characterized by an ability to swell spontaneously to water contents that may be as high as about 1000 % if the major

adsorbed cation is sodium. Thus, if such materials can be introduced in fractures with an initial density of 500 %, the swelling potential is sufficient to fill up the fracture even if the aperture would expand by about 100 % due to tectonic processes, thermal changes or stress changes caused by excavation activities. Such clay gels also exhibit a very low hydraulic conductivity; at low hydraulic gradients and fresh-water conditions the coefficient of permeability is less than 10^{-8} m/s as long as the water content is less than about 500 %.

The granular and mineralogic compositions of smectite-based sealings are determinants of their physical properties, but large deviations from the hydraulic conductivity cited above are not expected even at low clay contents provided that the density of the interstitial gel filling between coarser grains remains approximately constant. It is important to notice, however, that the expandability is significantly reduced when the clay content drops below 30-50 %.

The matter of erodibility is important since hydraulic gradients driving water from the rock towards the deposition holes in the operational time of a repository, tend to erode fracture sealings. Vast experience from earth dam construction (44) shows that soft Na smectite gels are easily eroded, the critical water flow rate to initiate significant release of particles and particle aggregates being of the order of 10^{-4}-10^{-5} m/s. This rate is certainly exceeded in repositories before the groundwater situation is ultimately restored after backfilling of tunnels, shafts and boreholes. The addition of a substantial amount of coarser grains, such as finely ground quartz, is expected to improve the erosion resistance significantly, and if a certain amount of cement is also added to quartz/smectite mixtures, it would create strong but brittle networks of the coarser particles which would largely increase the erosion-resistance. However, this would require a content of silt-sized quartz particles of at least 60-80 % which, in turn, would reduce the expandability of the mixture considerably. It would actually be completely eliminated through ion exchange of the clay from sodium to calcium emanating from the cement. The cement may, however, have a limited lifetime and disappear at a late stage when its erosion-resistant properties are no longer required.

We conclude from these considerations that the composition of grouts has to be a compromise between those which yield a strong swelling power and flexibility and those which represent very erosion-resistant substances. A guide is offered by Table 9 in which the smectite component is represented by the commercial Wyoming bentonite MX-80, which has a Na smectite content of 70-80 % by weight. The physical properties refer to a water content equal to the liquid limit.

Table 9 Main physical properties of Na smectite-based sealings. (Fresh water conditions)

MX-80/quartz-filler. Ratio of solids	Water content w, %	Estimated hydraulic conductivity, m/s	Swelling ability	Erodibility
10/90	30- 50	$\geqq 10^{-8}$	Insignif.	Insignif.
50/50	150-300	10^{-8}-10^{-9}	Moderate	Low
75/25	300-400	10^{-9}-10^{-10}	Considerable	High/mod.
100 %	400-600	$\leqq 10^{-9}$	High	Very high

It is concluded that a mixture of 50-75 % Na bentonite and quartz filler, i.e. finely ground quartz with a maximum grain size of 50 µm, and a water content of about 150-400 % may represent optimum conditions with a hydraulic conductivity of less than 10^{-9} m/s and a certain swelling ability, and still with a relatively high erosion resistance. The introduction of such sealings would actually make the rock mass practically impervious. Admittedly, a change from fresh water conditions to a brackish water state like that in Forsmark, would increase the hydraulic conductivity by approximately 10 times and significantly reduce the swelling ability. The erosion resistance, on the other hand, would be increased.

It should be added that present investigations of alternative clay mineral candidates, like illite, may yield clay sealing blends with suitable physical properties and chemical durability.

4.5.1.2 Chemical stability

The major point with which we are concerned is the long term stability of the sealing. Since the near-field conditions where the temperature will be raised to about 80-90°C are of major concern, the same stability problem appears as for the highly compacted bentonite forming the canister overpack. Pure bentonite is expected to survive this heat treatment but there may be some doubt as to the survival of bentonite/quartz mixtures. Thus, the solubility of quartz increases dramatically in the high pH environment created by the bentonite and it is further increased by the temperature. This may lead to cementation through silification of both the smectite particles and the quartz grains. Thereby, much of the spontaneous swelling potential will be lost and the ultimate state may be that of a clayey siltstone or a silty claystone. Disregarding from the loss of swelling ability, these end products are excellent sealings, however, and such composite materials may be accepted for certain purposes.

4.5.2 Physical properties of sealing substances in the grouting phase

The thixotropy of smectite clays is of vital importance in the present context. It is known that when pure bentonite or bentonite/silt mixtures with the presently discussed water contents are remoulded and then left to rest, a major part of their maximum shear strength is built up in a few minutes (45). This means that the mixture regains a rather high shear strength soon after its preparation for grouting, and that even a rather short pause before and during the injection will increase the viscosity so much that there are difficulties in bringing the material into even wide fractures. Naturally, the successively reduced rate of penetration in the course of the grouting operation yields thixotropic stiffening and a rapid increase in viscosity.

If agitated, the gel-sol transformation of the smectite particle system yields easy sliding of the particles and a viscosity that is sufficiently low to allow them to be injected into narrow fractures. The explanation of this reduction in viscosity on mechanical disturbance is offered by the classical concept of clay quickness. Thus,

since the bulk density is low, the particles are arranged in unstable edge-to-face networks held together at rest by electrostatic forces. This fragile system is easily disrupted by mechanical agitation by which it is transformed to innumerable separate crystallites with the same overall negative surface charge, which produces particle repulsion and easy slip. The shear strength is insignificant in this state.

Finely ground quartz may also show flow properties like those of quick-clays (46). This is the case when the system is in a loose layering and exposed to shear. Thereby, the particles become dispersed and tend to fall into a denser layering and if porewater is not expelled, zero effective pressure and hence very soft conditions prevail.

4.6 A new grouting technique, "dynamic injection"

4.6.1 General

As shown in the preceding text, injection under a constant pressure of several megapascals will not bring even soft clay slurries into fractures with an aperture of less than 0.1-0.2 mm, while the injection of a grout that is continuously agitated should be effective. Such a technique, based on vibration of pressurized grouts was developed years ago by Karl Erik Nyman and it has long been used by the Swedish enterprise Svensk Grundundersökning, Arlöv, for injecting cement slurries into sediments consisting of sandy silts. The vibrations keep the silt particles in motion and help to build up the pore overpressure that yields the desired condition of strongly reduced effective pressure. After the treatment, the relatively pervious soil permits rapid consolidation of the injected zone, which then solidifies in the course of the time-dependent formation of various hydrous aluminum silicates.

A similar effect is expected if clay grouts are injected into rock fractures under the combined action of static pressure and shear waves but in this case the intrinsic physical properties of the smectite minerals are assumed to be of major importance. Thus, the thixotropy of low-density smectite gels would yield a low viscosity

in the soft state that results from the mechanical agitation, while stiffening caused by spontaneous gelation would appear at rest. A slight expansion of the fractures would be caused by the injection pressure, whereby the slurry would logically enter also remote parts of a fracture set. On pressure release, at the end of the treatment, the rebound would yield slight consolidation and further stiffening of the clay gel.

Dynamic injection of quartz filler or mixtures of such filler and smectite would also yield the desired flow properties. Here, a similar effect as in the soil injection case would appear, i.e. the silt-sized quartz grains would be floating in excess water or in a dispersed clay matrix without making contacts as long as the water content is higher than or about equal to the liquid limit.

In practice, the desired low-viscous condition of fine-grained grouts may be achieved by applying a constant injection pressure with superimposed shear waves induced by percussion. This technique, termed "dynamic injection", has been investigated in a number of tests, which are reported in the subsequent chapters.

5 EXPERIMENTAL

5.1 Introduction

The test program comprised viscometer measurement of the flow properties of a number of grouts of potential interest, and a series of laboratory tests in which they were injected into narrow slots between 1 m^2 concrete slabs under static pressure, as well as by applying the dynamic injection technique. A pilot test was also made in which the latter technique was used to bring bentonite into a simulated fracture intersecting a large borehole. Finally, a full scale field test was made in which the groutability and sealing effect of bentonite was tested under realistic conditions.

5.2 Characterization and measurement of flow properties of grouts

5.2.1 Test procedure and program

As indicated earlier in this report the viscosity and the "Bingham yield stress" are relevant parameters for the characterization of grouts used in conventional rock sealing. These properties were determined in a preliminary study, which comprised a number of fine-grained materials of possible use for sealing. For this purpose a Swedish BOHLIN Viskosimeter 82 with computer-based recording units was used (43). Three different equipments were applied for the determination of flow data and for checking their suitability. These were the standard concentric cylinder device, the standard plate/cone equipment and a set of specially made laboratory vanes.

5.2.2 Test results

The study, which is fully described in a separate report (47), comprised tests of pastes as well as cement/bentonite/water mixtures and cement/bentonite/filler/water mixtures. A few tests were made also of pure bentonites, which have been rather thoroughly investigated in earlier research projects (43). A complete list of investigated materials is given in Table 10, MX-80 being the SKB reference sodium

bentonite. Filler is the term used here for quartz powder with a grain size smaller than 50 μm, while the cement was a sulphate-resistant, low alkali grout cement (Cementa Co) with a grain size smaller than 75 μm.

It appears that the τ_o - and η-values are very sensitive to changes in water content; for pure bentonite they logically drop rapidly in the vicinity of the liquid limit. For pure sodium smectite this means that the water content has to be somewhat higher than about 400-500 % in order to bring the clay into a semiliquid state, while the corresponding value is ten times lower for pure cement. Applying the recommendations of Wittke et al we conclude that pure MX-80 would not be groutable for w<2000 % and that the same goes for all the MX-80/filler mixtures. Cement and cement/bentonite mixture with a lower water content than 60 % would not be groutable either.

Characteristic plottings of the shear stress versus strain rate of bentonite and cement are shown in Figs 43 and 44. Fig 43 demonstrates that a high shear stress peak (1850 Pa) appears at the very start of the rotation which is probably explained by gel-sol transformation of this highly thixotropic material. The shear resistance is then almost independent of the shear rate. Fig 44 shows the typical behavior of a soft cement gel. In the tests with the lowest water contents, there were considerable difficulties in evaluating the flow properties from the cone/plate tests, while vane testing may be more relevant.

The major conclusions from this study were that the conventional viscometer equipment is not very suitable for the testing of relatively stiff grouts, and that the imposed mechanical disturbance may be considerably less than that produced at dynamic injection. This suggests that the investigated substances may be groutable at lower water contents than the liquid limit, a matter that was amply demonstrated in the injection tests.

Table 10 Viscometer-tested materials for possible use in grouting operations (43, 47)

Test no	Material, ratio of solids	Water content w, %	Water composition (Na dominant)	τ_o Pa	η Pas
1	100 % MX-80	300	Weakly brackish	1700	750
2	100 % MX-80	400	Dist	360-700	
3	100 % MX-80	500	Dist, brack, salt	300-900	110-800
4	100 % MX-80	1000	" " "	6-40	5-26
5	100 % MX-80	2000	" " "	1-3	1-3
6	100 % MX-80	5000	" " "	<0.1	<0.1
7	75/15/10; MX-80/filler/cement	375	Distilled	180-400	1-2
8	75/15/10; MX-80/filler/cement	400	"	160-510	1-2
9	60/40; MX-80/filler	300	"	400-740	1-2
10	50/40/10; MX-80/filler/cement	200	"	240-1200	0.5-1
11	98/2 cement/MX-80	50	"	100	8
12	98/2 cement/MX-80	75	"	41	2
13	98/2 cement/MX-80	125	"	11	0.2
14	100 % cement	40	" (vane)	95	0.8
15	100 % cement	40	" (cone/plate)	-	6
16	100 % cement	50	" (vane)	32	0.3
17	100 % cement	50	" (cone/plate)	3	0.8
18	100 % cement	50	" (cylinders)	20	0.8
19	100 % cement	60	"	8	0.4
20	100 % cement	75	"	5	0.1
21	100 % cement	100	"	1.5	<0.1
22	100 % cement	125	"	1	<0.1

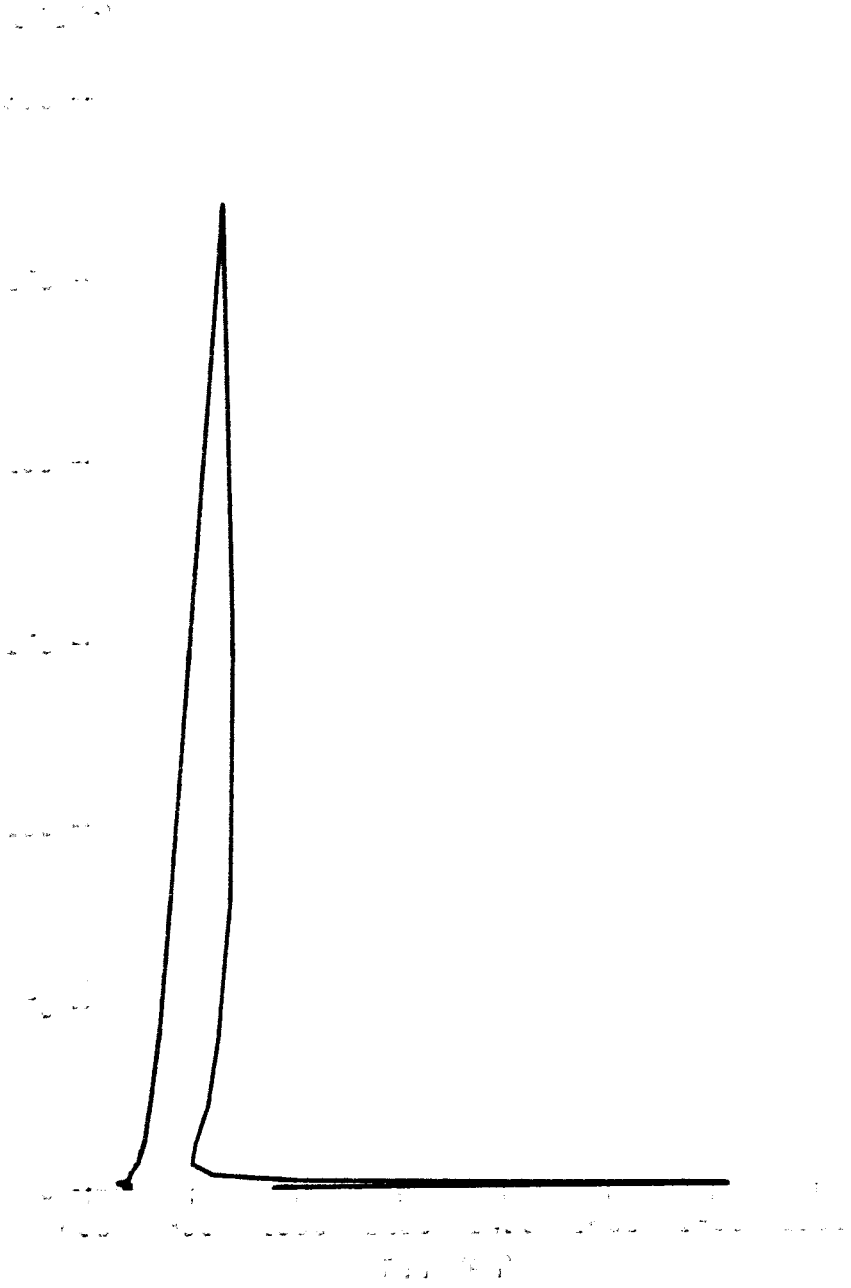

Fig 43. Typical viscometer diagram for bentonite at a lower water content than the liquid limit

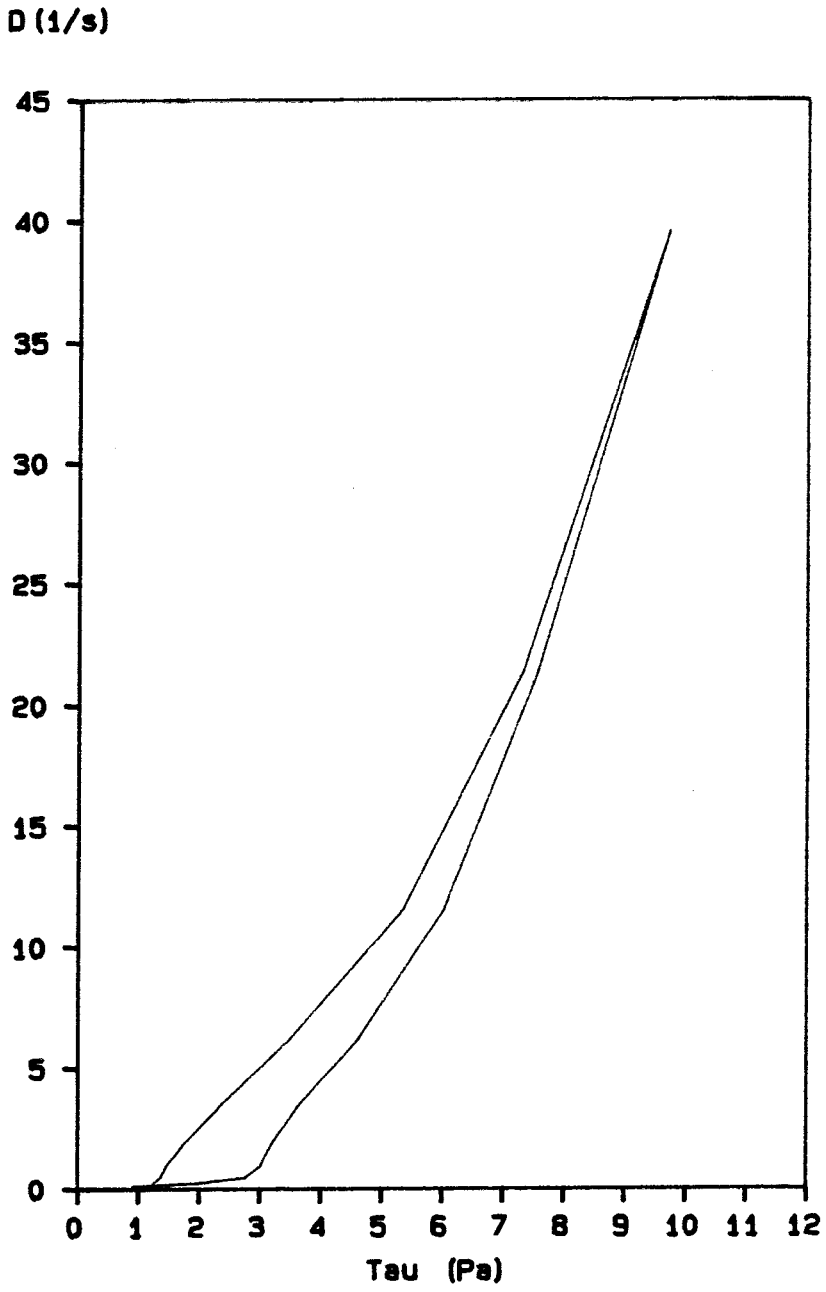

Fig 44. Viscometer diagram of cement which shows the typical increase in shear resistance at increased strain rate at relatively high water contents

5.3 Laboratory plate grouting experiments

5.3.1 Test procedure and program

An exploratory test series was made by SGAB in Lund to check the validity of the principle of dynamic injection. It involved injection of clay slurries and cement suspensions and pastes into thin parallel joints between concrete slabs. Rock fractures were simulated by bolting two concrete slabs together with small ring-shaped foils to keep the 10 cm thick slabs apart where the bolts passed through. The foils were 0.1, 0.2. 0.3 and 0.5 mm in different tests to yield apertures of the same width. The slabs had a side length of 1 m and one of them was equipped with a cast-in 20 mm pipe at its center, through which the sealing substance was injected. The distance between the bolts was only 20 cm in order to keep the slot aperture constant.

The injection equipment consisted of a rather small cylinder from a hydraulic jack with a tightly fitting piston, the cylinder being connected to a small container in which the slurry was applied, and to the pipe in the concrete slab. Two valves were arranged so that the cylinder could be filled by pulling the piston, while, at injection, the connection to the container was closed and a free passage opened to the injection point. The driving source was a hand-held TEX-50 percussion machine with a frequency of 1170 blows per minute, the air pressure being 0.7-0.8 MPa. In most tests, a 0.7-0.8 MPa static air pressure was applied on the back side of the piston while, at the same time, air was also let into the valve mechanism of the machine to produce the hammering (cf. Figs 45 and 46). This increased the injection pressure which was measured by using a Kistler piezoresistive transducer Type 4043 equipped with an amplifier and a digital multimeter (voltage) attached to the flexible injection tube.

Before each injection test, ordinary tap water was flushed through the slot to wet the concrete surfaces, which were carefully washed after each test. The slab surfaces were very even since form plywood was used for the casting operation. However, numerous voids ranging in size from that of colloidal particles to that of gravel were exposed at the surface and these were filled in the course of the

respective injection test by which they caused a delay in penetration that is not relevant to the conditions in actual rock fractures.

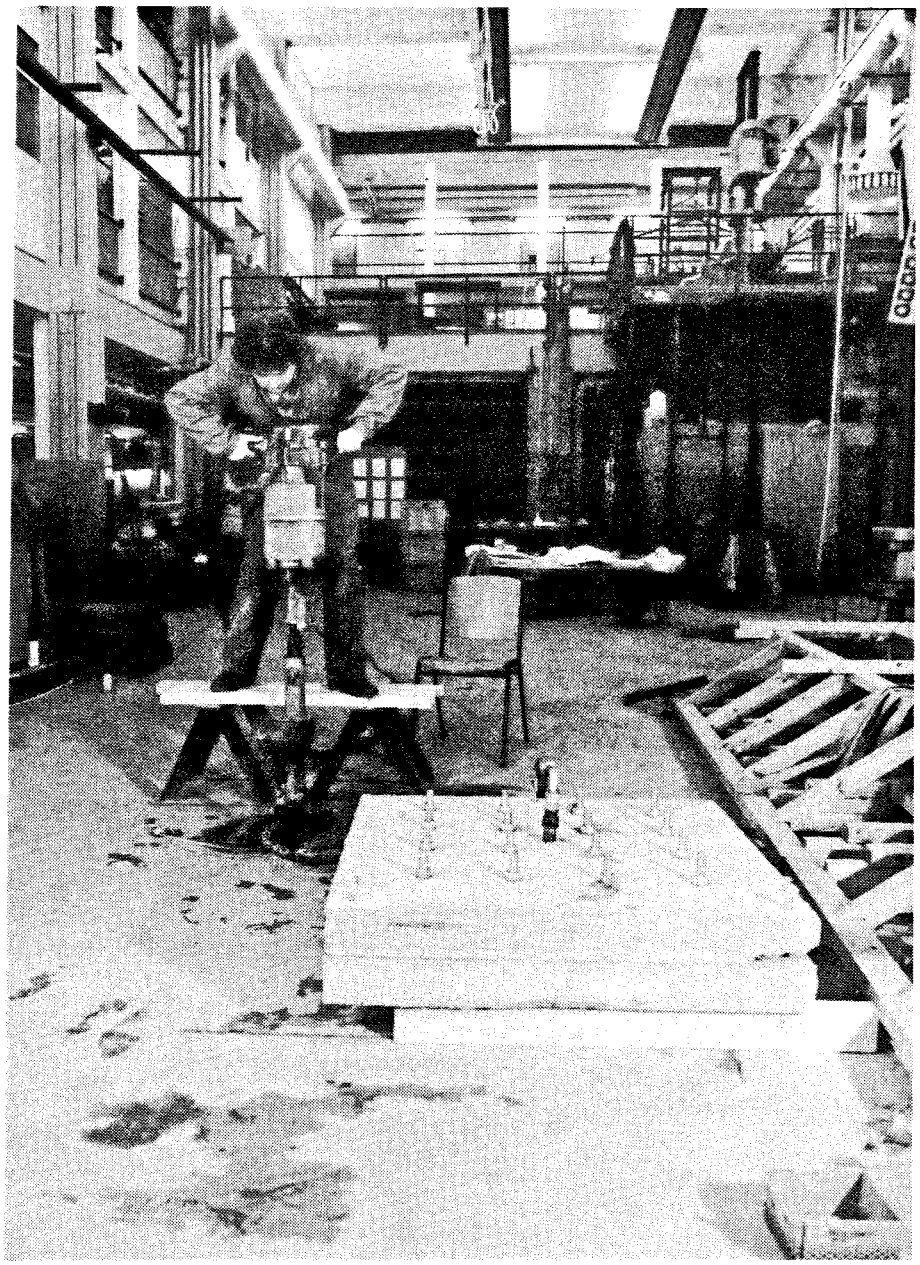

Fig 45. Setup of the plate injection test

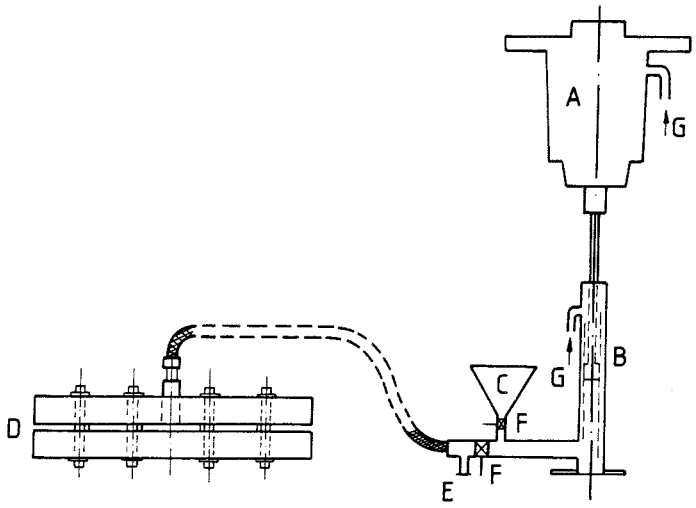

Fig 46. Schematic test arrangement for the plate injection.
A) percussion drilling machine, B) steel cylinder,
C) slurry container, D) slot between concrete slabs,
E) transducer, F) valves, G) air pressure

Twelve plate injection tests were made with bentonite, bentonite/filler and bentonite/filler/cement, the test data being specified in Table 11.

Table 11 Exploratory dynamic injection tests

Test no	Material, ratio of solids	Water content w, %	Slot aperture mm	Remark
A	75/15/10 MX-80/ filler/cement	400	0.3	Only dynamic injection
B	100 % MX-80	500	0.5	"
C	100 % MX-80	500	0.5	Only static pressure (0.8 MPa)
D	100 % MX-80	500	0.2	Dynamic injection combined with static pressure (0.7 MPa)
E	100 % MX-80	500	0.1	Dynamic injection with static pressure (0.8 MPa)
F	75/15/10 MX-80/ filler/cement	400	0.1	Dynamic injection with static pressure (0.7 MPa)
G	75/15/10 MX-80/ filler/cement	375	0.1	"
H	70/30 MX-80/filler	400	0.1	"
I	70/30 MX-80/filler	300	0.1	"
J	100 % cement	70	0.1	"
K	100 % cement	50	0.1	"
L	100 % cement	40	0.1	"

5.3.2 Test results

Test A Compound: 75 % MX-80
15 % filler
10 % cement

Water content: 400 %

Slot aperture: 0.3 mm

In this first test no static pressure was applied, only the percussion was in operation at 0.7 MPa air pressure for about 15 minutes. Practically no intrusion of the semiliquid substance took place as observed from the almost constant position of the piston, and this

was also confirmed when the slabs were taken apart for inspection. Thus, the grouts had entered the slot only to a few millimeters depth despite the rather long treatment. In this first test a manometer was used to measure the injection pressure, i.e. the pressure generated in the flexible tube leading to the injection point, but self-plugging of the connection occurred and no pressure reaction was observed. It is not known whether other frequencies or a higher air pressure would have yielded more favorable results but it is probable that a much higher dynamic energy input would have improved the penetration power of the grouting.

An alternative explanation of the unsuccessful treatment was that consolidation, i.e. densification through dewatering, and arching effects caused by piling up of larger particles, plugged the slot at the point of injection. This would be a natural effect if the slurry had not been effectively agitated.

Test B	Compound:	100 % MX-80
	Water content:	500 %
	Slot aperture:	0.5 mm

This experiment was conducted in the same way as Test A, i.e. percussion was applied without superimposing a static pressure. This time the grout went in 25-30 cm from the injection (cf. Fig 47) point but the penetration can still be regarded as insignificant. The impression was that the energy input was insufficient to make the slurry move deep into the slot. Thus, the pressure waves induced by the percussion did not seem to reach through to the injection point, so the larger part of the slurry appeared to have stiffened thixotropically in the slot.

Test C	Compound:	100 % MX-80
	Water content:	500 %
	Slot aperture:	0.5 mm

This test was made with the same grouting as in the preceding test but with only static pressure of 0.8 MPa. No penetration at all could be noticed this time.

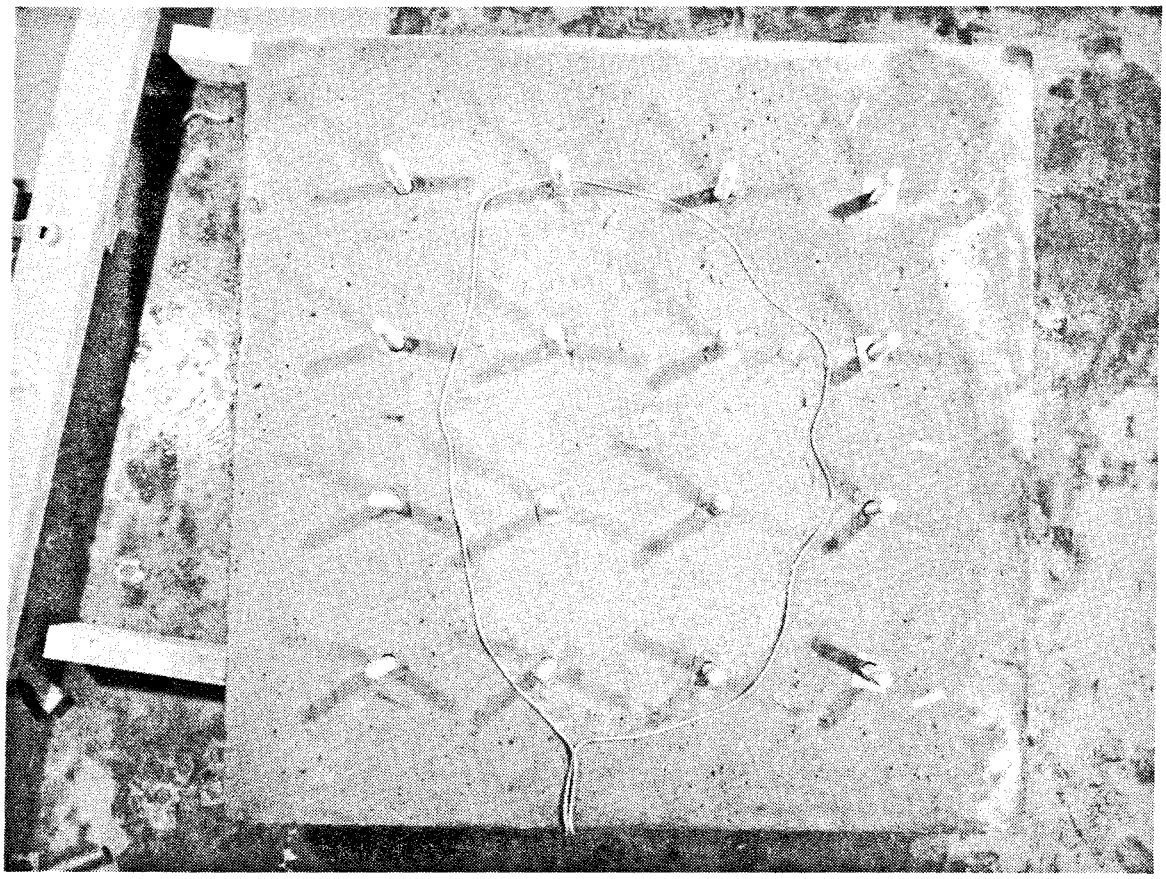

Fig 47. View of the surface of the lower concrete slab showing the extension of the clay grout (Test B). The white string marks the gel front

Test D	Compound:	100 % MX-80
	Water content:	500 %
	Slot aperture:	0.2 mm

The impression that the transfer of the dynamic pressure through the injection tube was insufficient in Tests A and B led to the idea to combine the hammering operation with a superimposed constant pressure on the piston. This was first tested with bentonite only, the water content being approximately equal to the liquid limit as in Test B and C.

The effect was very good. Thus, the slurry passed through, filled up and flowed out of the narrow slot within a few seconds (cf. Fig 48). The principle of applying a constant pressure of 0.7 MPa on the lid, by which the imposed pressure waves were effectively transferred throughout the slurry, was applied in all subsequent tests.

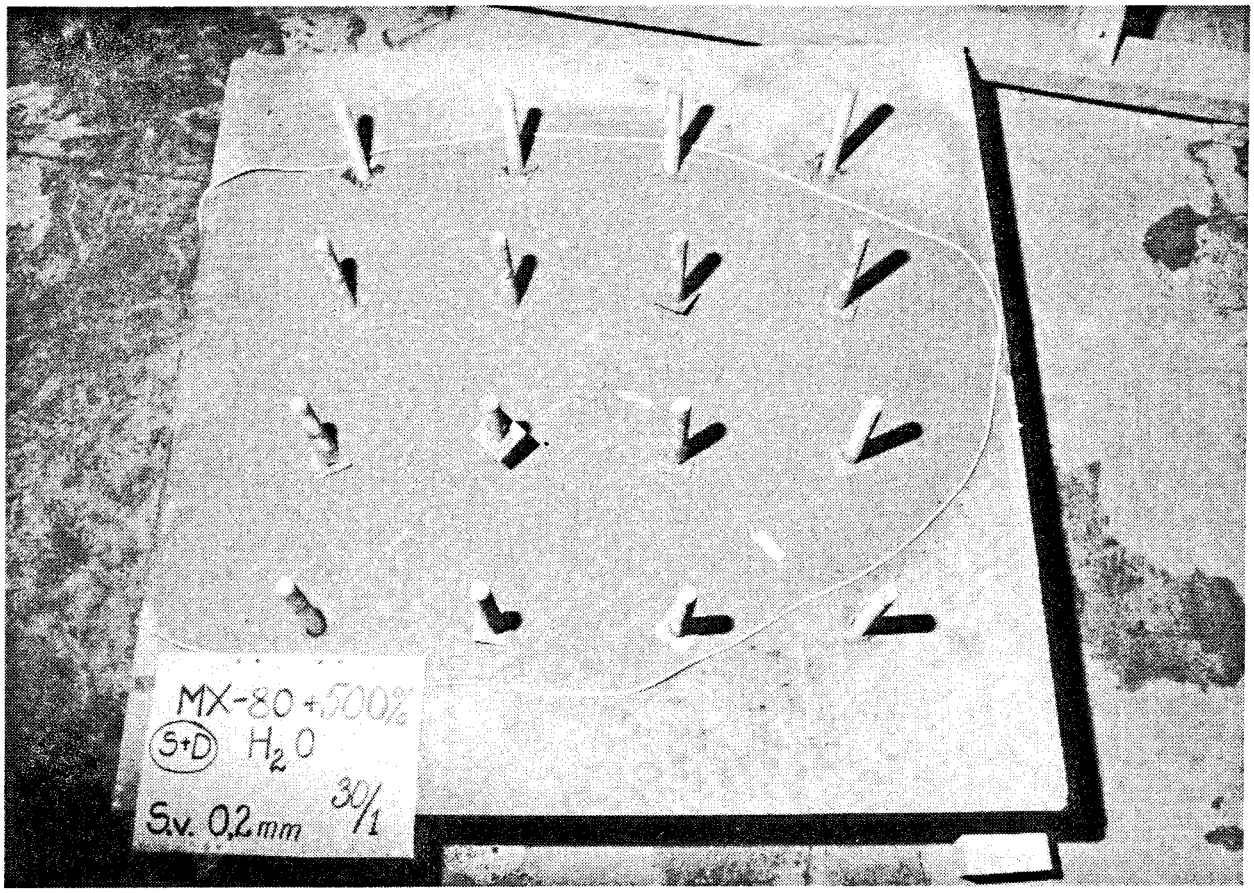

Fig 48. View of the surface of the lower concrete slab showing the extension of the clay grout (Test D)

Test F	Compound:	75 % MX-80
		15 % quartz filler
		10 % cement
	Water content:	400 %
	Slot aperture:	0.1 mm

All the particles of this composite grout were smaller than 75 μm and there was some doubt as to the possibility of bringing it into the slot but the treatment was again successful; the slurry behaved as the bentonite/water mixtures and no separation of the individual components took place.

Unfortunately, the prepared volume of the relatively stiff mixture was too small and the injected mass did therefore not fill the entire slot. A 10-15 minute pause was taken shortly before the termination of the injection in order to refill the cylinder, but during this period of rest the mass stiffened so much that additional injection was impossible. The appearance of the filling at the end of the test is shown in Fig 49.

Test G	Compound:	75 % MX-80
		15 % quartz filler
		10 % cement
	Water content:	375 %
	Slot aperture:	0.1 mm

This test was aimed at finding the lower limit of the water content range for which the dynamic injection technique can be used. The value 375 % must have approached this limit since the flow was much slower than that at 400 % water content. A temporary stop was made also in this test and continued treatment was not successful until the percussion machine was strongly pressed towards the piston shaft. The mass then turned liquid again and an outflow at one of the edges took place (Figs 50 and 51). Here, a tendency of the components to separate was observed which may be related to different mobilities at the reactivation of the flow of the filler and cement on the one hand, and of the clay on the other. The matter requires further study.

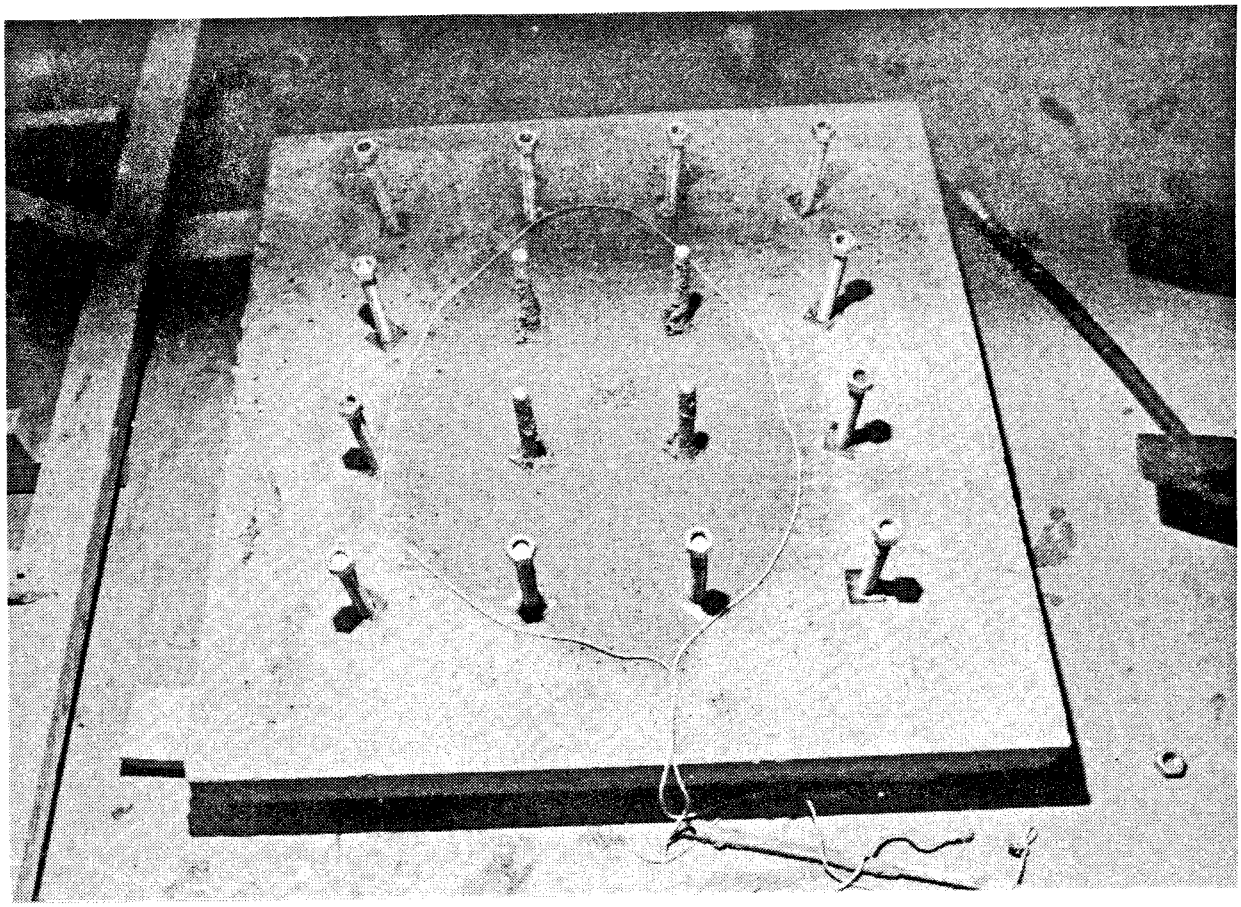

Fig 49. View of the extension of the grout in Test F. The front is not more than 10 cm from the closest edge

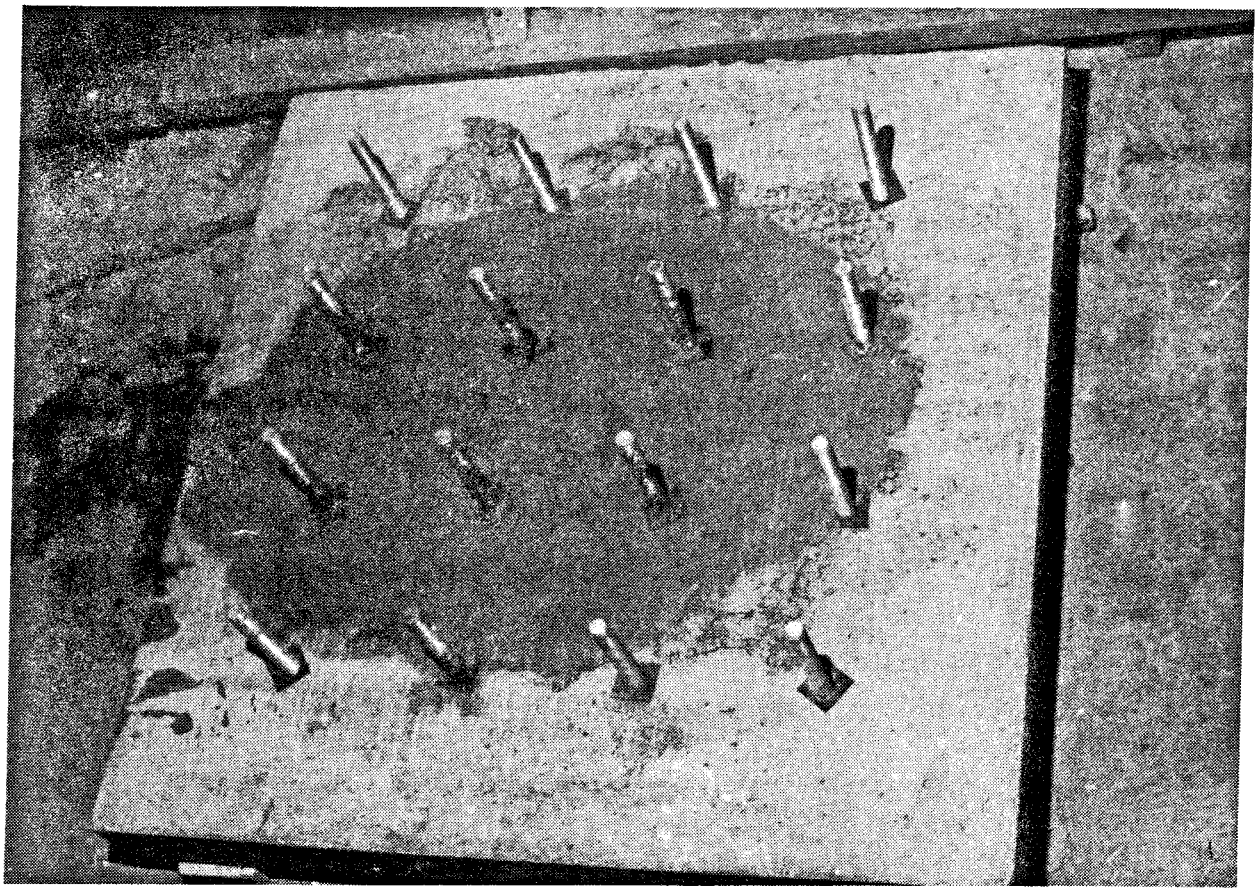

Fig 50. View of the extension of the clay/quartz/cement grout in Test G. The mass finally flowed out through the slot at the left side

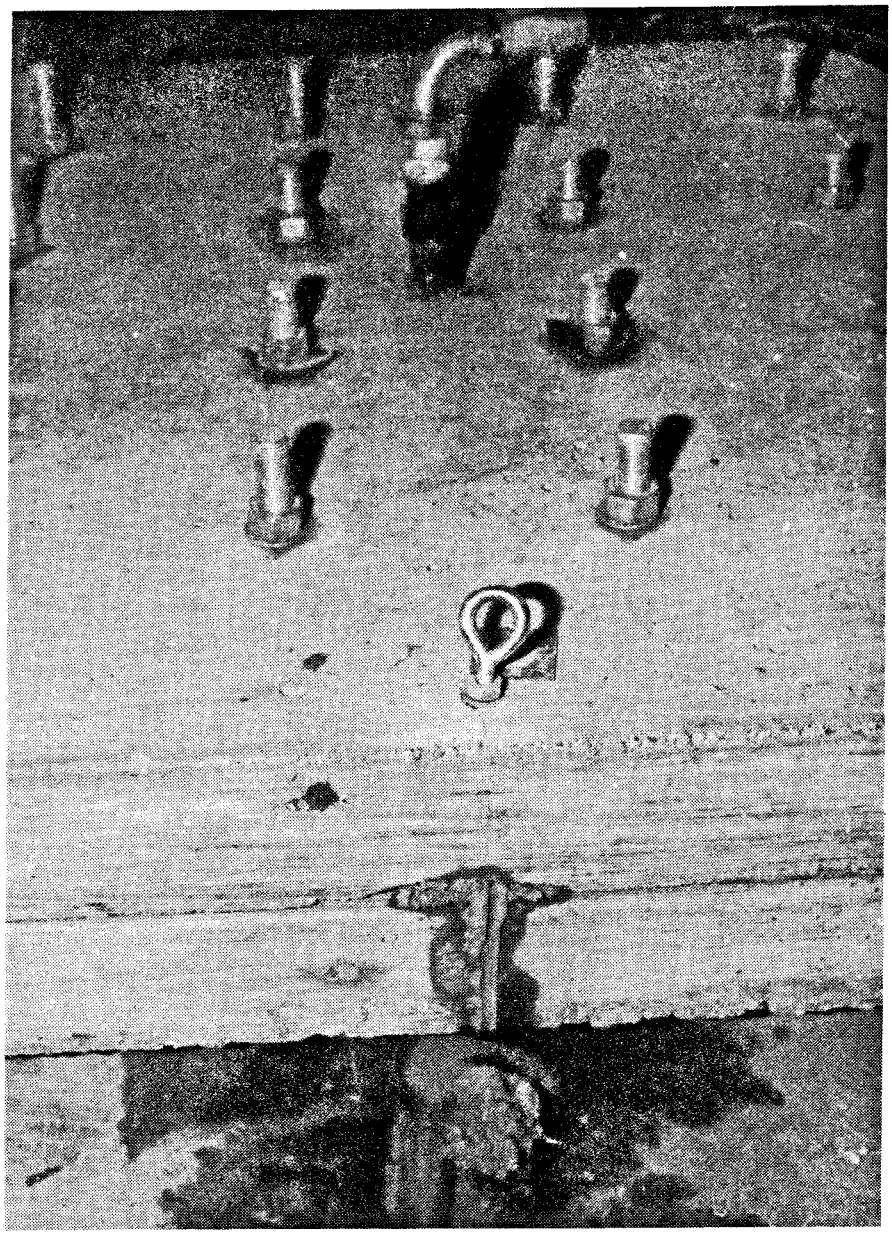

Fig 51. Close-up of the mass outflow in Test G

Test H	Compound:	70 % MX-80
		30 % filler
	Water content:	400 %
	Slot aperture:	0.1 mm

Static pressure alone did not bring in the grout at all, while it flowed in and filled the slot as in Test D in a few seconds when the percussion machine was started.

Test I	Compound:	70 % MX-80
		30 % filler
	Water content:	300 %
	Slot aperture:	0.1 mm

The result was identical to that of Test H, but the inflow at the onset of the dynamic treatment was slower.

Test J	Compound:	100 % cement (Cementa)
	Water content:	70 %
	Slot aperture:	0.1 mm

Static pressure did not bring in the grout to a depth of more than 1-2 centimeters, while it flowed in and filled the slot as in Tests D and H when the dynamic treatment started.

Test K	Compound:	100 % cement
	Water content:	50 %
	Slot aperture:	0.1 mm

Static pressure alone did not bring in the grout at all while it flowed in and filled the slot as in Test J but significantly slower.

Test L	Compound:	100 % cement
	Water content:	40 %
	Slot aperture:	0.1 mm

For this test a larger percussion machine was used but the grout could only be forced into the slot to about 20 cm depth despite the 7

min long treatment. It was concluded that the groutability limit was reached in this test.

5.3.3 Conclusions

It is clear that clayey compounds with a composition that may represent optimum conditions with respect to swelling ability, strong thixotropic behavior, low hydraulic conductivity, and erosion resistance through a suitable content of silt-sized grains, can be forced into very narrow fractures to a depth of several decimeters and probably even meters by use of the dynamic injection technique. The limiting factor is the grain size of the grout. The degree of filling is concluded to be very high and uniform because of the fluid character of the grouts. Since injection most probably increases the aperture of the fracture temporarily, the visco-elastic rebound of the rock after pressure release is expected to distribute and consolidate the grouting over the entire cross section.

The tests were sufficiently encouraging to suggest a continuation on a larger scale, as described in Chapters 5.4 and 5.5. It should be noticed, though, that no water backpressure, simulating the pressure component p_2 in Wittke's Eq (6), was applied and that the groutability may therefore be less good in practice.

It should also be added that a pilot test was made for identification of the penetration of soft clay grout by use of radar technique.* Antennae were placed on the upper concrete slab and profiles taken immediately before and after the grouting operation and about 2 hours after its completion. A clear difference in signal amplitude was obtained, particularly between the first and second recordings, which shows that the technique is feasible. The additional amplitude change that was found to take place between the two last measurements suggests that consolidation of the grout had taken place.

---

* The test was conducted by Dr Peter Ulrichsen, Lund University of Technology and Natural Sciences

5.4 Injection test in simulated deposition hole

5.4.1 General

An ideal application of the dynamic injection technique to the case of sealing of canister "near-field" rock, would be to make the grout enter fractures that are exposed in deposition holes (Fig 52).

5.4.2 Test arrangement

The testing of the injection technique required the use of packers with a very effective sealing ability, for which a prototype has been manufactured and tested. It was designed by SGAB, Lund, and manufactured by Svensk Grundundersökning Co, Arlöv, and consists of a device in which the borehole with an intersecting 0.1 mm fracture is simulated by two steel tubes with an inner diameter of 76.5 cm diameter (Fig 53). The packer has the form of a steel cylinder equipped with pneumatically operated rubber sealings at its ends. These sealings were specially made by Trelleborg Co.

5.4.3 Test results

A larger percussion drilling machine was used in this test than in the preceding plate tests, the frequency being 1800 blows per minute in the recent test. The grout was pure MX-80 bentonite with a water content of 450 %, and it was successfully injected into the 0.1 mm wide slot in a few seconds. No water backpressure was applied and the test certainly needs to be repeated in rock before safe conclusions can be drawn.

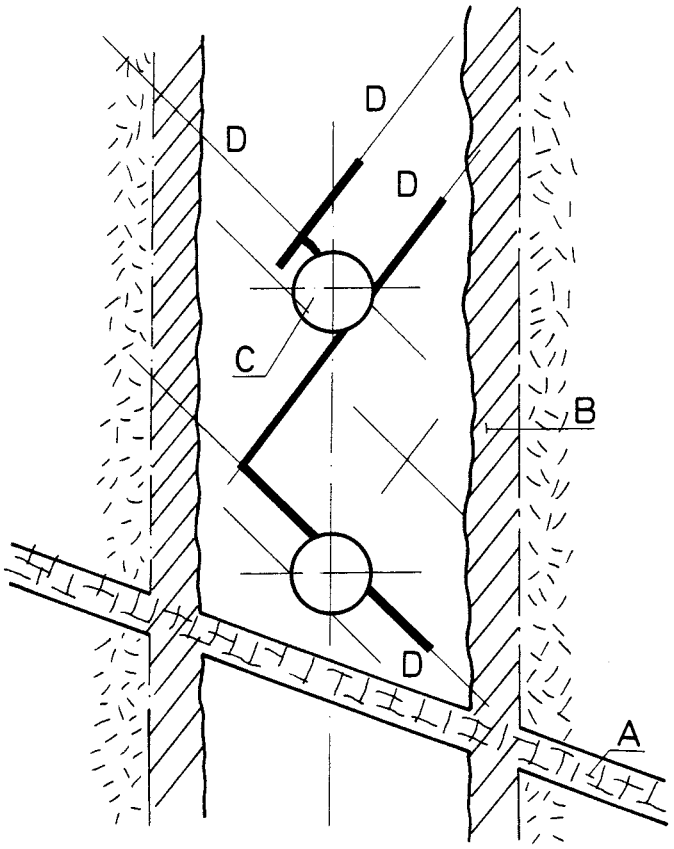

Fig 52. Principle of shunting off fractures (D) serving as short-circuits; thick lines indicating sealed parts. A is major hydraulically active rock zone, B is zone of increased permeability due to blasting and stress release ("super-conductor"), C is canister hole.

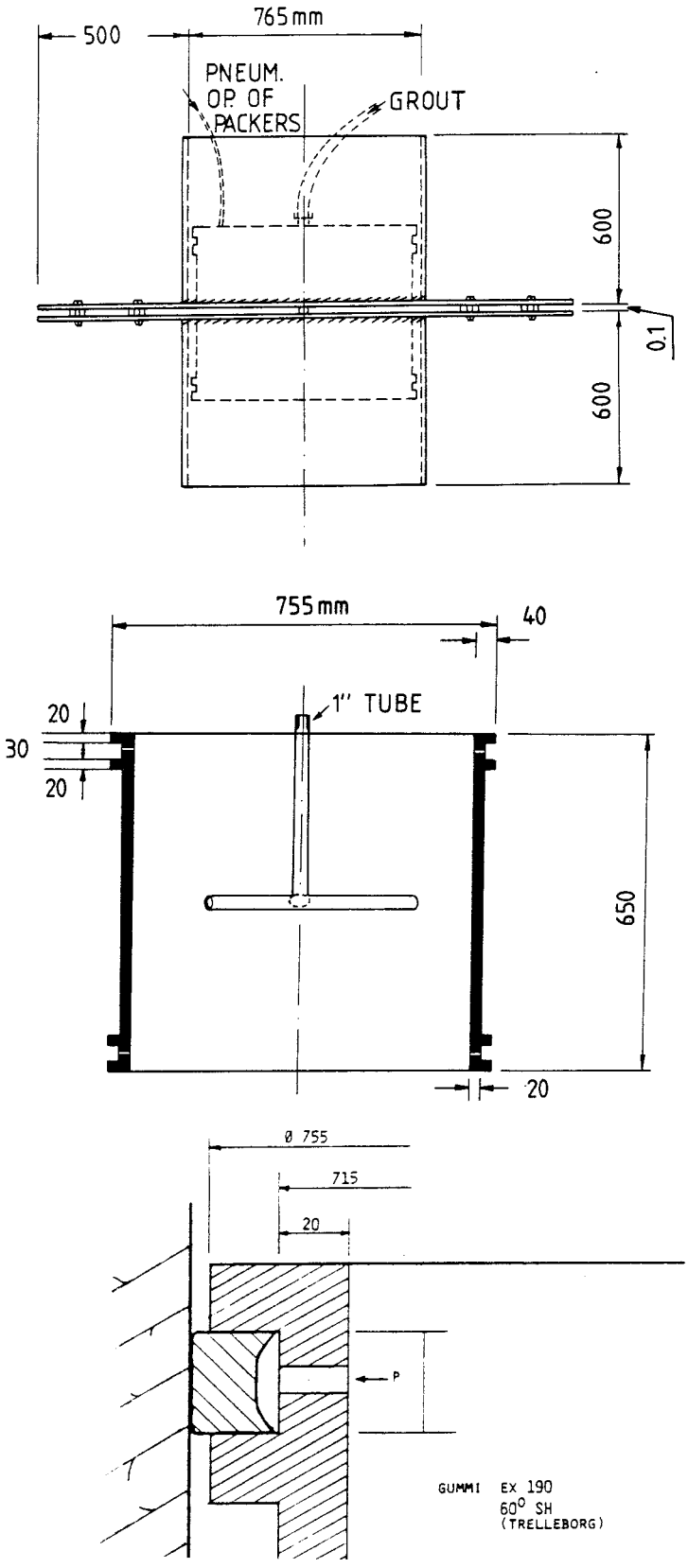

Fig 53. Equipment for pilot injection test in simulated deposition hole. Upper picture shows steel tubes representing the borehole while the lower picture shows the packer and detail of rubber sealing

5.5 Field test

5.5.1 General

At the end of the current tunnel "HP" plugging experiment in the Stripa mine, it appeared to be possible to test the applicability of the dynamic injection method in granite. This experiment, which is conducted in granite at 350 m depth, has the form of a huge double packer test with two concrete walls at about 8 m distance sealing off a drift with 20 m^2 cross section, the walls being connected by a Ø 1.5 m steel tube (Fig 54). Highly compacted bentonite blocks were arranged as "O-ring"-sealings at the interface between the concrete and the rock in the construction period in early 1983, and in late 1985 the blocks had fully developed their sealing ability, as concluded from continuous measurement of the water outflow from the pressurized sand-filled space confined by the concrete walls, the rock and the steel tube. The water pressure had been maintained at 3 MPa for 10 months and the leakage through the rock had become constant and equal to about 85-100 liters per hour. A large part of this water was assumed to be discharged through two major rock structures, one of them being a steeply oriented fracture (I in Fig 55) which is interconnected with and drained by fractures exposed at the outer end of the tunnel plug (II and III in Fig 55), the other consisting of two sets of steeply oriented fractures in the tunnel floor (IV and V in Fig 55). It was estimated from several series of tracer tests that these structures were responsible for about 50 % of the total leakage and that successful sealing of them would therefore reduce the total outflow by 50 %, i.e. to about 10 liters per hour at 1 MPa pressure, 25 liters per hour at 2 MPa pressure, and about 50 liters per hour at 3 MPa pressure. Figs 55 and 56 also show suitable positions of injection holes and expected spread of grouts.

The groundwater pressure in the rock at the interface between the rock and the bentonite/concrete walls is assumed to have been approximately equal to the water pressure in the sand-filled space throughout the "HP"-test. This pressure was kept constant at 250 kPa during the grouting experiment to simulate a piezometric head of a common order of magnitude.

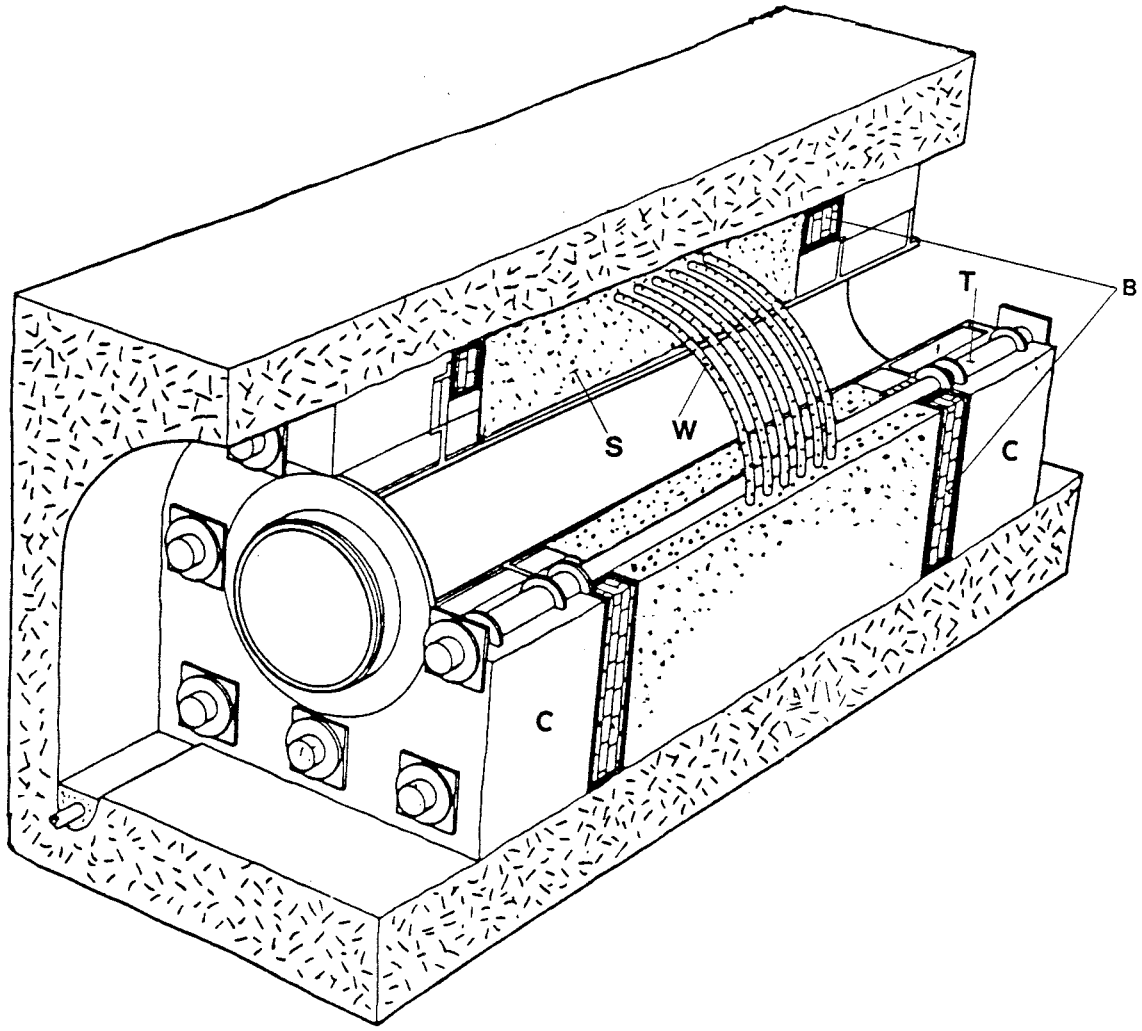

Fig 54. The tunnel plug experiment in Stripa. C represents concrete walls with bentonite "O-ring" sealings (B). S is the sand-filled injection chamber in which the water pressure was varied from 0-3 MPa, W pipes for water injection, and T tie-rods

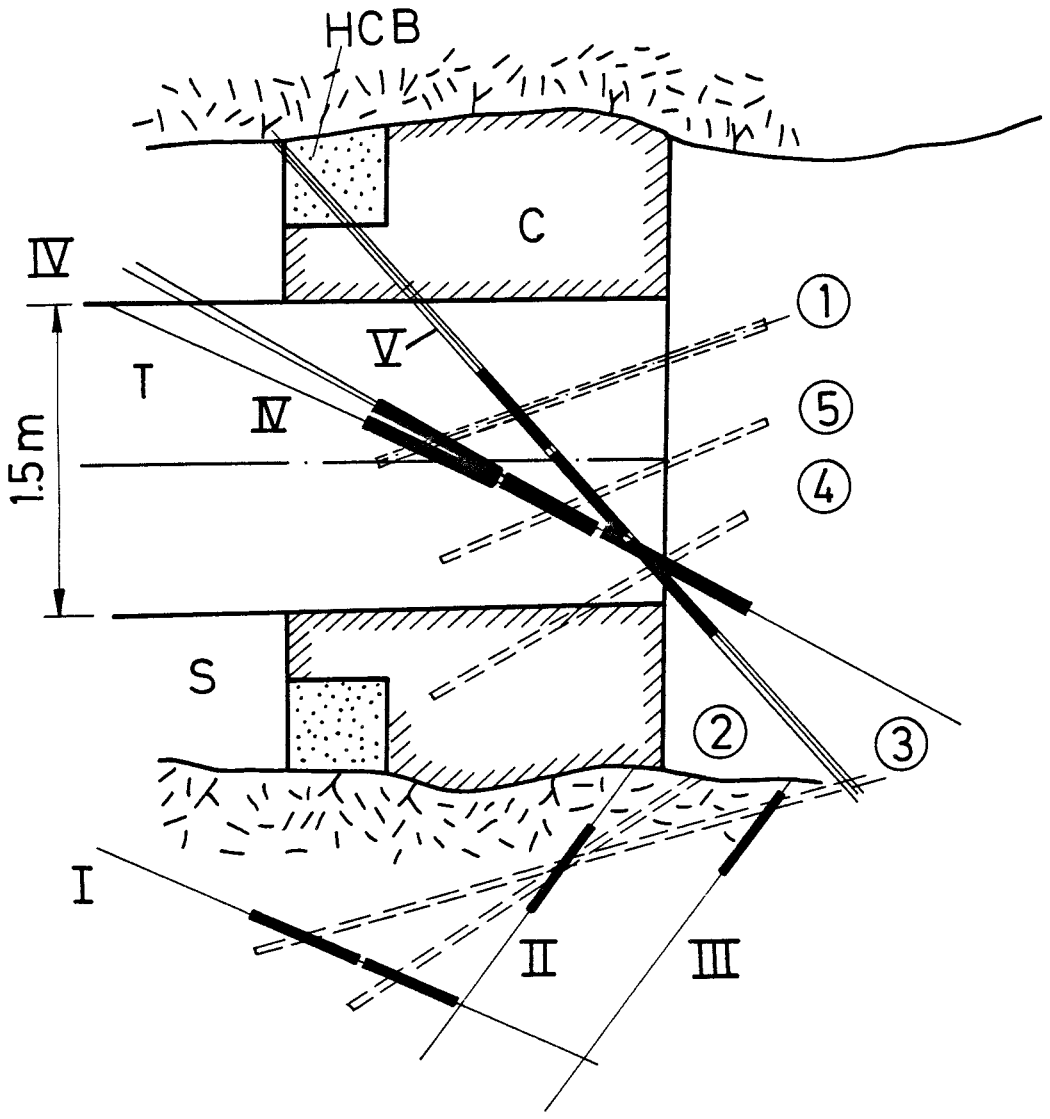

Fig 55. Major rock fractures, I-V at the outer end of the tunnel plug. C represents concrete, HCB highly compacted bentonite and T steel tube. The space S is water saturated sand in which the water pressure can be raised to 3 MPa. Holes 1-5 for grouting are also shown, the thick black zones indicating the expected spread of the injected grout

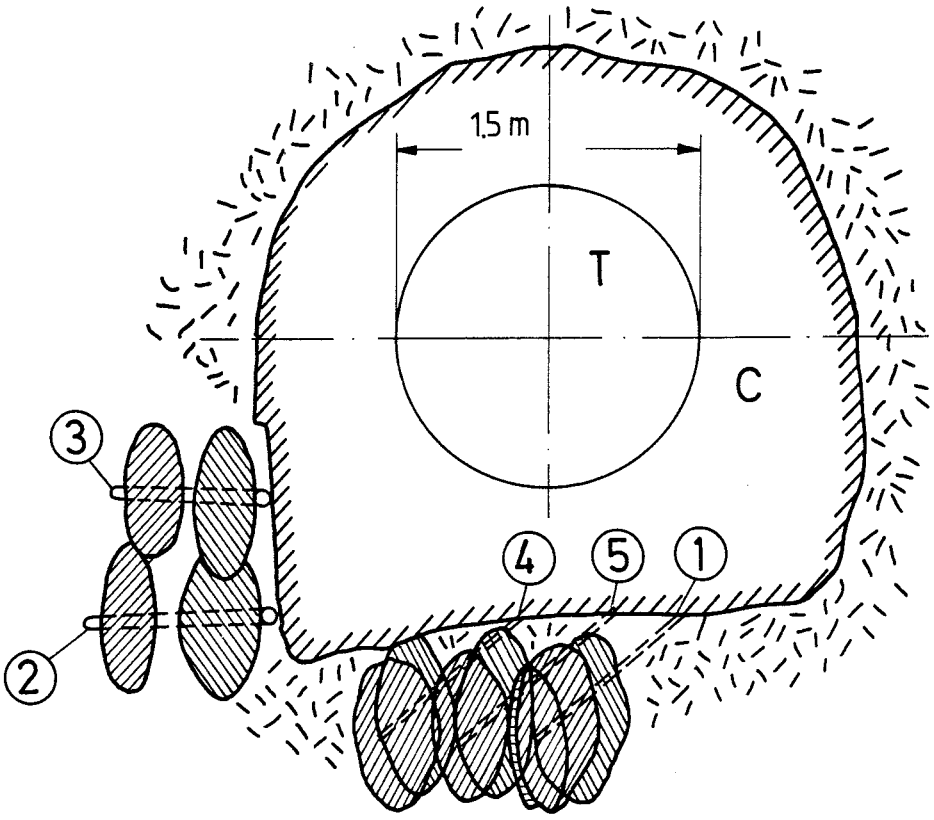

Fig 56. Front view of the tunnel plug with approximate positions of the injection holes and expected spread of grouts.

5.5.2 Field work

Five Ø 56 mm boreholes, located according to Figs 55 and 56, were diamond-drilled to intersect the major water-bearing structures and to seal them. The cores were carefully mapped to identify major fractures and to select suitable positions for the mechanical packers, which were used for the grouting and for measuring the pressure during and after the injections. The character of the rock as evaluated from the cores is shown in Figs 57-59. The high fracture frequency of all the five cores strongly supports the authors' hypothesis that blasting produces disintegration and a high hydraulic conductivity of the rock close to the periphery of tunnels and shafts.

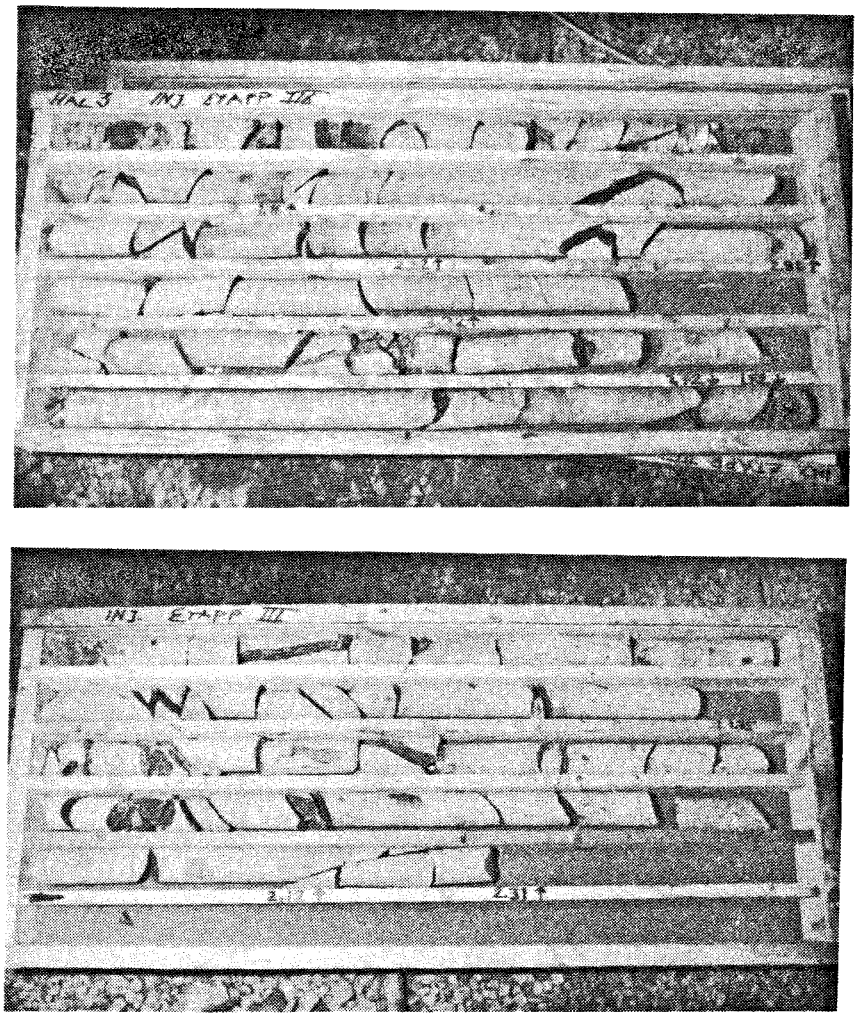

Fig 57. Typical appearance of the cores, indicating a high degree of fractures generated by the blasting

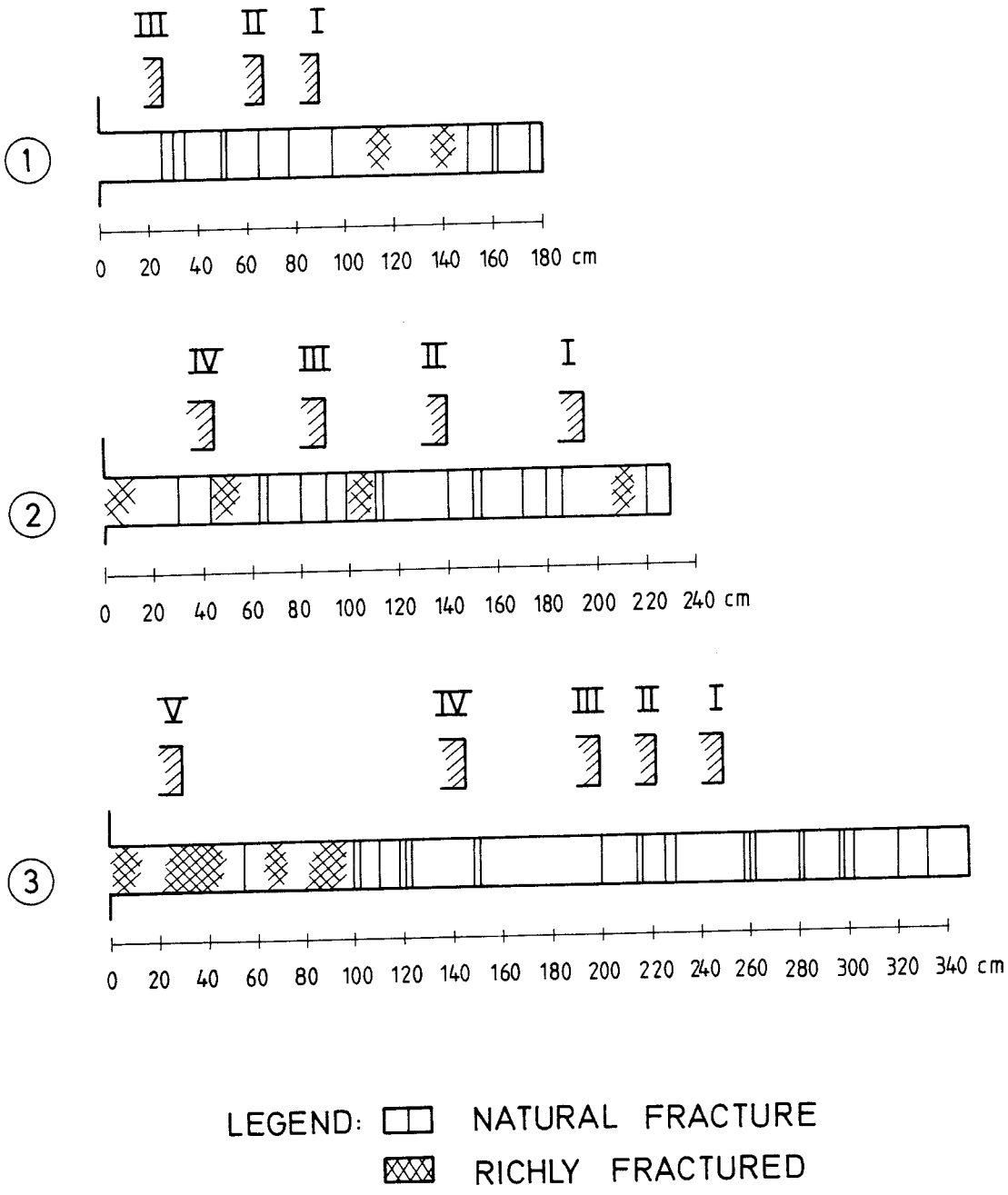

Fig 58. Core mapping of holes no 1, 2 and 3. Figures I, II etc represent the position of the inner end of the packer at each grouting stage

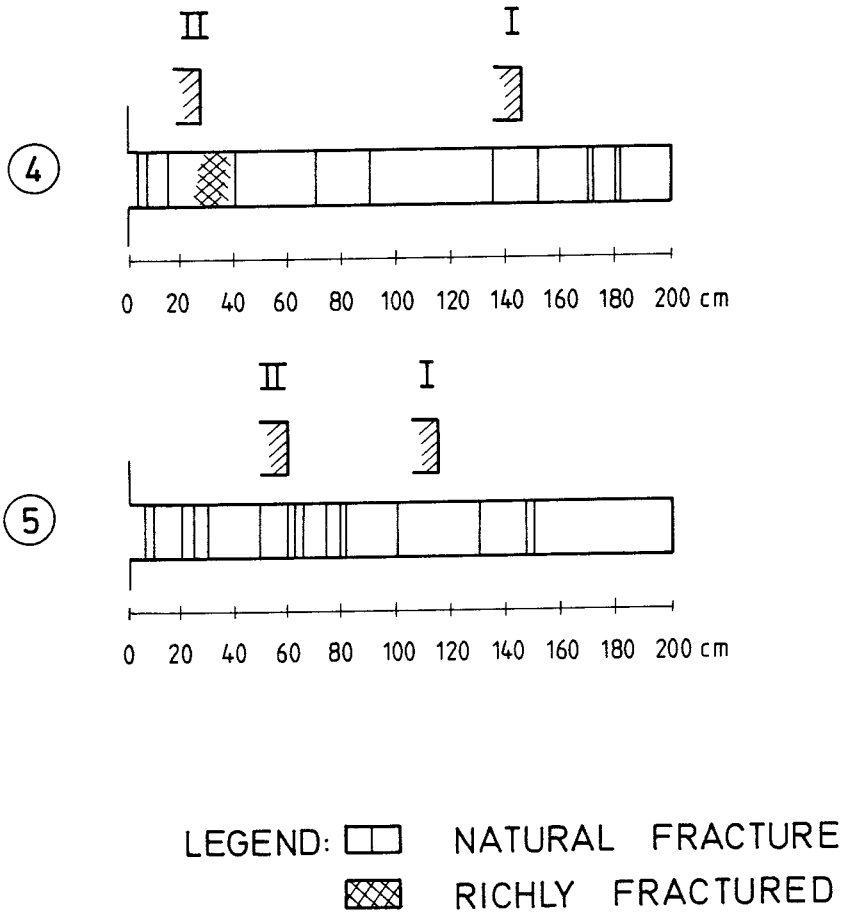

Fig 59. Core mappings of holes no 4 and 5. Figures I, II etc represent the position of the inner end of the packer at each grouting stage

5.5.3 Grouting equipment and procedure

The equipment used for the grouting was developed by the company Svensk Grundundersökning, Arlöv. It consisted of a large cylinder hosting the grouting, on which a static pressure of 1 MPa was exerted by a tightly fitting piston. The required superimposed dynamic loading was achieved by use of a heavy percussion drilling machine, which was operated at about 1800 blows per minute. Several special arrangements were made to facilitate the filling of the grouting into the cylinder and certain improvements of the machine are still required for optimum performance (Fig 60).

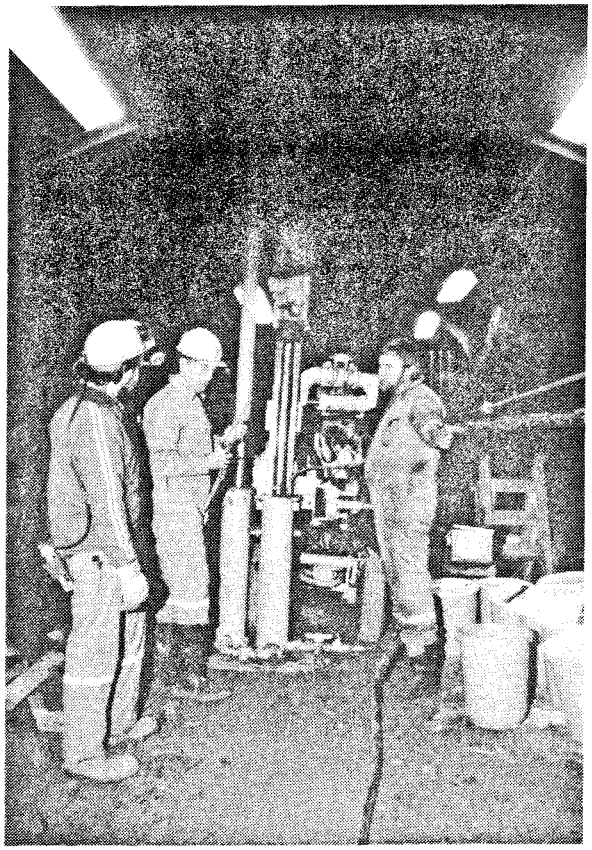

Fig 60. View of the grouting equipment

One hole at a time was grouted, starting with the packer in the innermost position and following the procedure in Fig 61. The percussion machine was operated for about 3 minutes after which the packer was moved to the next position and the grouting continued. The packer was left in the outermost position with the valve closed so that pressure changes could be recorded after the completion of the grouting work. The pressure reading at this late stage was made by use of manometers, while the pressures which were built up in the course of the injections were measured by means of a Druck PTX 110/W transducer and an Ultralette UV plotter. The high resolution power of the latter equipment was required for the identification of the detailed pressure pattern.

The grouting substance was a commercial bentonite, Tixoton, from Süd-Chemie (West Germany). This clay is usually delivered in sodium form with a liquid limit of about 450 %. Since sodium bentonite is being used in the HP experiment and it is required that the two bentonites can be distinguished at the excavation that is planned in spring 1986 to identify to what extent the two clay sealings have interacted with the rock, an ion-exchanged version of this same clay was used for the injection. Thus, clay in lithium form was prepared for grouting by mixing it with tap water to a water content of 500 %, which was found to be the liquid limit of the clay. Methylene Blue was added as well to make it directly visible at the injection stage, the concentration of the dye being 200 ppm.

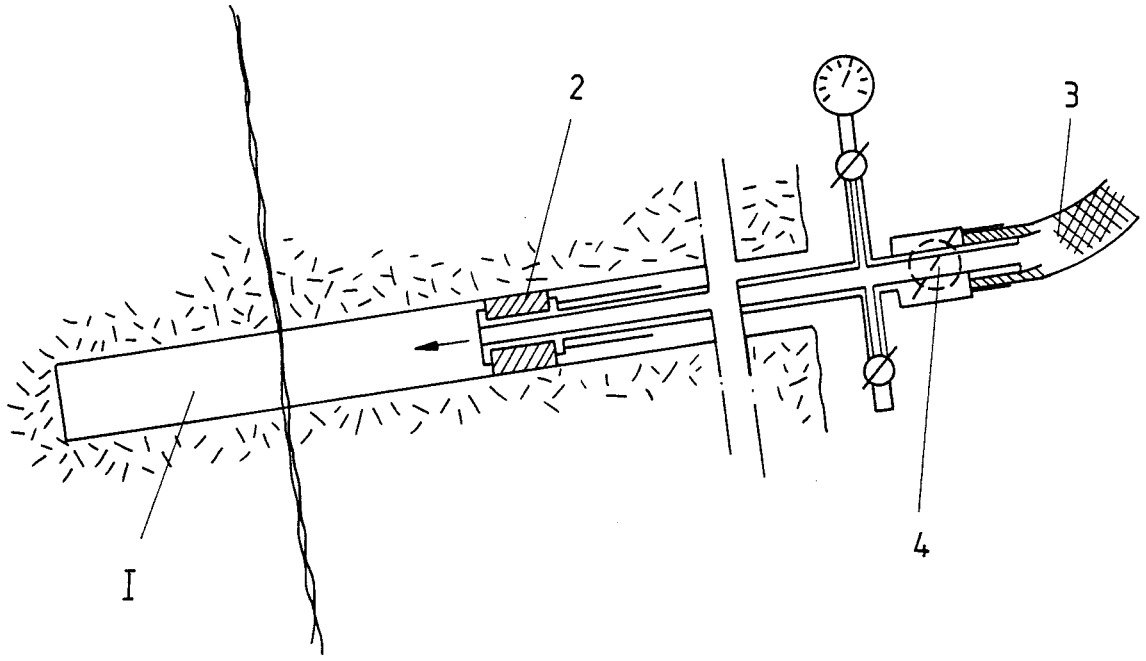

Procedure: a The hole (1) is first filled with the clay slurry by use of the packer tube (2)

b The flexible tube (3) from the large cylinder with the clay slurry is attached and 1 MPa static pressure is applied

c Percussion hammering

d Valve (4) closed, injection device removed

Fig 61. Detail of the packer equipment in the holes and specification of the grouting procedure

5.5.4 Results

The grouting experiment was evaluated with respect to:

1 Amount of injected material
2 Build-up and retention of injection pressures
3 Sealing effect and erodibility

5.5.4.1 Amount of injected material

The amount of clay slurry that entered rock fractures was estimated by direct measurement of the displacement of the piston which pressed against the clay. Since the penetration depth was not assumed to exceed one or a few meters and the average fracture aperture was estimated at 0.1 mm, the expected volume was assumed to be less than one liter in each hole. The accuracy of the measurements was low because of various slight leakages but rough estimates indicate that 2.5-3 liters were injected into the fractures intersected by the respective hole. This discrepancy may partly be explained by larger actual apertures than the assumed ones and by pressure-induced expansion of the fractures. A conservative conclusion is that clay had entered wider fractures, i.e. the ones forming the major sets in Figs 55 and 56, to a depth of at least one meter. Very probably, the distribution patterns were irregular and fingerlike with local deep intrusions alternating with very limited penetration depths. Since the first-mentioned are also primary water passages the sealing effect should be significant.

In two of the holes clay was pressed out through fractures when the packer was in the outer position (Fig 62). The way the clay appeared, proves that groutings of the present sort can be effectively driven through narrow fractures by the applied method.

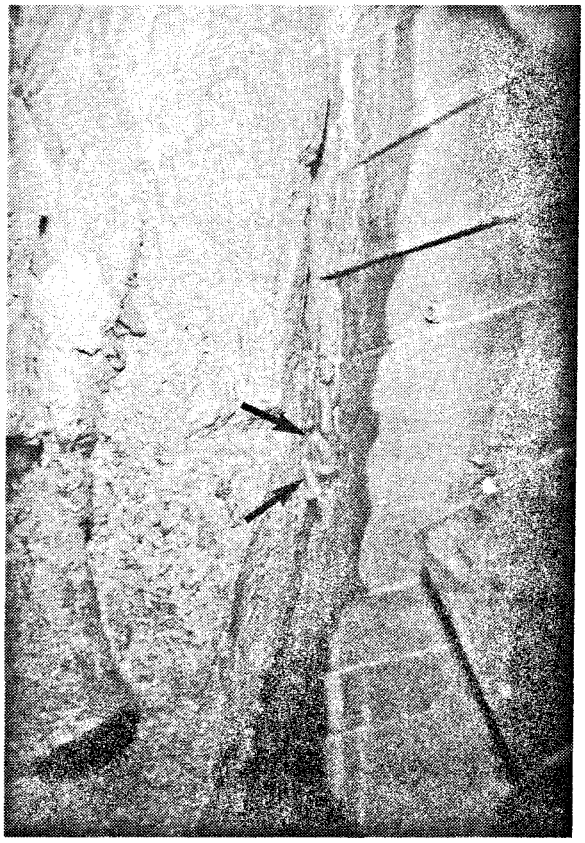

Fig 62. Clay is being pressed out through a fracture (arrow)

5.5.4.2 Build-up and retention of injection pressures

The high resolution power of the recording equipment showed that pressure peaks of 3.5-4 MPa, lasting for about 1 millisecond, were produced at each blow, the detailed pressure pattern being illustrated by Fig 63. This diagram demonstrates that the pressure did not drop below the static pressure and this is probably one reason for the efficiency of the applied injection technique.

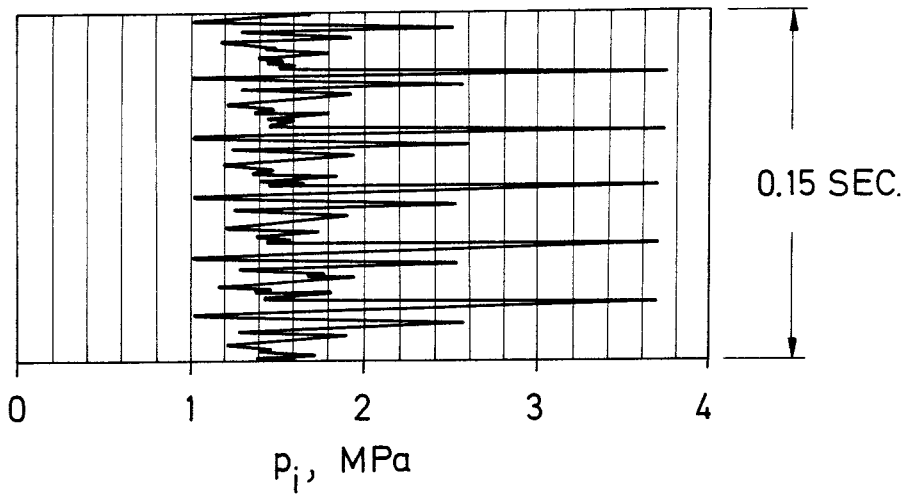

Fig 63. Example of pressure recording

At the end of the last injection stage in each hole, pressure readings were taken at regular intervals. Immediately after the injection, the pressure was found to be in the interval 2-3 MPa in all the holes but it dropped successively to about 0.5 MPa in 0.5-3 hours, and to 0-0.25 MPa after several hours or days. The recorded pressure drop is assumed to be caused by pore pressure dissipation causing consolidation of the clay gel in the expanded fractures. This would suggest that the injected gel turned stiffer, which would, in turn, bring down its hydraulic conductivity and make it less vulnerable to erosion.

5.5.4.3 Sealing effect

The sealing efficiency of the clay grouting was tested by measuring the water outflow from the sand-filled space of the tunnel plug at various water pressures, and comparing it to the recorded leakage immediately before the sealing operations. The outcome of the investigation is shown by the diagrams in Figs 64, 65 and 66.

We see that the leakage was reduced by 50-75 % at the low pressures 0.25 and 1 MPa, which is actually better than expected (cf. p. 114) and indicates that the injected fractures were effectively sealed. At 2 MPa pressure the reduction in leakage was about 20 %, which may indicate that the clay sealing tended to be damaged or that non-sealed, previously unimportant water passages had been activated.

At 3 MPa pressure the leakage was almost identical to that before the sealing, which suggests that erosion or piping had taken place. This is evidenced by the observation that a few deciliters of clay was instantly extruded from one fracture and that water was then ejected from this point of break-through. The fact that the clay fillings stayed intact at the considerable pressure 1 MPa and the associated high hydraulic gradients, demonstrates that the shear strength and erosion resistance were unexpectedly high. Such severe conditions are not probable in repository tunnels as concluded from the measurement of groundwater pressures in the Buffer Mass Test area, which is located a few hundred meters from the test site.

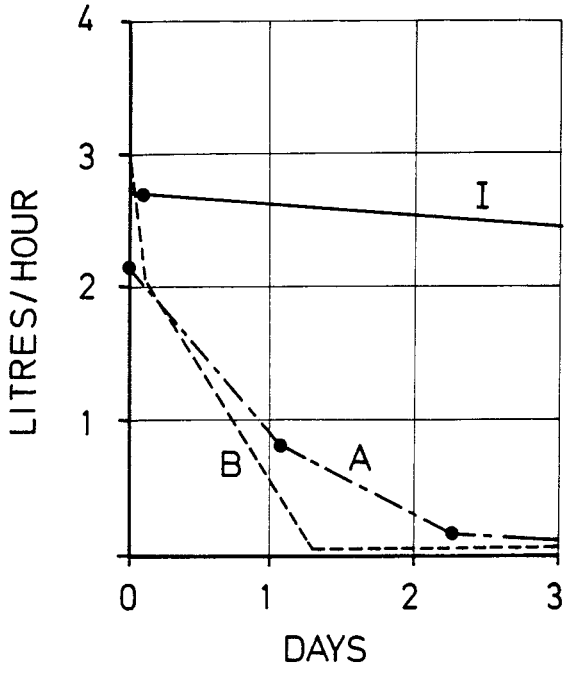

Fig 64. Leakage curves at 0.25 MPa water pressure before the sealing (Curve A) and after its completion (Curve B). I represents the leakage when this water pressure was applied at the start of the HP test in 1984, i.e. before the highly compacted bentonite had matured

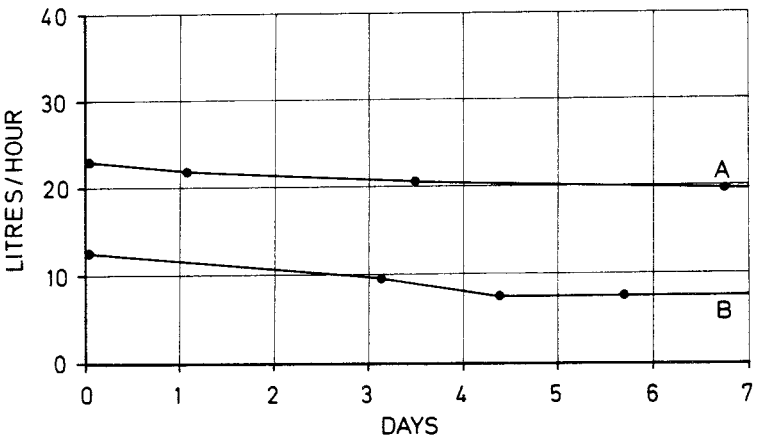

Fig 65. Leakage curves at 1 MPa water pressure before the sealing (Curve A) and after its completion (Curve B).

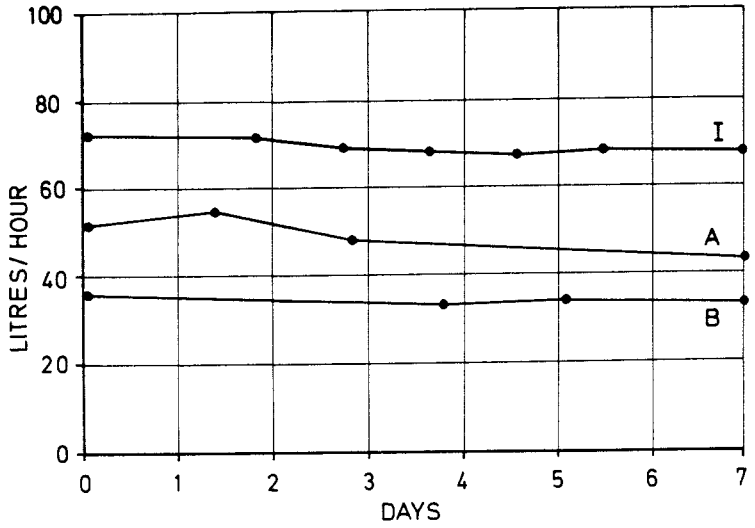

Fig 66. Leakage curves at 2 MPa water pressure before the sealing (Curve A) and after its completion (Curve B) I represents the leakage when this water pressure was applied at the start of the HP test in 1984

The manometers in the injection pipes reacted in the course of the water pressure increase in the sand chamber of the plug. The first pressure step 1 MPa gave reactions varying between 0.3 and 0.8 MPa in all the holes, except in no 3 in which the recorded pressure was first 1 MPa and then dropped to 0.95 MPa. At the next step 2 MPa, holes no 2 and 4 showed a reaction pressure of 0.4 MPa while all the others gave values in the range of 1.1 to 1.7 MPa. They dropped, however, to zero in hole no 1 and to 0.5 MPa in holes no 2 and 4 and to 1.6 MPa in hole no 3 in one day, indicating local piping. The highest step 3 MPa generated an increased reaction pressure only in hole no 3 but it dropped rapidly from the maximum value 2.2 MPa to 0.8 Mpa in connection with the previously mentioned extrusion of clay through a fracture that was intersected by this hole. Also in the other holes, the reaction pressures decreased, which shows that all the injected fractures are interconnected and that the local water break-through altered the flow and pressure pattern significantly.

5.5.5 Conclusions

The field test shows that soft smectite-rich clay slurries can be successfully injected in narrow rock fractures, and that they appear to be physically stable even at high rock water pressures. This stability may be due to consolidation, but this conclusion requires systematic tests under relevant field conditions. It is also required that long term pressure tests be made to certify that clay gels are durable from a physical point of view, not to forget that chemical longevity is needed as well.

As to the planning of the test it appears that the simple fracture mapping of the drift was sufficient for a proper selection of suitable positions of the injection holes to intersect the right water passages, although it may be possible that the fluid condition of the grout automatically gave an effective filling of the interconnected fracture system.

Finally, it was concluded that the equipment for injecting clay gels should be improved in various ways, a number of innovations being planned by Karl-Erik Nyman, Svensk Grundundersökning, Arlöv.

6 GENERAL ASPECTS AND CONCLUSIONS

Starting, as we did in this report, from the basic view that those fractures can be foreseen and identified that intersect canister deposition holes or are otherwise critical to the isolating function of the canister "near field", a number of possible techniques can be suggested for sealing them. Some of these techniques involve simulation of nature's own fracture sealing mechanisms but much research remains to be done in order to test their feasibility and the longevity of the filling substances.

At present, clay-based fracture fillings applied by use of the dynamic injection technique that was developed in the course of the project, seem to be of greatest potential use. However, additional research is required, particularly with respect to the efficiency of the grouting equipment and to the composition of the grouts. The latter has to be selected with respect to the durability from a chemical point of view, as well as to the physical properties, both in the injection phase and after the filling operation. Relevant rheological testing methods and parameters still remain to be developed and defined, while the matter of erodibility requires basic research as well as the development of practical methods for quantification purposes.

For the special case of high water flow through pervious rock zones that are intersected by boreholes, rapid stabilization by use of mechanically strong substances is required for which clay-based grouts are hardly sufficient. For such purposes there is an urgent need to develop in-hole techniques which yield chemically stable plugs.

Development of stochastic fracture flow models for the prediction of the penetration of grouts would be helpful, as would also refined field techniques for remote sensing of the spread of grouts in the course of the injection.

7 ACKNOWLEDGEMENTS

The authors wish to express their gratitude to Jeanette Stenelo at our office for her painstaking transformation of the scribblings to the present readable form.

Thanks are extended to Kjell Nilsson, SGAB, who solved major practical problems and made a number of valuable improvements of the test setups. The authors are also very grateful to Gunnar Ramqvist and Per Andersson, Stripa, for invaluable assistance in the field test, and to Karl-Erik Nyman, Svensk Grundundersökning AB, and his coworkers for valuable discussions and devoted work with the injection device.

8 REFERENCES

1 Asmis, H.W. Aspects of Seismic Mechanisms Related to Vault Design. Atomic Energy of Canada, Ltd, TR-228, 1984

2 Haimson, B.C. & Lee, C.F. Hydrofracturing Stress Determinations at Darlington, Ontario, 13th Can. Rock Mech. Symp., Toronto, Ontario, CIM Special Vol. 22

3 Sanford, B.V. & Thompson, F.J. Phanerozoic and Recent Tectonic Movements in the Canadian Shield and Their Significane to the Nuclear Fuel Waste Management Program. Workshop on Transitional Processes, Whiteshell Nuclear Res. Establishment, May, 1984. Atom Energy of Canada, Ltd, 7822

4 Gramberg, J. Axial Cleavage Fracturing, a Significant Process in Mining and Geology. Engineering Geology, Elsevier Publ. Co., Vol. 1, No. 1, 1965 (pp. 31-72)

5 Paul, B. & Gangal, M. Initial and Subsequent Fracture Curves for Biaxial Compression of Brittle Material. Failure and Breakage of Rock, 8th Symp. Rock Mech., Amer. Inst. Mining, Metallurg. and Petr. Engrs. (pp. 113-141)

6 Griffith, A.A. The Phenomenon of Rupture and Flow in Solids. Phil. Trans. Roy. Soc., London, Vol. A221, 1921 (pp. 163-198)

7 Griffith, A.A. The Theory of Rupture. Proc. 1st Int. Congr. Appl. Mechanics, Delft, 1924 (pp. 55-63)

8 Carlsson, A. & Olsson, T. Caracteristiques de Fracture et Proprietes Hydraulique d'une Region au Sous-sol Cristalline en Suede. Bull. B.R.G.M., Vol. 2, No. III, 1980/1981

9 Wilkins, B.J.S. Slow Crack Growth and Delayed Failure of Granite. Int Journ. Rock Mech. Min. Sci. & Geomech. Abstr., vol. 17, 1980 (pp. 365-369)

10 Pusch, R. Creep in Rock as a Stochastic Process. Engineering Geology, Vol. 20, 1984 (pp. 301-310)

11 Ramsay, J.G. The Crack-seal Mechanism of Rock Deformation. Nature, Vol. 284, March 1980 (pp. 135-139)

12 Bergman, S. Funktionell Bergklassificering. Bergmekanik, IVA Medd. 142, 1965 (pp. 115.123)

13 Thorpe, R. Characterization of Discontinuities in the Stripa Granite Time-scale Heater Experiment. Swedish-American Coop. Program on Radioactive Waste Storage in Mined Caverns in Crystalline Rock. Techn. Int. Rep. No 20, 1979

14 Pusch, R., Nilsson, J. and Ramqvist, G. Final Report of the Buffer Mass Test - Volume I: Scope, preparative field work, and test arrangement. Stripa Project Technical Report 85-11, 1985

15 Baecher, G.B. and Lanney, N.A. Trace Length Biases in Joint Surveys. Proc. 19th US Symp. on Rock Mechanics, Vol. I, 1978 (pp. 56-65)

16 Stephansson, O. (Ed.) Fundamentals of Rock Joints. Proc. Int. Symp. on Fundamentals of Rock Joints, Björkliden, 15-20 Sept. 1985. Centek Publishers, Luleå, Sweden

17 Montazer, P.M. and Hustrulid, W.A. An Investigation of Fracture Permeability Around an Underground Opening in Metamorphic Rocks. OCRD, Battelle Memorial Institute, Technical Report, BMI/OCRD-4(5), October 1983 (p. 56)

18 Kelsall, P.C., Case, J.B. and Chabannes, C.R. A Preliminary Evaluation of the Rock Mass Disturbance Resulting from shaft, Tunnel and Borehole Excavation. D'Appolonia Battelle Mem. Inst. Project No NM 79-137, July 1982

19 Pusch, R. A Multi-Purpose Rock Fracture Model. Internal Report, SKBF/Swedish Geological Co, IRAP 85502, May 1985

20 Johansson, C.H. Rock Motion in Bench Blasting. Swedish Detonic Research Foundation. Report DL 27, 1968

21 Andersson, B. and Halen, P.-A. Mining Methods Used in the Underground Tunnels and Test Rooms at Stripa. Swedish-American Coop. Program on Radioactive Waste Storage in Mined Caverns in Crystalline Rock, LBL-7081, SAC-08, UC-70, 1978

22 Lindgren, W. Mineral Deposits. Mc Graw-Hill, Book Co., New York,(4th ed) 1933

23 Fyfe, W.S., Turner, F.J. and Verhoogen, J. Metamorphic Reactions and Metamorphic Facies, 1958

24 Tullborg, E.-L. and Larson, S.Å. Fissure Fillings from Gideå, Central Sweden. SKBF/KBS Technical Report 83-74, 1983

25 Deloule, E. The Genesis of Fluorspar Hydrothermal Deposits at Moutroc and Le Burc. The Tarn as Deduced from Fluid Inclusion Analysis. Economic Geology. Vol 77, 1982 (pp 1867-1874)

26 Kristmannsdottir, H. and Tomasson, J. In Natural Zeolites. Occurrence, Properties, Use. Ed L.B. Sand and F.A. Mumpton. Pergamon Press, Oxford, 1978

27 Olkiewicz, A., Scherman, S. and Kornfält, K.-A. Kompletterande Berggrundsundersökningar inom Finnsjö och Karlshamnsområdena. SKBF/KBS, Technical Report, 79-05, 1979

28 Tullborg, E.-L. and Larsson, S.Å. Fissure Fillings from Finnsjön and Studsvik, Sweden. Identification, Chemistry and Dating. SKBF/KBS Technical Report 82-20, 1982

29 Posnjak, E. The System, $CaSO_4$-H_2O. Amer Jour Science, Amer. Vol. 235-A, 1938 (pp 247-272)

30 Larsson, S.Å. Sprickmineralogisk Sprickstudie. Rapport Prav 4.13, 1980

31 Larsson, S.Å., Tullborg, E.-L. and Lindblom, S. Sprickmineralogiska Undersökningar. Report Prav 4-20, 1981

32 Mtschedlow-Petrossian, O.P. and Worobjow, J.L. Die Aussichten der Verwendung einiger naturlicher Magnesiumhydrosilikate in der Industrie. Silikattechnik, Vol. 11, No. 10, 1960

33 Bergman, L. and Lindberg, B. Phanerozoic Veins of Galena in the Åland Rapakivi Area, Southwestern Finland. Bull Geol. Soc. Finland 51, 1979 (pp 55-62)

34 Martinsson, A. Neue Funde Kambrischer Gänge und Ordovizischer Geschiebe im sudwestlichen Finnland. Bull. Geol. Inst. Uppsala, Vol. 36, No. 5, 1956, (pp 79-105)

35 Tanner, V. Uber eine Gangformation von fossilien-fuhrendem sandstein auf der Halbinsel Långbergsödaöjen im Kirschspiel Saltvik, Åland Inseln. Bull. Comm. Geol. Finnlande 25, 1911

36 Pusch, R. Mineral-Water Interactions and Their Influence on the Physical Behavior of Highly Compacted Na Bentonite. Canadian Geotechnical Journal, Vol. 19, No. 3, 1982

37 Pusch, R. Clay Microstructure. Nat. Swed. Building Research Council, Document D8:1970

38 Pusch, R. Influence of Salinity and Organic Matter on the Formation of Clay Microstructure. Proc. Int. Symp. Soil Structure, Gothenburg, 1973

39 Wittke, W., Pierau, B. and Plischke, B. Erfahrungen mit Zementpasten bei Injektionsarbeiten in Kluftigen Fels. Ver. des Institutes fur Grundbau, Bodenmechanik, Felsmechanik und Verkehrswasserbau der RWTH Aachen. Heft 7, 1978

40 Andreasson, L. et al. Provning av Injekteringsmedel för Fintätning av Berg. Byggforskningsrådet, Rapport R 121:1980

41 Bergman, S.G.A. Tunneltätning. Injekteringsmedel-Inträngning i Sand och Smala Spalter. Byggforskningen Rapport R 45:1970

42 Chan, H.T. Laboratory Study of Clay-type Grouting Materials. Internal Report, CNS Conference, Winnipeg, Sept 13-15, 1982

43 Pusch, R. Rock Sealing with Bentonite by means of Electrophoresis. Bull Int Ass Engng Geology No 18, 1978

44 Pusch, R. Stability of Bentonite Gels in Crystalline Rock - Physical Aspects. SKBF/KBS Technical Report 83-04, 1983

45 Arnold, M. A Study of Thixotropic Action in Bentonite Clay. Diss. Univ. of Adelaide, 1968

46 Smalley, I., Cabrera, J.G. and Hammond, C. Particle Nature in Sensitive Soils and its Relation to Soil Structure and Geotechnical Properties. Int. Symp. Soil Structure, Gothenburg, Sweden, 1973

List of Technical Reports

1977–78
TR 121
KBS Technical Reports 1 – 120.
Summaries. Stockholm, May 1979.

1979
TR 79–28
The KBS Annual Report 1979.
KBS Technical Reports 79-01 – 79-27.
Summaries. Stockholm, March 1980.

1980
TR 80–26
The KBS Annual Report 1980.
KBS Technical Reports 80-01 – 80-25.
Summaries. Stockholm, March 1981.

1981
TR 81–17
The KBS Annual Report 1981.
KBS Technical Reports 81-01 – 81-16.
Summaries. Stockholm, April 1982.

1982
TR 82–28
The KBS Annual Report 1982.
KBS Technical Reports 82-01 – 82-27.
Summaries. Stockholm, July 1983.

1983
TR 83–77
The KBS Annual Report 1983.
KBS Technical Reports 83-01 – 83-76
Summaries. Stockholm, June 1984.

1984
TR 85–01
Annual Research and Development Report 1984
Including Summaries of Technical Reports Issued during 1984. (Technical Reports 84-01– 84-19)
Stockholm June 1985.

1985
TR 85–01
Annual Research and Development Report 1984
Including Summaries of Technical Reports Issued during 1984.
Stockholm June 1985.

TR 85–02
The Taavinunnanen gabbro massif. A compilation of results from geological, geophysical and hydrogeological investigations.
Bengt Gentzschein
Sven-Åke Larson
Eva-Lena Tullborg
Swedish Geological Company
Uppsala, January 1985

TR 85–03
Porosities and diffusivities of some non-sorbing species in crystalline rocks.
Kristina Skagius
Ivars Neretnieks
The Royal Institute of Technology
Department of Chemical Engineering
Stockholm, 1985-02-07

TR 85–04
The chemical coherence of natural spent fuel at the Oklo nuclear reactors.
David B. Curtis
New Mexico, USA, March 1985

TR 85–05
Diffusivity measurements and electrical resistivity measurements in rock samples under mechanical stress.
Kristina Skagius
Ivars Neretnieks
The Royal Institute of Technology
Department of Chemical Engineering
Stockholm, 1985-04-15

TR 85-06
Mechanical properties of granitic rocks from Gideå, Sweden
Christer Ljunggren
Ove Stephansson
Ove Alm
Hossein Hakami
Ulf Mattila
Div of Rock Mechanics
University of Luleå
Luleå, Sweden, October 1985

TR 85-07
Complex forming properties of natural occurring fulvic acids
Part 1. Complexes with cadmium, copper and calcium
Jacob A. Marinsky,
A. Mathuthu,
M. Bicking and
J. Ephraim
State University of New York at Buffalo
Buffalo, New York 14214,
July 1985

TR 85-08
In situ one-year burial experiments with simulated nuclear waste glasses
Larry L Hench, Derek Spilman and T Buonaquisti
College of Engineering, Univ. of Florida, Gainesville, USA
Alexander Lodding
Chalmers Univ. of Technology, Gothenburg, Sweden
Lars Werme
SKB, Stockholm, Sweden

TR 85-09
Concentration and distribution of natural radionuclides at Klipperåsen and Bjulebo, Sweden
Björn Sundblad, Ove Landström, Rune Axelsson
Studsvik Energiteknik AB, Nyköping, Sweden

TR 85-10
Chemical interactions between the bentonite and the natural solutions from the granite near a repository for spent nuclear fuel
Bertrand Fritz and Marie Kam
Université Louis Pasteur de Strasbourg, Institut de Géologie, France
July 1985

TR 85-11
Hydrochemical investigations in crystalline bedrock in relation to existing hydraulic conditions: Experience from the SKB test-sites in Sweden
John Smellie, Nils-Åke Larsson
Swedish Geological Company, Uppsala, Sweden
Peter Wikberg
Royal Institute of Technology, Stockholm Sweden
Leif Carlsson
Swedish Geological Company, Göteborg, Sweden
November 1985

TR 85-12
Hydrogeological investigations and tracer tests in a well-defined rock mass in the Stripa mine
Peter Andersson
Carl-Erik Klockars
Swedish Geological Company
Division of Engineering Geology
Uppsala 1985-11-29

TR 85-13
Analysis of hydrodynamic dispersion in discrete fracture networks using the method of moments
Anders Rasmuson
Dep of Chemical Engineering, Royal Inst of Technology Stockholm
June 20, 1985

TR 85-14
Radionuclide migration in strongly fissured zones—The sensitivity to some assumptions and parameters
Anders Rasmuson, Ivars Neretnieks
Dep of Chemical Engineering, Royal Inst of Technology Stockholm
August 7, 1985

TR 85-15
Diffusion measurements of cesium and strontium in biotite gneiss
Kristina Skagius, Ivars Neretnieks
Dep of Chemical Engineering, Royal Inst of Technology Stockholm
1985-12-30

TR 85-16
The corrosion of spent UO_2 fuel in synthetic groundwater
R S Forsyth
Studsvik Energiteknik AB, Nyköping, Sweden
L O Werme
The Swedish Nuclear Fuel and Waste Management Co (SKB), Stockholm, Sweden
J Bruno
Royal Institute of Technology, Dept of Inorganic Chemistry, Stockholm, Sweden
October 1985